2014

Evaluation of Iowa asphalt pavement joint cracking

Can Chen
Iowa State University

Evaluation of Iowa asphalt pavement joint cracking

by

Can Chen

A dissertation submitted to the graduate faculty

in partial fulfillment of the requirement for the degree of

DOCTOR OF PHILOSOPHY

Major: Civil Engineering (Civil Engineering Materials)

Program of Study Committee:
R. Christopher Williams, Major Professor
Jeramy Ashlock
Mervyn Marasinghe
Thomas Rudolphi
Vern Schaefer

Iowa State University
Ames, Iowa
2014

TABLE OF CONTENTS

ACKNOWLEDGMENTS

First, I would like to thank my mother who has fully supported me through a hard journey in my life.

I would like to thank my major professor, Dr. Christopher Williams, for all his help and support throughout my studies at Iowa State University. I owe my deepest gratitude to him for placing me in the doctoral program, providing guidance, and also constantly looking out for my interests and career development. This would not have been possible without his generosity and kindness.

I would also like to extend my great thanks to Drs. Jeramy Ashlock, Vern Schaefer, Jennifer Shane (substitute for Vern Schaefer in final oral exam), Mervyn Marasinghe, and Thomas Rudolphi for serving as my graduate committee and providing me generous help in my Ph.D studies. Their knowledge in non-destructive testing, geotechnical/transportation engineering, statistical analysis and numerical simulation that I learned in my four year Ph.D study will definitely benefit me for many years.

Last, but not least, I would like to thank my dear friends and colleagues. Your companionship made living in Ames at Iowa State a memorable experience.

CHAPTER 1. INTRODUCTION

1.1 Background

Flexible pavements are constructed of bituminous and granular materials. The common asphalt pavement distresses are provided in Table 1. Many of the distresses commonly occur in the pavement joint area and good pavement joint connection and attachment are vital to control pavement cracking and pavement movement. In this thesis, two major types of asphalt pavement joint cracking; reflective cracking and longitudinal joint cracking, are discussed.

Table 1 Types of major asphalt pavement distresses

Cracking	Distortion	Disintegration
Transverse cracking	Rutting	Raveling
Longitudinal cracking	Shoving	Segregation
Fatigue cracking	Upheaval	Stripping
Edge cracking	Depression	Bleeding

Reflective Cracking

Transverse cracking in a flexible overlay surface that occurs over joints in underlying concrete pavements is generally called reflective cracking. This type of cracking usually happens in composite pavements (flexible overlay of a rigid pavement). The existing concrete joints or cracks cause stress concentrations at the bottom of an asphalt overlay, which will lead to continued crack growth into the asphalt overlay layers. Several strategies exist to mitigate reflective cracking depending upon the pavement structure, and include the use of crack relief layers in the form of membranes and specialty asphalt mixtures (e.g. Strata), crack & seat, rubblization, cold in-place recycling of existing asphalt overlays, and full-depth reclamation. Depending upon the pavement structure, the pavement condition, and

traffic level, varying strategies to improve the performance of the pavement economically exist.

However, despite the availability of numerous crack mitigation strategies, many of the methods do not have construction criteria to assist in ensuring the intended design life of the strategies is met. One such example is the use of rubblization. There have been many instances where a pavement has been rubblized, yet upon later investigation it is found that the jointed concrete pavement was only rubblized in the top 3-4 inches and not the full depth of the concrete. There is also substantial variation in the fracture particle size of rubblized pavements.

The Iowa Department of Transportation (DOT) currently does not have a guideline or specification on reflective cracking control and mitigation in conventional composite pavements. A standard technical guide is needed for the State of Iowa to provide detailed guidance on choosing the optimal reflective cracking mitigation strategy for a project. The guide should provide pavement designers with a crack control selection method that is in part based upon a reliability-based analysis and life cycle cost analyses. It also needs to specifically address rubblization and crack & seat mitigation techniques by giving recommendations for construction specifications and structural capacity based on the most advanced research available. In addition, newly developed rock interlayers have been commonly used in Iowa's county roads, and the performance data is readily available to the research team including the original material properties and designs. The study also needs to verify the practical aspects of the rock interlayer in Iowa.

Longitudinal Joint Cracking

Many asphalt pavement cracks also develop at the longitudinal joint area, and these are called longitudinal joint crackings. A longitudinal joint is the interface between two adjacent and parallel hot-mix asphalt (HMA) mats. Longitudinal joint quality is critical to the long-term performance of asphalt roadways, and many asphalt pavement failures occur at the longitudinal joint. In general, low joint densities have been believed to be primarily responsible for the longitudinal joint cracking because low densities generally indicate higher levels of permeability, meaning that air and water can enter the joint area and accelerate the potential for deterioration. Many state agencies are moving toward the implementation of a longitudinal joint specification. According to the information provided at the Research in Progress database on the Transportation Research Board (TRB) Website, current available longitudinal joint research projects in the U.S. include *the Evaluation of Longitudinal Joint Density* conducted by the Colorado DOT, *Quality Assurance/Quality Control Testing for Joint Density and Segregation of Asphalt Mixtures* by the Iowa DOT, *the Improved Longitudinal Joint Construction* sponsored by the Kentucky Transportation Cabinet and *the HMA Longitudinal Joint Deterioration Investigation* supported by the National Center for Freight & Infrastructure Research and Education. Simply, the assessment of longitudinal joint construction quality can be beneficial to improve the performance of the joint and it has drawn a significant amount of research attention in recent years.

The Iowa Department of Transportation (IDOT) currently does not have a test method or specification for identifying segregation and quality control/quality assurance for longitudinal joint density. A number of specific questions are to be answered in this thesis:

1. What is the best method for constructing longitudinal joints in Iowa?

2. Is permeability of longitudinal joints related to joint' performance?
3. If permeability is related to longitudinal joint performance, what are the appropriate quality assurance criteria?
4. What types of tests can be used to detect the segregation of asphalt mats and longitudinal joints?
5. Does segregation have a significant effect on the longitudinal joint performance?

1.2 Objective

A first objective is to evaluate the reflective cracking in flexible pavements at both network and project-levels. The second purpose of this thesis is to obtain necessary field and laboratory test data to investigate the flexible pavement longitudinal joint construction method in Iowa.

1.3 Organization of Dissertation

This dissertation consists of six chapters including the introductory one as the first. The second chapter provides a comprehensive literature review discussing the causes of reflective cracking and longitudinal joint cracking in asphalt pavement. The commonly used mitigation strategies for reflective cracking and longitudinal joint cracking control are also provided in this chapter. Statistical survival analysis was applied and is in chapter three for reflective cracking mitigation strategy selection in a network-level approach. The fourth chapter evaluates the pavement layer structural condition and field performance condition for different reflective cracking treatments in a project-level approach. The fifth chapter considers the available test methods for longitudinal joint quality control and the effect of segregation on longitudinal joint density performance. Finally, the sixth chapter outlines the findings, conclusions and makes recommendations. A numerical simulation for HMA

material is provided in the appendix to better understand the interaction of air void (porosity) and moisture damage.

CHAPTER 2. LITERATURE REVIEW IN REFLECTIVE CRACKING AND LONGITUDINAL JOINT CRACKING

2.1 Causes and Mechanism of Reflective Cracking

Reflective cracking is one of the most common types of distresses that occur early in the service life of composite pavements. When HMA overlays are placed over jointed or severely cracked Portland cement concrete (PCC) or HMA pavements, the cracks rapidly propagate through the HMA overlay thickness and reflect to the surface causing reflective cracks. Although reflective cracks do not generally reduce the structural capacity of a pavement, subsequent ingress of moisture and the effects of the natural environment and traffic can result in premature distress and even failure of the pavement.

Reflective cracks propagate through the HMA overlay surface due to the movement at the crack (joint in case of existing concrete pavements) producing tensile stresses which are caused by (a) discontinuities in the underlying layers, (b) differential temperature conditions, and (c) longitudinal cracks in the old surface (Roberts et al. 1996). Schematic diagrams of thermally-induced and traffic-induced reflective cracking mechanisms are shown in Figure 1 (Von Quintus et al. 2009). The combined effect of traffic and environmental loadings is considered to cause reflective cracks which can initiate either at the top or bottom of the HMA overlays. The propagation rate of reflective cracks is dependent on a number of factors including the thickness of the overlay, properties of the HMA overlay, type of reinforcement (if used), and the subgrade condition (Von Quintus et al. 2009). Reflective cracks observed in HMA overlays at different levels of severity are shown in Figure 2 (Al-Qadi et al. 2009).

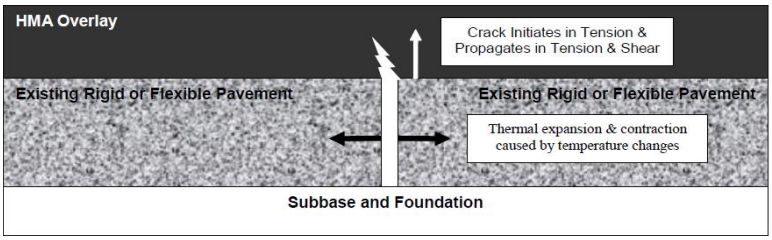

(a) Thermally-induced Reflective cracking of HMA overlays: Horizontal movements

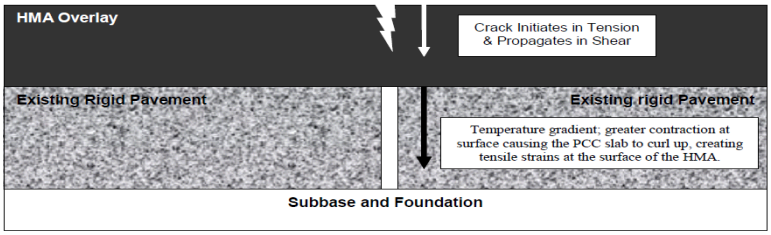

(b) Thermally-induced Reflective cracking of HMA overlays: Curling of PCC slab

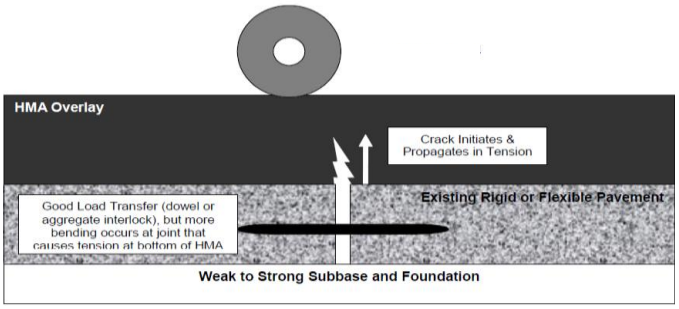

(c) Traffic-induced Reflective cracking of HMA overlays

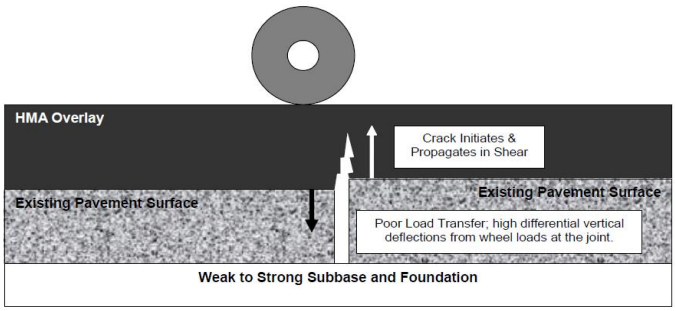

(d) Traffic-induced Reflective cracking of HMA overlays

Figure 1 Mechanisms of reflective cracking of HMA overlays (Von Quintus et al. 2009)

Von Quintus et al. (2009) summarized the most commonly attributed factors that cause movements at joints and cracks in the existing pavement (termed as trigger factors for reflective cracking) as follows:

- Low temperatures (temperature drop)
- Wheel loads
- Freeze-thaw cycles
- Aging of HMA near surface (air voids level)
- Shrinkage of PCC, HMA, and cement-treated base (CTB)

From the perspective of fracture mechanics, cracks are classified in accordance with three loading modes. In mode I (opening mode), principal loading is applied normally to a crack plane, and cracks grow perpendicular to the crack plane, and cracks grow perpendicular to the crack plane. In modes II and III, cracks occur in in-plane shear direction and out-of-plane shear direction, respectively. Typically, both temperature and traffic loading can result in mode I fracture. Horizontal strain accumulates in an HMA overlay due to horizontal movements of PCC slabs due to temperature variations and pure bending in HMA when a tire is located directly over a joint. Traffic loading can also result in mode II fractures due to the differential shear movement of PCC slabs. Mode III fracture may be induced by lateral (longitudinal) movement of concrete slabs, but it is rarely observed in HMA overlays (Mukhtar and Dempsey, 1996). Temperature and traffic loadings applied usually are together in HMA overlays, so that reflective cracking may develop in a mixed mode. In the simulation of reflective cracking development, a cohesive zone model is usually selected because of its accuracy and efficiency in accounting for material response ahead of

the crack tip in the fracture process zone (region of micro-cracking, crack branching, material softening, etc.).

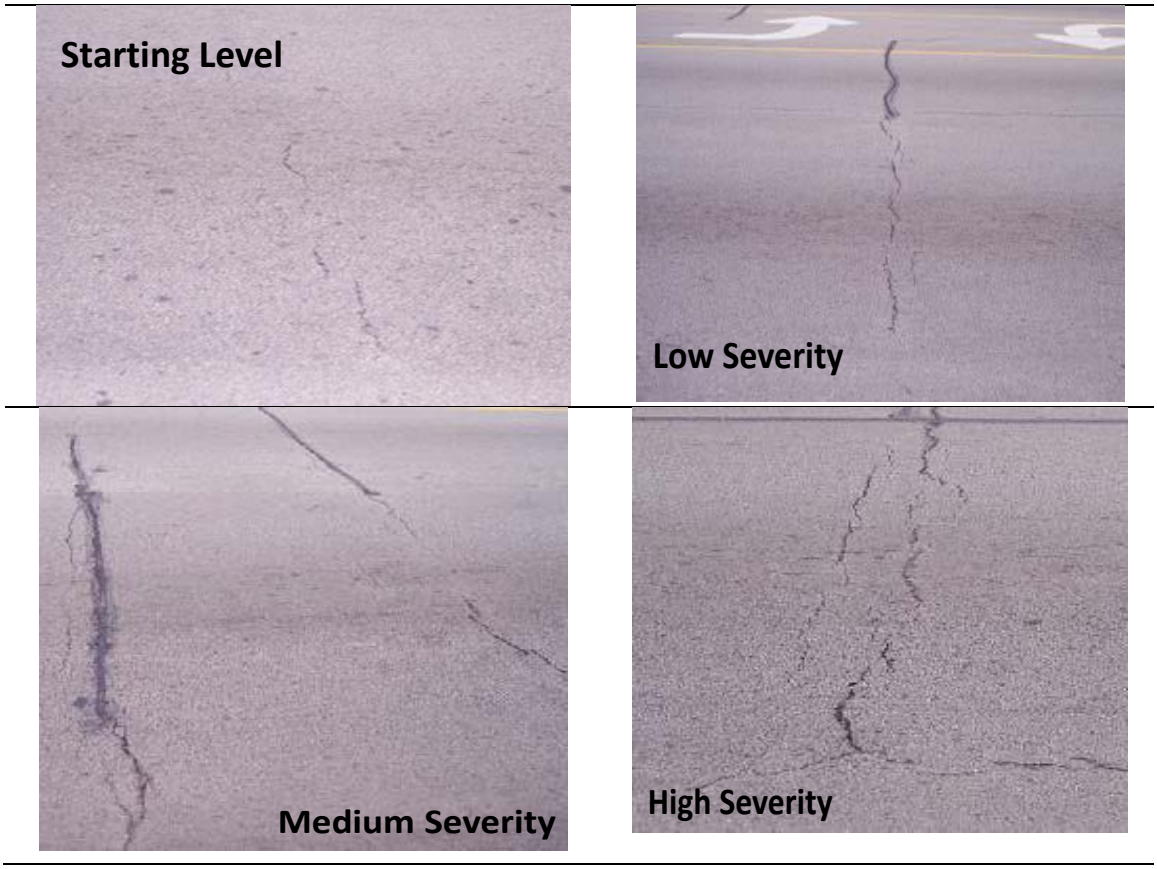

Figure 2 Reflective cracking severity levels (Al-Qadi et al. 2009)

2.2 Types of Reflective Cracking Mitigation Strategies

The following are the various pre-overlay techniques used by different States to mitigate reflective cracking in existing HMA and PCC pavements (Von Quintus et al. 2009; Bandaru 2010):

- **Modification/Treatment of existing PCC pavement surface**
  - Crack-and-seat or Break-and-seat
  - Rubblization

- **Existing HMA surface**
  - Mill and replace wearing surface
  - Heater scarification
  - Hot In-Place Recycling (HIPR)
  - Cold In-Place Recycling (CIPR)
  - Full-Depth Reclamation (FDR)
- **Pre-overlay repairs of existing pavement surface**
  - Undersealing PCC slabs
  - HMA inlay
  - HMA patches
  - Use of leveling courses
- **Stress/Strain relieving interlayer**
  - Stress Absorption Membrane Interlayer (SAMI)
  - Geosynthetic fabrics
  - Soft asphalt interlayer
  - Rubber modified asphalt interlayer
  - Strata® Reflective Crack Relief System
  - Interlayer Stress Absorbing Composite (ISAC)
  - Bond breaker
- **HMA mixture modification**
  - Polymer-modified asphalt
  - Rubberized asphalt
  - Stone Matrix Asphalt

- Sulfur asphalt
- Carbon black
- **HMA overlay reinforcement**
- Steel-reinforcing nettings
- Geotextiles
- Geogrids
- Geocomposites
- Geomembranes
- **Crack control**
- Sawing and sealing joints in HMA overlays
- Chip seal (HMA surface treatment)

Bennert (2010) recently completed a national survey on the reflective cracking experience of different States in the US. A total of 26 State Highway Agencies (SHAs), who reported that they overlay PCC pavements with HMA, participated in this survey and Iowa was one of the participants. Based on the survey results, the answers to the following questions were analyzed: relationship between the aggregate base type and years until reflective cracking observed, relationship between joint spacing and time until reflective cracking observed, common PCC treatment used by SHA prior to HMA overlay. A majority of the SHAs (22 or 85%) reported that reflective cracking was observed within the first four years of the placement of the HMA overlay while 7 SHAs reported observing reflective cracking within the first two years.

An overall conclusion drawn by Bennert (2010) based on the results of the national survey was that "there currently exists a large gap in the current practice of evaluating the

potential for reflective cracking of asphalt overlays when placed on composite/rigid pavements." Similarly, Loria-Salazar (2008) conducted a comprehensive literature review on reflective cracking mechanisms and mitigation techniques which is summarized in Table 2.

Table 2 Summary of a recent review on reflective cracking treatments (Loria-Salazar 2008)

Treatment	Description	Performance
Cold in-place recycling	Remove and mill the upper layers of the existing pavement with specialized recycling equipment then mix with virgin materials to produce a strong flexible base course	Promising performance for roads with up to 13,000 ADT and 200,000 annual equivalent single axle loads
Glassgrid	Geosynthetic material consisting of connected parallel sets of intersecting ribs with openings of sufficient size	Benefits in retarding or preventing reflective cracking are not clear. Field performance has varied from excellent to very poor. Concerns when used on rough surfaces
Fabric interlayer	Geosynthetic comprised solely of textiles. A paving fabric interlayer provides the generally acknowledged functions of stress-absorbing interlayer and a waterproofing membrane. The stress-related performance has been easily verified by the observed reductions of cracking in pavement overlays	Effective when used for load-related fatigue distress. It did not perform well when used to delay or retard thermal cracking. Optimum performance highly associated with proper construction procedures. The key factor is properly reinforced overlays with fabrics have shown better performance than unreinforced overlays under same conditions
Asphalt rubber	Asphalt rubber chip seal overlaid with conventional dense-graded HMA or gap-graded HMA	Reduce or delay reflective cracking for a period of 5 years
Stress absorbing membrane	A thin layer placed between an underlying pavement and an HMA overlay for the purpose of dissipating movements and stresses at a crack in the underlying pavement before they create stresses in the overlay. SAMIs consist of a spray application at the stress relieving material, followed by placing and seating aggregate chips	Successful in reducing the rate of reflective cracking.
Crumb rubber overlay	Produced by adding ground tire rubber to HMA using the wet process	Ranged from successful to devastating failures depending on percent of crumb rubber in mix

Among the various reflective cracking mitigation techniques documented in the literature, the following are the primary techniques used in Iowa: rubblization, crack-and-

seat, CIR, FDR, crack relief or stress/strain relieving interlayer (e.x., Strata®), and others (engineering fabrics, saw-and-seal, polymer-modified mixes, etc.). Apart from these techniques, milling and filling HMA overlay, sawing and sealing the joints in HMA overlays have also been employed on some projects. Additionally, experimental studies of fabric applications in Iowa have not been conclusive. A brief summary of each of these techniques is provided below.

The following are some of the major research studies carried out in Iowa to study the effectiveness of different reflective cracking strategies:

- **Cold In-Place Recycling (CIPR)**
  - HR-1020: Transverse Cracking Study of Asphalt Pavement (1981)
  - HR-303: Field Evaluation of Cold In-Place Recycling of Asphalt Concrete (1993)
  - HR-392: Review of Cold In-Place Recycled AC Projects (1998)
  - TR-502: Evaluation of Long-Term Field Performance of CIPR Roads (2007)
- **Paving Fabrics and Geosynthetics**
  - HR-158: Prevention of Reflective Cracking in HMA Overlays with Structufors, Petromat, and Cerex (1963)
  - MLR-83: Performance of Reinforcement Fabric Used Under AC Overlays (1983)
  - HR-535: Glasgrid Fabric to Control Reflective Cracking (1990)
  - HR-360: Field Evaluation of Experimental Fabrics for AC Resurfacing – Audobon County (2001)
- **Rubblization and Crack-and-seat**
  - HR-158: Prevention of Ref. Crack. in AC Overlays with Structufors, Petromat, and Cerex (1963)

- HR-279: Cracking and Seating to Retard Reflective Cracking – Fremont County (1993)
- HR-527: Crack and Seat PCC Pavement Prior to Resurfacing US 59 – Shelby County (1993)
- HR-315: Iowa Development of Rubblized Concrete Pavement Base – Mills County (1995)
- TR-473: Rehabilitation of PCC Pavements Utilizing Rubblization and Crack and Seat (2005)
- TR-550: Performance Evaluation of Rubblized Pavements in Iowa (2008)

Crack-and-Seat

Crack and seat is a fractured slab technique that uses a drop hammer to break the existing concrete pavement slabs into smaller pieces (typically, 12-48 in.) thereby reducing the effective slab length and minimizing its movement from thermal stresses. This strategy is gaining popularity in Iowa since its original use in 1986 on JPCPs from county roads to interstate highways.

Four major steps are involved in implementing crack-and-seat techniques (see Figure 3): cracking the concrete slab (using a drop hammer or guillotine or modified pile driver or whip hammer), seating the cracked slab, applying special treatments, and placing the HMA overlay. The cracking of the existing pavement reduces the slab movement due to thermal action, thus minimizing or controlling the reflective cracking in the HMA overlay. The resulting pieces should be large enough to retain aggregate interlock between aggregates, and yet small enough to minimize the unreinforced PCC slab joint movement (PCS 1991).

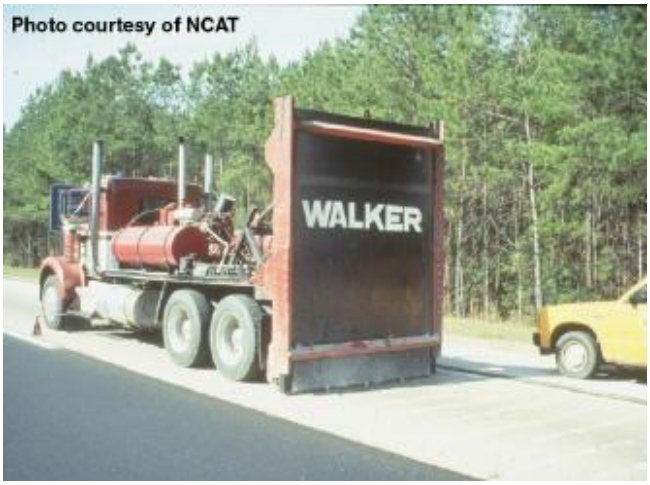

Figure 3 Crack-and-seat

It has been reported that crack-and-seat fractured slab technique, when used properly, has the potential to significantly delay the reflective cracking, but not completely eliminate them in the HMA overlay (Thompson 1999). They have also been reported to be effective in eliminating blowups in JPCPs (Drake 1988). Although smaller cracked PCC pieces mean larger potential reduction in reflective cracking, they also lead to larger reduction in the concrete pavement structural strength (Eckrose and Poston 1982).

A previous study conducted in Iowa (IHRB Project TR-473) identified crack and seat as a viable strategy for Iowa pavements that minimizes reflective cracking (Ceylan et al. 2005). Still, several challenges exist in the design and construction phases of a project when selecting this strategy. Sharpe et al. (1987) identified the following main concerns of the Kentucky Department of Highways when implementing this strategy:

- Selecting acceptable breaking equipment,
- Validating the extent of breaking or cracking,
- Determining acceptable seating/rolling patterns, and
- Establishing minimum asphalt overlay thicknesses.

The breaking equipment used and the cracking pattern chosen have an effect on the structural capacity of the pavement. With the use of crack-and-seat technique, the structural capacity of the pavement is generally reduced. Since the structural capacity affects the thickness of the HMA layer, proper construction criteria are necessary to achieve the intended design.

Rubblization

Rubblization is defined as "breaking the existing pavement into pieces and overlaying with HMA." It destroys the slab action of the rigid pavements. The sizes of the broken pieces usually range from sand size to 3 in. at the surface and from 12 to 15 in. on the bottom part of the rubblized layer (Von Quintus et al. 2007). The results from a comprehensive investigation conducted by PCS/Law (1991), the National Asphalt Pavement Association (NAPA) study (NAPA 1994), and a nationwide survey conducted by the Florida DOT (Ksaibati et al. 1999) all indicate that rubblization is the most effective procedure for addressing reflection cracking. It has been concluded that the rubblized PCC behaves like "a high-strength granular base," with strength between 1.5 to 3 times greater than a high-quality, dense-graded, crushed-stone base in load-distributing characteristics (PCS/Law 1991).

In general, two types of equipment are used in the rubblization process (see Figure 4): Resonant Pavement Breaker (RPB) and Multiple-Head Breaker (MHB). The RPB uses vibrating hammers to break the concrete slab and destroy the bond between the concrete and the steel. The other common rubblizing equipment is the self-contained and self-propelled MHB used by Antigo Construction which is capable of rubblizing the pavement over a minimum width of 13 ft. per pass.

Figure 4 Rubblization: Resonant Pavement Breaker (left) and Multi-Head Breaker (right)

During rubblization the PCC is converted to small, interconnected pieces that serve as an aggregate base course. IHRB Project TR-473 concluded that rubblization can be a viable, rapid, and cost-effective rehabilitation method for deteriorated PCC pavements. Several State highway agencies (Illinois, Michigan, Wisconsin, etc.) have also completed studies on the performance of rubblized pavements and have concluded similar results (Von Quintus et al., 2009). To address the various construction challenges when implementing this strategy, in February 2004 the Federal Aviation Administration (FAA) adopted and published FAA Engineering Brief (EB) No. 66, *Rubblized Portland Cement Concrete Base Course*. The document includes guidance and criterion for rubblizing PCC pavements.

The Iowa DOT recognized the potential of rubblization in rehabilitating old concrete pavements and conducted a research project to rehabilitate and evaluate a severely deteriorated concrete roadway using a rubblization process as early as 1995. A 3.0 km (1.9 mi.) section of L-63 in Mills county was selected and divided into 16 sections. In 1985, HMA overlay construction was done in 13 sections after rubblizing the existing pavement with a RPB and in three sections without rubblization. This research concluded that the rubblization process prevents reflective cracking and that edge drains improved the structural rating of the rubblized roadway. In addition, it was noted that a 5-in. (125-mm) thick HMA

overlay on a rubblized base provided an excellent roadway regardless of soil and drainage conditions; whereas a 3-in. (75-mm) thick HMA overlay on a rubblized base can provide a good roadway if the soil structure below the rubblized base is stable and well drained.

After the completion of this research (Tymkowicz and DeVrie 1995), the use of rubblization has steadily increased in Iowa state highways and county roadways. However, there were some changes in the rubblization practices adopted in Iowa due to poor subgrade, lack of crushed aggregate base, and the use of thin concrete pavements (Jansen 2006). The modified rubblization method was proposed and adapted in the rehabilitation project of W-14 in Winneshiek County by Antigo in 2003.

Ceylan et al. (2008) recently evaluated the performance of rubblized pavements in Iowa using field surveys (Falling Weight Deflectometer, visual distress surveys, DCP, and coring) and concluded that Iowa's rubblized pavement sections are performing well. The predominant distresses exhibited on HMA-overlaid rubblized PCC sections are non-load associated distresses, such as low-temperature cracking and/or longitudinal cracking. Similarly, based on long-term field monitoring results of different mitigation strategies applied to Iowa pavements, Kim et al. (2008) reported that the rubblization technique was the most effective method in retarding reflection cracking whereas the test sections with a crack relief layer exhibited the highest amount of reflection cracking. However, it is important to note that the rubblized sections had much thicker HMA overlay than the other test sections. Several State highway agencies (Illinois, Michigan, Wisconsin, etc.) have also completed studies on the performance of rubblized pavements and have reported success with the use of this technique (Von Quintus et al., 2009).

To address the various construction challenges when implementing this strategy, in February 2004 the Federal Aviation Administration (FAA) adopted and published FAA Engineering Brief (EB) No. 66, *Rubblized Portland Cement Concrete Base Course*. The document includes guidance and criterion for rubblizing PCC pavements. Similarly, the Wisconsin DOT Standard Specifications give guidance to the contractors with respect to size requirements for rubblized pieces in slab surface, top half of slab, and bottom half of slab as shown in Figure 5.

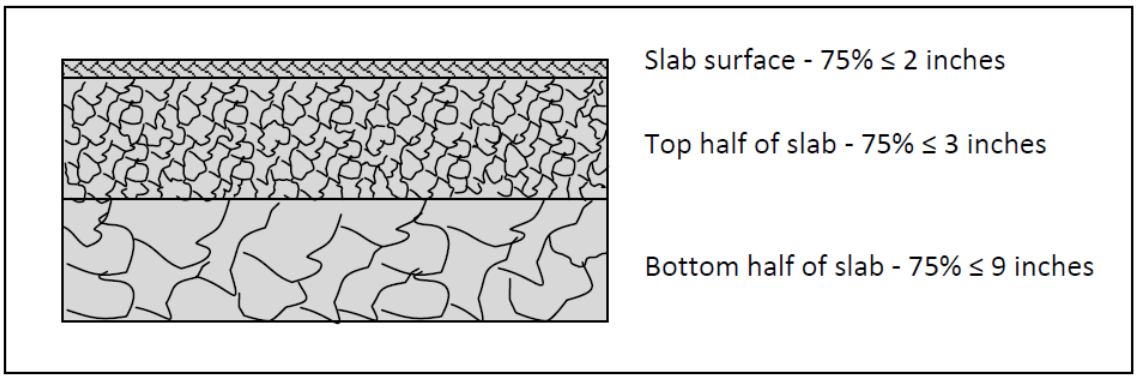

Figure 5 Rubblized particle size requirements as per WisDOT standard specifications

Recently, Battaglia and Paye (2011) investigated premature distress formation in Wisconsin rubblized pavements by analyzing design parameters, soil properties, historic distress levels, and several additional factors for 19 good- and poor-performing pavements. It was recommended that major cracks and distressed joints in the existing PCC pavement be repaired before rubblizing/HMA overlay to prevent reflection cracking. According to Battaglia and Paye (2011), joints with heavy deterioration, spalling, and/or evidence of pumping following the PCI rating system guidelines are candidates for repair. Recommended PCC joint repair and test rolling guidelines were also proposed by Battaglia and Paye (2011) as shown in Figure 6.

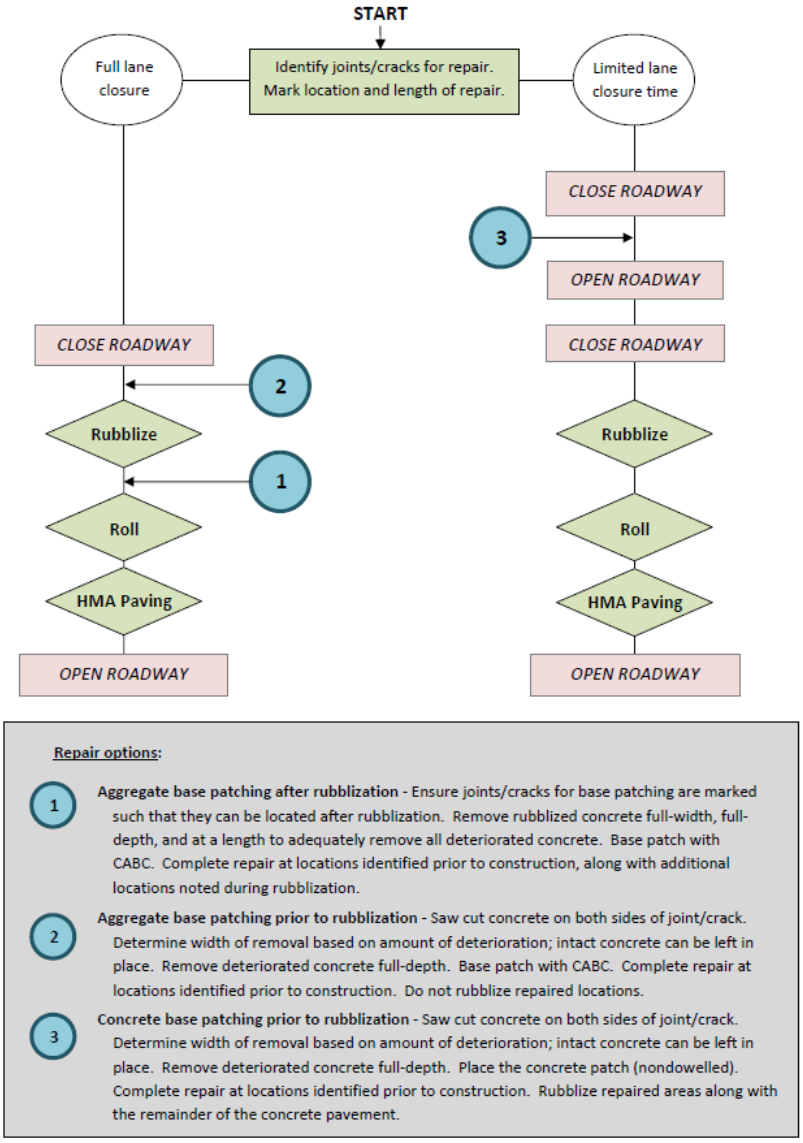

Figure 6 PCC joint and crack repair options and construction sequence for rubblization projects (Battaglia and Paye 2011)

Reflective Crack Relief Interlayer

A reflective cracking relief interlayer is a low stiffness pavement layer that relieves the stresses and strains built up in an underlying pavement layers by dissipating energy during vertical and horizontal deformations. Typically these layers are less than 2 inches and do not increase the structural value of the pavement, but they are designed to reduce

reflective cracking. Various interlayer techniques have been developed and successfully used under the right application.

These include a stress absorption membrane interlayer (SAMI), a rubber modified asphalt interlayer, a soft asphalt interlayer, geosynthetics (paving fabrics), and Strata®.

Strata is a reflective crack relief interlayer system promoted by SEM Materials, Inc. (now Road Science LLC, a Division of ArrMaz Custom Chemicals) that protects the existing pavement structure from water damage and delays reflective cracks . According to Road Science LLC, the Strata system has several advantages: it significantly delays reflective cracking longer than paving fabrics and HMA overlays; it provides an impermeable interlayer to protect pavement structure from moisture damage; it provides a highly fatigue resistant material; it uses readily available aggregates and it lengthens pavement service life; ease of mixing, placement, and compaction through the use of conventional HMA paving equipment and standard construction methods; and savings in construction time and facilitating easy maintenance of pavement (Von Quintus et al. 2009).

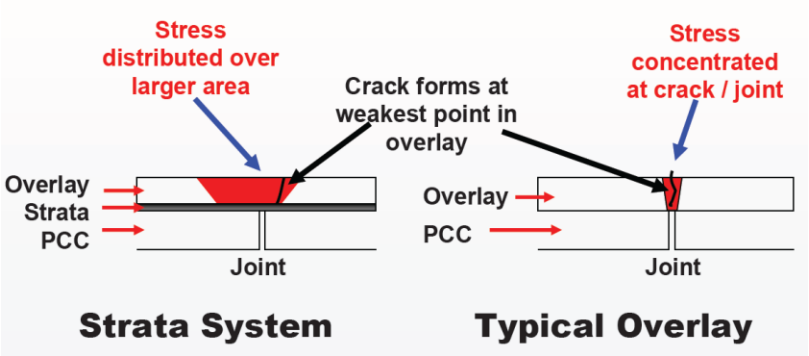

Figure 7 Strata system

The Strata system was applied on an Iowa highway project in northeast Iowa on State Highway 9 near Decorah (Winnesheik County) in 2001 and was studied by Wagoner et al.

(2006) using field observations, laboratory testing as well as finite element analysis. The IA-9 project consisted of three sections (a control section, section 1 and section 3 with a nominal overlay thickness of approximately 6.3 in.) in a two-lane pavement with an average of 3800 vehicles per day and 18 percent truck traffic. The Strata system was placed above the leveling course in sections 1 and 3 and annual surveys were conducted to monitor the development of reflective cracks. The study concluded that the Strata layer was beneficial in retarding reflective cracking. Figure 8 illustrates the reflective cracking performance of the Strata sections 1 and 3 as well as the control section.

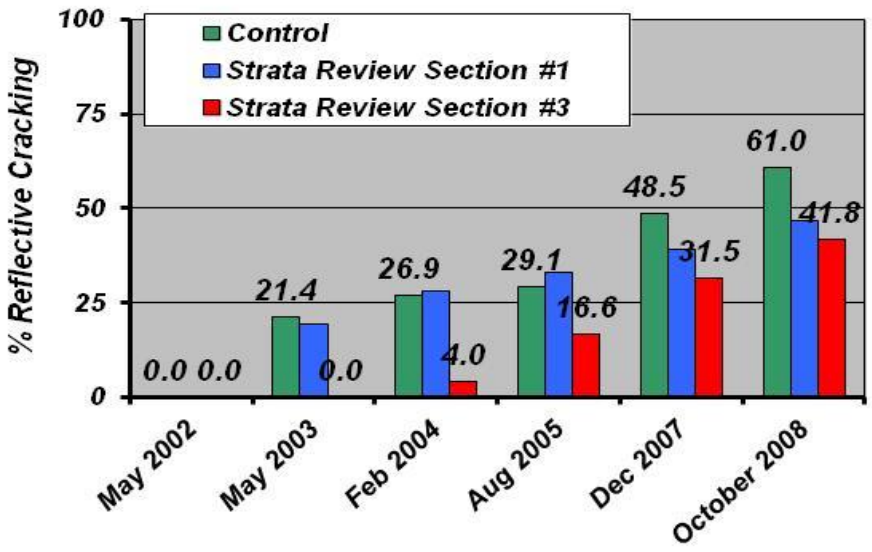

Figure 8 Reflective cracking performance of Strata sections 1 and 3 and the control section

Cold In-Place Recycling (CIPR)/Full-Depth Reclamation (FDR)

Full-depth reclamation (FDR) and cold in-place recycling (CIR) are viable strategies to remove cracks in HMA pavements. Cold In-Place Recycling (CIR) involves cold milling the existing HMA surface; mixing the cold milled materials with emulsified asphalt or other modifiers to improve the properties of original HMA mix; screeding, spreading and

compacting the recycled mixture in one continuous operation (see Figure 9). The *NCHRP Synthesis 421: Recycling and Reclamation of Asphalt Pavements Using In-Place Methods*, defines FDR as a process that pulverizes an existing asphalt pavement along with one or more inches of the underlying base or subgrade; the pulverized material is mixed with or without additional binders, additives, or water, and then placed, graded, and compacted to provide an improved base layer for placement of surface layers (see Figure 10).

FDR works well when the pavement layer has a minimal total thickness (e.g. 6 inches) while CIR works well when only the top 3 to 4 inches need to be repaired. Although FDR has potential cost-saving, engineering, and other sustainability benefits, and is considered a viable rehabilitation alternative, information reported in the literature is scant with respect to the material properties of FDR to facilitate the structural design of pavements incorporating FDR-stabilized base materials. In fact, there is some controversy on how to characterize the FDR layer stabilized with asphalt emulsions (Thompson et al. 2009).

Schram (2011) recently reported on Iowa's experience with CIPR and FDR techniques. Over a 5-year total, there have been 53 CIPR projects (foam and emulsion) in Iowa costing $118 Million and totaling 1,800 lane-miles. On the other hand, FDR (using fly ash stabilization) over a 5-year total amounts to only 3 projects costing $8.6 Million and totaling 100 lane-miles. The IHRB Project TR-502, *Evaluation of Long-Term Field Performance of Cold In-Place Recycled Roads: Field and Laboratory Testing*, studied the performance of CIR in Iowa projects extensively. The study concluded that a CIR layer effectively acts as a stress relieving layer to mitigate reflective cracking.

Figure 9 Cold In-Place Recycling (CIR or CIPR) (Source: FHWA)

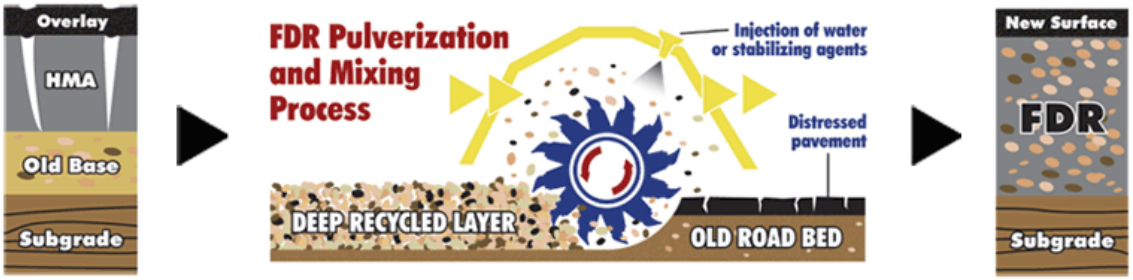

Figure 10 Full-Depth Reclamation (FDR) (Source: American Road Reclaimers)

Although all these techniques have been successfully used with recommendations for further investigation and expanded use in Iowa, they still continue to be used modestly due to lack of proper technical guidance. While limited performance data is available for many of the existing and newer methods and products (including the proprietary ones), the performance data available for other reflective cracking mitigation techniques have not been examined or documented from the perspective of providing technical guidance on the appropriate use of various pre-overlay techniques for different situations. This need to provide practical guidance to owners, industry, and practitioners regarding proper project

selection, design, and quality control of reflective crack mitigation techniques forms the basis of this proposed research.

Von Quintus et al. (2009) reviewed products and processes that have been used to mitigate reflective cracks in rigid and flexible airport pavements. Decision trees providing guidance to select the appropriate mitigation treatment method for the site and in place pavement condition were developed (see Figure 11 and Figure 12). Similar decision trees would be greatly beneficial to Iowa design engineers when selecting a reflective cracking mitigation strategy for a particular project.

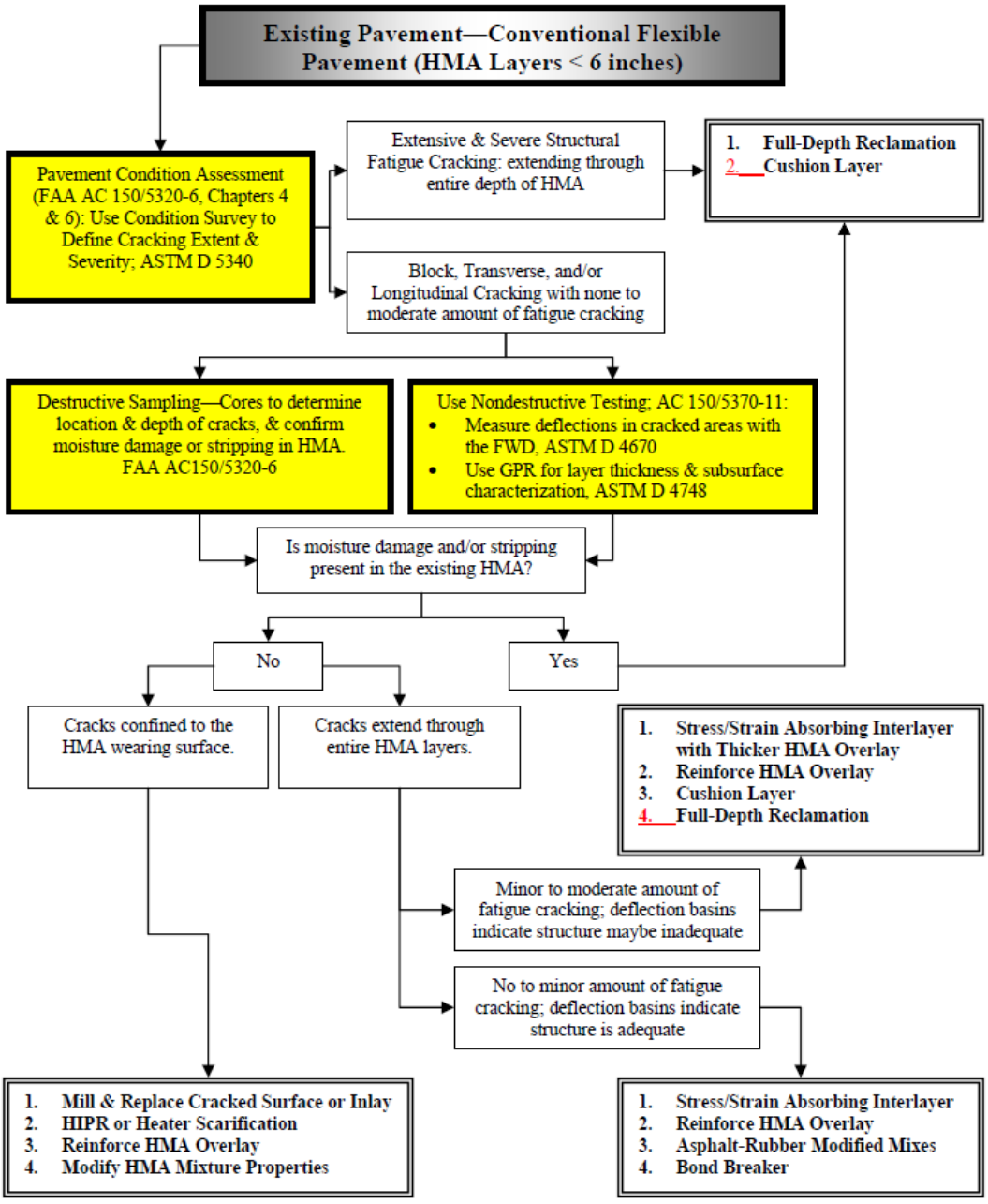

Figure 11 Decision tree for providing guidance reflective cracking mitigation in HMA overlays of existing conventional flexible airport pavements (Von Quintus et al. 2009)

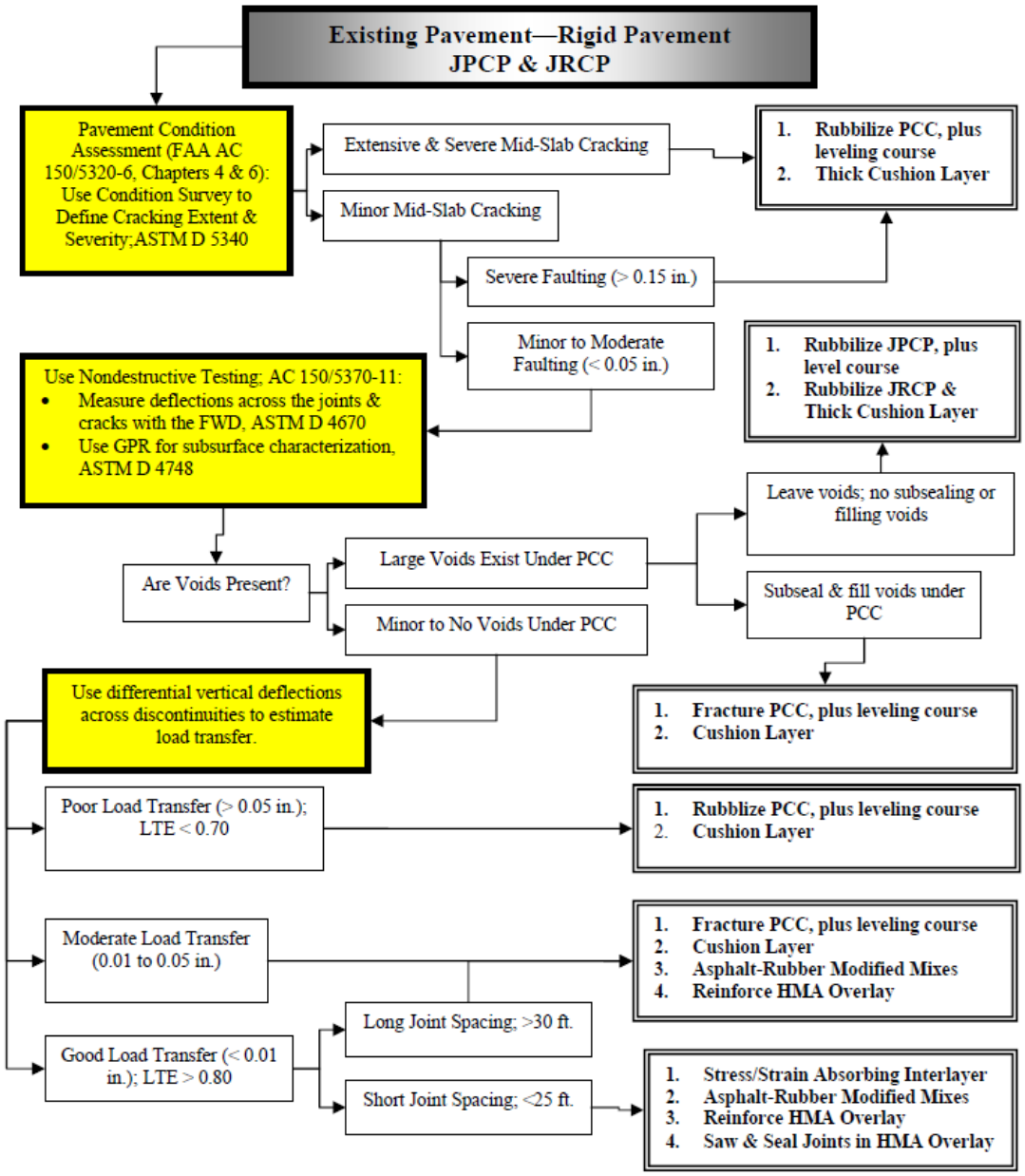

Figure 12 Decision tree for providing guidance reflective cracking mitigation in HMA overlays of existing conventional rigid airport pavements (Von Quintus et al. 2009)

2.3 Causes and Mechanism of Longitudinal Joint Cracking

The premature deterioration of longitudinal joint occurs in the form of cracking and/or raveling. The distresses are caused by relatively low density and surface irregularity at the joints. A density gradient exists across a typical longitudinal joint. The density gradient is

mainly caused by the low density at the unconfined edge when the first lane (also called the cold lane) is paved and a relatively high density at the confined edge, when the adjacent lane (also called the hot lane) is paved. In addition, more rapid cooling of the HMA mix occurring near the unconfined edge of the cold lane can easily result in relatively low roller compaction efficiency and lower density. Therefore, it is not uncommon to encounter low densities at the joint, which are significantly lower than those in the mat away from the joint. Traffic load may also accelerate the development of longitudinal joint cracking. Once the residual stress under traffic loading are higher than the existing tensile strength, the construction joint splits apart (Kandhal et al., 2002).

Typically, a crack can develop at the longitudinal joint in very short time, sometimes as soon as one year in service (Figure 13). The crack becomes wider and more ragged every year. This phenomenon is more prevalent and severe in areas with very cold climatic conditions, which may also cause transverse shrinkage cracking in HMA pavements. It is also not uncommon for the HMA pavement to develop raveling on one side of the longitudinal joint. Usually, raveling occurs on the side of the cold lane, which usually has lower density at the unconfined edge. Raveling can also occur on the side of the hot lane due to inadequate compaction, which may result from bridging action if the edge of the cold lane is higher than the hot lane due to excessive material. Both cracking and raveling allow intrusion of water into the pavement system, which weakens the foundation of the pavement requiring extensive repairs. Longitudinal joints often look coarse in surface texture. This can happen primarily for two reasons: segregation and handwork. Because longitudinal joints occur at the edge of the paver screed and auger system and the HMA has been moved beyond the end of the auger, there is a potential of HMA being segregated. Typically, HMA from the

hot lane, which overlaps the cold lane, is luted back onto the hot side of the joint. This handwork usually results in a coarse surface texture (Kandhal and Mallick, 2007).

Figure 13 Survey on a project one year after construction (IA-13)

2.4 Types of Longitudinal Joint Construction Method

A longitudinal joint is the interface between two adjacent and parallel HMA mats. Several types of longitudinal joint construction techniques are generally used in Iowa. These include butt joint, notched wedge joint, joint with heat treatment and joint with edge restraint.

The traditional method for constructing a longitudinal joint in Iowa is the butt joint (see Figure 14). The challenge of butt joint is to achieve adequate density on the unconfined edge of the cold lane. This is because at the time of its compaction, there is no lateral confinement to compact against the cold lane, therefore, the unconfined edge is able to move laterally when the downward compaction force is applied and reduce its density. Pinching the butt joint by adding extra material for compaction near to the joint is a way to achieve better butt joint density. Kandhal et al., (2002) reported that rolling from the hot lane (6 inches) away from the joint during the first pass can provide a better butt joint confinement. They found that this technique would push the material between the roller and joint towards the

joint during the initial roller pass, which crowds and pinches the mix at the butt joint area and produce a higher density (see Figure 15 a). However, this method may make the longitudinal joint appears slightly humped as shown in Figure 15 (b). Researchers in Canada reported that warm mix asphalt (WMA) may produce a tighter butt joint than hot mix asphalt (HMA) as the temperature differential for continuous paving is reduced (Hughes et al., 2009). The heat loss associated with WMA is less, which makes it more versatile during various weather conditions. However, they also remarked that although the WMA is very workable, it has a stiffer makeup than the corresponding HMA and thus held the mix together to reduce gradation segregation.

Temperature is always considered as the key in longitudinal joint construction. It is generally believed that higher temperature can help increase compaction of the material at the joint and improve the bond between the cold mat and hot mat. The basic premise of the joint heat treatment is that after the cold lane is placed, the joint area can be pre-heated just prior to placement of the hot lane, make the constituent asphalt binder in cold lane more viscous and stickier. Daniel (2006) reported that the infrared heat can penetrate the existing pavement and heat the mixture within 25 to 50 mm of joint up to the temperatures of about 60 ^{o}C during the initial compaction by the first roller. The temperature would drop down to about 50 ^{o}C when the finishing roller passes. Results of the field trials in Kentucky, Tennessee and New Hampshire have all reported that the use of joint heater can effectively reduce permeability/increase density, increase the indirect tensile (IDT) strength of the asphalt mixtures and provide a smooth joint (Fleckenstein, et.al. 2002, Huang and Shu, 2010, Daniel, 2006).

The notched wedge joint was originally developed in Michigan and has been gradually considered as a good option for longitudinal joints construction. As shown in Figure 16, an extended joint taper placed on the first paved lane can help reduce joint air voids and the notches should be at least as deep as the nominal maximum aggregate size (NMAS) of the mix and the taper is usually spread out over about 0.3 m (1 ft.). The hot lane should overlap the cold lane notch by about 12.5 to 25 mm (0.5 to 1 inch) to ensure enough material at the notch for adequate compaction. Buchanan (2000) compared the notched-wedge joint technique with the conventional butt joint technique in Colorado, Indiana, Alabama, Wisconsin, and Maryland. The evaluation consisted of comparing the in-place densities obtained through pavement cores at five locations across the longitudinal joint of the pavement: at the centerline and at 150 mm (6 in.) and 450 mm (18 in.) on either side of the centerline. The results of the study indicate that the notched-wedge joint can be successfully used to increase the in-place density at the longitudinal joint. Some decrease in the in-place density was observed at the 150-mm (6-in.) location in the hot lane when the notched-wedge joint was used. However, some construction-related problems for the notched wedge joint were observed and pointed out by Fleckenstein et.al. (2002). These include maintaining the upper notch during compaction, raveling on the lower portion of the wedge and aggregate pickup by the small wedge roller. Bulging of the notch was also observed in some cases. It appears that the wedge is restraining the mix from pushing sideways during compaction is the cause of the bulging.

A new longitudinal joint construction technique using the milling operation to form edge restraints for both the cold lane and hot lane is applied in Iowa. In this method, one old lane is milled and the adjacent traffic lane can make a natural vertical edge face for the first

new paving lane during compaction. After the first paving lane becomes cold, the adjacent traffic lane would be milled and the first paving lane can serve as the edge restraint for the second paving lane. Since the confinement can be formed during both the paving process of the cold and hot lanes, it is believed that this technique would result in a better joint performance.

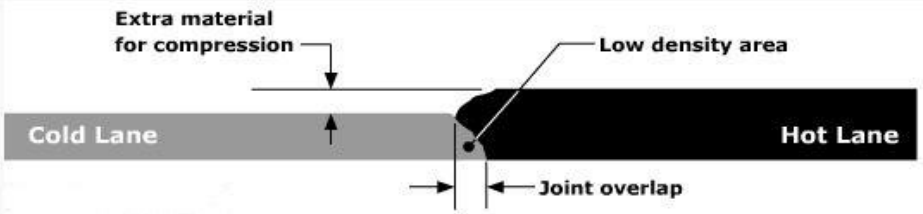

Figure 14 Butt longitudinal joint schematic (WSDOT, 2012)

Figure 15 Butt joint construction with hot pinch (pictured on US-61)

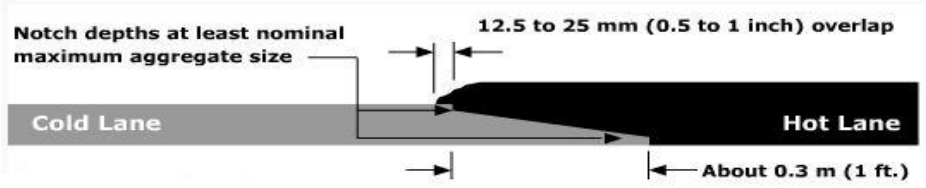

Figure 16 Notched wedge joint schematic (WSDOT, 2012)

2.5 References

Al-Qadi, I., Buttlar, W. G., and Baek, J. 2009. Cost-effectiveness and performance of overlay systems in Illinois. Volume 2: Guidelines for Interlayer System Selection Decision

When Used in HMA Overlays. Illinois Center for Transportation Series No. 09-045, University of Illinois at Urbana-Champaign.

Bandaru, R. 2010. Cost effective prevention of reflective cracking in composite Pavements. M.S. Thesis. Department of Civil and Environmental Engineering, Louisiana State University, Baton Rouge, LA.

Buchanan, M.S. 2000. Evaluation of notched-wedge longitudinal joint construction" *Transportation Research Record 1712: 50-57.*

Battaglia, I. and Paye, B. (2011). *Investigation of early distress in Wisconsin rubblized pavements*. WisDOT Research Report WI-02-11, Wisconsin Department of Transportation, Madison, WI.

Bennert, T. 2010. *Flexible overlays for rigid pavements*. Final Report. Department of Civil and Environmental Engineering, Center for Advanced Infrastructure and Transportation (CAIT), Rutgers, The State University, Piscataway, NJ.

Ceylan, H., Mathews, R., Kota, T., Gopalakrishnan, K., and Coree, B. J. 2005. *Rehabilitation of concrete pavements utilizing rubblization and crack and seat methods*. Final Report, IHRB Project TR-473, Institute for Transportation, Iowa State University, Ames, Iowa, December 2005.

Ceylan, H., Gopalakrishnan, K., and Kim, S. 2008. *Performance evaluation of rubblized pavements in Iowa.* Final Report, IHRB Project TR-550, Institute for Transportation, Iowa State University, Ames, Iowa, April 2008.

Chen, D. and C. Jahren. 2007. *Evaluation of long-term field performance of cold in-place recycled roads: Field and Laboratory Testing*. Final Report, IHRB Project TR-502, Institute for Transportation, Iowa State University, Ames, Iowa.

Daniel, J.S. 2006. Use of an infrared joint heater to improve longitudinal joint performance in hot mix asphalt pavements. *Journal of Performance of Constructed Facilities, 20(2), pp. 167 – 175.*

Drake, E.B. 1988. Pavement Rehabilitation by Breaking and Seating Existing Portland Cement Concrete Pavement Prior to Bituminous Concrete Overlays. *Presented at the 1988 Annual Meeting of the Transportation Research Board.*

Eckrose, R.A., and W. E. Poston, Jr. 1982. Asphalt Overlays on Cracked and Seated concrete Pavements. Information Series 83, National Asphalt Pavement Association.

Fleckenstein, L.J., Allen, D. and Schultz, D. 2002. *Compaction at the longitudinal construction joint in asphalt pavements*. Kentucky Research Center, Report No.KYSPR-00-208.

Hughes, T., Davidson, J.K. and Cormier, A. 2009. Performance of Warm Mix Technology in the Province of New Brunswick" *Proceedings of 54th Conference, Canadian Technical Asphalt Association.*

Huang, B.S., and Shu, X. 2010. *Evaluation of longitudinal joints of HMA pavements in Tennessee*. Tennessee Department of Transportation, Project No. RES1304.

Jansen, J. 2006. Rubblization vs. crack and seat. *Presented at 2006 Great Iowa Asphalt Conference, Iowa.*

Kandhal, P.S., Ramirez, T.L. and Ingram, P.M. 2002. *Evaluation of Eight Longitudinal Joint Construction Techniques for Asphalt Pavements in Pennsylvania*. NCAT Report No. 02-03.

Kandhal, P.S. and Mallick, R.B. 2007. Evaluation of various longitudinal joint construction techniques for asphalt airfield pavements. *Presented at 2007 FAA Worldwide Airport Technology Transfer Conference, New Jersey, USA.*

Ksaibati, K., Miley, W., and Armaghani, J. 1999. Rubblization of concrete pavements. *Transportation Research Record* 1684. TRB, National Research Council, Washington, DC., pp.165-171.

Loria-Salazar, L. G. 2008. Reflective Cracking of Flexible Pavements: Literature Review, Analysis Models, and Testing Methods. Department of Civil Engineering, University of Nevada, Reno.

Mukhtar, M. and Dempsey, B. 1996. *Interlayer Stress Absorbing Composite (ISAC) for Mitigating Reflection Cracking in Asphalt Concrete Overlays*. Project IHR-533, Report No. UILU-ENG-96-2006, Illinois Cooperative Highway Research Program, Illinois Department of Transportation.

National Asphalt Pavement Association (NAPA).1994. Guidelines for Use of HMA Overlays to Rehabilitate PCC Pavements. Information Series 117.

PCS (Pavement Consultancy Services). 1991. *Guidelines and Methodologies for the rehabilitation of Rigid Highway Pavements Using Asphalt Concrete Overlays*. Engineering Report prepared by NAPA and SAPAE, Maryland.

Roberts, L. F., Kandhal, S., P., Brown, E., R., Lee, D., H., T. W. Kennedy. 1996. Hot Mix Asphalt Materials, Mixture Design, and Construction. NAPA Research and Education Foundation, Lanham, Maryland.

Schram, S. 2011. Iowa's Best Practices for Full Depth Reclamation and Cold In-Place Recycling. *Proceedings of the 15th Annual TERRA Pavement Conference*, University of Minnesota, St. Paul, MN.

Sharpe, G.W., M. Anderson, and R.C. Deen. 1987. *Breaking and Seating of Rigid Pavements*. UKTRP Report 87-26.

Thompson, M., R. 1999. Hot mix asphalt overlay design concepts for rubblized Portland cement concrete pavements. *Transportation Research Record* 1684, 147-155.

Thompson, M.R., Garcia, L., and Carpenter, S.H. (2009). Cold in-Place recycling and full-depth recycling with asphalt products. Illinois Center for Transportation, Research Report ICT-09-036. http://ict.illinois.edu/Publications/report%20files/FHWA-ICT-09-036.pdf. Accessed November 5, 2009.

Tymkowicz, S. and DeVries, S. 1995. *Iowa development of Rubblized pavement base - Mills County*. HR- 315. Iowa Department of Transportation, Ames, Iowa.

Von Quintus, H. L., Rao, C., Mallela, J., and Aho, B. 2007. *Guidance, parameters, and recommendations for rubblized pavements*. Final Report WHRP 06-13. Wisconsin Department of Transportation, Madison, Wisconsin.

Von Quintus, H. L., Mallela, J., Weiss, W., Shen, S. and Lytton, R. L. 2009. *Techniques for mitigation of reflective Cracks*. Final Report AAPTP 05-04. Airfield Asphalt Pavement Technology Program, Auburn University, AL.

Wagoner, M. P., Buttlar, W. G., Paulino, G. H., and Blankenship, P. 2006. Laboratory testing suite for characterization of asphalt concrete mixtures obtained from Field Cores, *Journal of the Association of Asphalt Paving Technologists*, pp. 815-851.

Washington State Department of Transportation (WSDOT) (2010). Factors effecting HMA permeability. Retrieved from http://pavementinteractive.org/index.php?title=WSDOT:Factors_Effecting_HMA_Permeability

CHAPTER 3. ASSESSMENT OF COMPOSITE PAVEMENT PERFORMANCE BY SURVIVAL ANALYSIS

A paper presented in the Transportation Research Board conference 2014, Washington, D.C. The paper is also under the review in the ASCE Journal of Transportation Engineering currently.

Authors: Can Chen, R. Christopher Williams, Mervyn G. Marasinghe, Jeramy C. Ashlock, Omar Smadi, Scott Schram

3.1 Abstract

The main objective of this paper is to identify the most appropriate rehabilitation method for composite pavements and to evaluate the influence of different factors for the reflective crack development in composite pavement by survival analysis.

Four composite pavement rehabilitation methods are evaluated: mill and fill, overlay, heater scarification, and rubblization. Survival analysis is used to evaluate the four methods using three pavement performance indicators: reflective cracking, International Roughness Index (IRI), and Pavement Condition Index (PCI). It is found that rubblization can significantly retard reflective cracking development compared with the other three methods. No significant difference for PCI is seen in the survival analysis for the four rehabilitation methods. Heater scarification shows the lowest survival probability for both reflective cracking and IRI, while overlay results in the poorest overall pavement condition based on PCI.

Parametric survival models are employed to further analyze the factors influencing reflective cracking for the four composite pavement rehabilitation methods. Traffic level is found to not be a significant factor for reflective cracking development. An increase in overlay thickness can significantly delay the propagation of reflective cracking for all

treatment methods (not include rubblization). Soil types in rubblization pavement sites are assessed, and no close relationship is found between rubblized pavement performance and subgrade soil condition.

Keywords

Reflective cracking; survival analysis; pavement management system; performance monitoring

3.2 Background

Composite pavements comprise a large portion of the paved highway surfaces in the U.S. Midwest. They are most commonly the result of concrete pavement rehabilitation. The traditional pavement design approach has been to construct full-depth Portland cement concrete (PCC) pavements. When they begin to fail years later, they are overlaid with 2-6 inches of hot-mix of asphalt (HMA). Composite pavements, compared to traditional flexible or rigid pavements, can be a more cost-effective alternative because they may provide better levels of performance, both structurally and functionally.

A composite pavement structure may develop different types of distresses throughout its service life. Several research studies have reported that reflective cracking is the most common type of distress in composite pavements (Von Quintus, et al., 2010; Lytton, et al., 2010). When HMA overlays are placed over jointed or severely cracked PCC or HMA pavements, reflective cracks rapidly develop through the HMA overlay extending to its surface. Although reflective cracking does not generally reduce the structural capacity of a pavement, subsequent ingress of moisture and the effects of the natural environment and traffic can result in premature distresses and early failure of the pavement. The basic

mechanisms leading to the occurrence of reflective cracks are horizontal and differential vertical movements between the original pavement and HMA overlay. Commonly attributed factors that cause movements at joints and cracks in the base pavement are low temperature (freeze-thaw cycles), wheel loading, and curling of concrete pavement slabs. Among these factors, temperature-induced cracking is considered to be a critical one. Bennert and Maher (2007) completed a national survey on the reflective cracking experience in different states highway agencies (SHAs). A majority of the SHAs (22 out of 28 participating states) reported that reflective cracking was observed within the first four years of HMA placement, while seven SHAs reported reflective cracking in the first two years. The survey results indicate that growth rates of reflective cracking could be very high during the early composite pavement service life.

Four widely used rehabilitation strategies for composite pavements are evaluated in this study. These include:

- HMA overlay,
- HMA mill & fill,
- Heater scarification (SCR), and
- PCC rubblization

The HMA overlays are simply the process of installing a new layer of HMA directly over an existing pavement structure. They generally provide good performance over flexible pavements, but their performance for composite pavements may depend on the extent of reflective cracking. Surface recycling has been reported by Federal Highway Administration (FHWA) to be successful in removing pre-existing reflective cracks prior to an HMA overlay (FHWA, 2002). Mill & fill and SCR are generally used in Iowa as two common ways to

remove cracks from old HMA overlays. In the SCR method, the pulverized pavement materials are used along with recycling agents in the re-paving process, while in the mill & fill process, the contractors typically use new asphalt concrete mix for repaving after milling. Therefore, the SCR treatment can be considered to result in "reclaimed asphalt pavement (RAP)". Rubblization is defined as "breaking the existing concrete pavement into smaller fragments and overlaying it with HMA". The extent of rubblization depends on the thickness and size of the broken concrete slab, and the intent of rubblization is to produce a structurally sound base which prevents reflective cracking by eliminating the existing pavement distresses and joints.

A suitable data source to monitor the pavement performance and reflective cracking conditions following the four pavement rehabilitation strategies is state transportation agencies' pavement management information system (PMIS). In Iowa, this information is contained in the Iowa PMIS database and the Iowa Pavement Management Program (IPMP). The Iowa PMIS database contains data about pavement condition, construction history, and materials from 1991 until the present for all of the state maintained roads (Interstate, National, and State highways). The IPMP database is a pavement condition information database for paved roads on the local system (counties and cities) in Iowa. Both databases include continuous testing and subsequent quantification that provides 100% coverage length of the network and roadway surface, as opposed to a smaller sample of representative sections. The surface distress information in both databases is based on the same technology and is collected in the same manner utilizing the same contractor. Therefore, information in the two databases is comparable with each other and they follow the same method for pavement performance surveys, as defined in the "Distress Identification Manual for the Long-Term

Pavement Performance (LTPP) Project" (Smadi and Maze, 1998). The literature has shown that reflective cracking can be rated in the same manner as transverse cracking for composite pavements (Lytton et al., 2010; Zhou, et al., 2010). In this study, only transverse cracks are considered as reflective cracks for each test section in the PMIS and IPMP databases.

The performance data are collected on a two-year cycle in the state. The Iowa Department of Transportation (Iowa DOT) has a contract with an independent contractor to collect the required information for their pavement management system. Roughness (IRI) is collected in each wheel path utilizing two laser sensors (South Dakota Profiler-SDP: Class I profiling device according to ASTM E950) behind the two front wheels. These two sensors measure the longitudinal profile of the road to determine IRI. The same laser sensors are used to determine the faulting between slabs in concrete pavements as well. In the back of the mobile device, two scanning lasers are used to measure the transverse profile of the pavement surface (14 feet wide) to determine rutting for asphalt pavements. Because of the wide footprint of the two lasers, the edge drop-off can also be determined. Surface distresses such as cracking and patching are collected using a 2D camera that captures images of the pavement surface which are later analyzed using image analysis and pattern recognition to determine the type of cracking and severity. Once all of the surface distresses are collected, the Iowa DOT calculates a pavement condition index (PCI) for each homogenous pavement management section. The sections can range between 0.5 miles to over 5 miles in length based on the original construction and rehabilitation history. The PCI calculation is based on pavement type (concrete, asphalt, and composite) and system (Interstate and other).

3.3 Survival Analysis

In order to track the growth rate of reflective cracking and composite pavement performance over time for each type of rehabilitation method, survival analysis, or more generally, time-to-event analysis is used. The term survival analysis s(t) is used predominately in biomedical and healthcare sciences where the interest is in observing the time to death of either patients or of laboratory animals. The engineering sciences have also contributed to the development of survival analysis, wherein it is referred to as "reliability analysis" or "failure time analysis". Early survival analysis application relies more on empirical methods than statistical procedures. The survival analysis approach simply considers the cumulative traffic as a surrogate for pavement life (Vepa et al., 1996). In recent years, more complicated survival analysis applications were conducted using comprehensive pavement databases and advanced statistical software (e.g. JMP, SAS, Minitab). Bausano, et al. (2004) compared the reliability of four different types of HMA pavement maintenance treatments using the Michigan PMIS database. Dong and Huang (2012) employed the survival function to evaluate four types of HMA pavement cracks using the LTPP database. Survival analysis focusing on the hazard function was applied by Yang (2009) to estimate the duration of pavement life in Florida. Survival data are generally described and modeled in terms of two related functions, namely the survival function s(t), and hazard function h(t), which are inter-related (see Eq.1). If either s(t) or h(t) is known, the other can be determined. Consequently, either can be the basis of statistical analysis (Hosmer and Lemeshow, 1998). The survival function s(t) measures the survival probability beyond a time t, while h(t) measures the failure probability occurring in the next instant, given survival to time t.

$$h(t) = -\frac{d}{dt}\left[\log s(t)\right] \qquad \text{Eq.(1)}$$

In this paper, three pavement performance indicators are applied, including reflective cracking, International Roughness Index (IRI), and Pavement Condition Index (PCI), with the emphasis on reflective cracking. From the perspective of statistics, the specific difference related to survival analysis arises largely from the fact that survival data should be divided into censored and uncensored groups. Censoring occurs when an observation is incomplete due to some random cause. In the area of pavement performance, censored data occurs if a pavement project performs well during the observation time and reaches the planned end of study, or is lost to follow up, while uncensored data (failure) is obtained when a pavement project is distressed beyond the performance indicators' threshold values during the observation period.

3.4 Objective and Scope

The objective of the present study is to compare the survival time of four different composite pavement rehabilitation methods and to evaluate the influence of different factors for the reflective cracking development in composite pavement by parametric survival analysis.

3.5 Threshold Value

Threshold values are used to delineate the censored and uncensored data. The threshold values are defined as the lowest acceptable pavement condition level before pavement preservation treatments become necessary. A lower threshold value is used for local county roads, as they usually have much lower traffic and longer service lives. Although there do not appear to be universal threshold values for the pavement maintenance or rehabilitation treatments, the IRI and PCI values shown in Table 1 are generally used for

pavements in fair or poor condition (Papagiannakis, et al., 2009). The range and description for each performance index are also provided. To quantify the severity and extent of reflective cracking, a simple reflective crack index (RCI) formula is developed, as shown in Table 3. The index is based upon the extent of reflective cracking and a weighting function of the crack severity to account for the condition of reflective cracking. Taking three levels of crack severity into consideration, the RCI provides a distress condition rather than merely evaluating only one facet of the cracking, such as the total crack length or amount of cracks per kilometer or mile. In Figure 17, a typical ascending trend for RCI can be observed. The RCI value is represented by the shaded area whose height is measured on the right axis. On the left axis, reflective crack numbers in the low severity level develop quickly at the beginning, and start to decrease later as more cracks move into medium and high severity levels in later service life. In other words, the RCI can represent not only changes in the total number of cracks, but also show the influence and dimensions of their severity. The threshold value for RCI is set to 420 by considering common concrete joint spacing (4.5 to 6.1 m) and the possible number of reflective cracks per kilometer. Based upon this threshold value, at least 420 low severity, 140 medium severity, or 70 high severity cracks are allowed per kilometer before triggering the threshold. This threshold is similar to those recommended by other highway agencies for reflective or transverse cracking. The threshold value used in the pavement health track analysis tool is 1500 ft/mi for primary and secondary roads, and Wisconsin calls for remedial action if more than 25 cracks per 100-meter section are found (Titus-Glover et al., 2010; Scott et al., 2011).

Table 3 Summary of Three Performance Indicators

Pavement Condition Index	Range	Trigger	Description
Reflective crack index (RCI)	0 to inf.	420 (primary road) 390 (county road)	RCI=Low ×1+Med×3+$High$×6; Low, Med., High: represent numbers of low, medium and high severity reflective cracks per km.
International Roughness Index (IRI)	(0 to inf.) in./mi	125 in/mi (primary road) 120 in/mi (county road)	Irregularities in pavement surface. Higher values indicate a rougher road. Measured in m/km and converted to in/mi in this study.
Pavement Condition Index (PCI)	0 to 100	64 (primary road) 68 (county road)	Composite index including cracking, ride quality & rutting. Lower values indicate poorer road conditions.

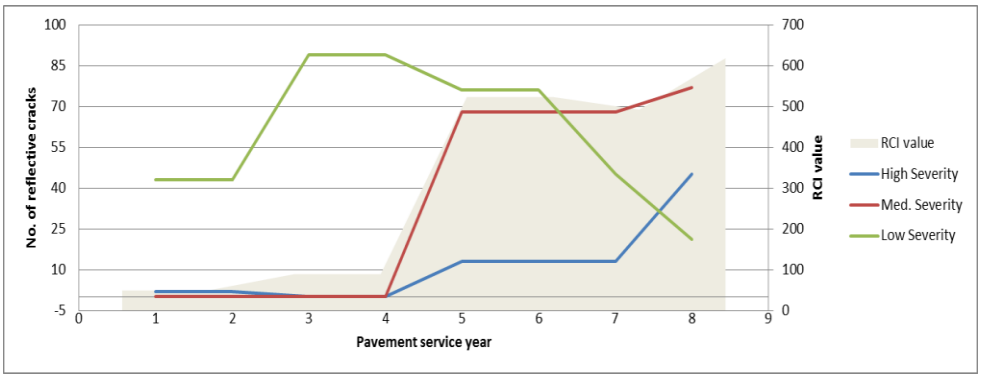

Figure 17 A typical relationship for reflective cracking and RCI

(IA-12 highway project, STP-12-(16)-2C-97)

3.6 Data Preparation

This study utilizes pavement performance, traffic, and pavement structural data from the Iowa PMIS and IPMP databases and represents pavements constructed from 1998 through 2008. The performance of these projects was tracked until the latest 2012 pavement performance survey representing 154 projects. These include 42 projects for mill and fill treatment, 32 projects for heater scarification, 51 HMA overlay projects, and 30 rubblization projects. The life distribution and survival platform is used in the data analysis via JMP software (SAS, 2012).

3.7 Discussion of Results

1 Kaplan-Meier Estimator

In statistical analyses, it is prudent to perform a univariate analysis before proceeding to more complicated models. In survival analysis, it is highly recommended to look at the Kaplan-Meier curves for all the categorical predictors. This will provide insight into the shape of the survival function for each group and provide an idea of whether or not the groups are proportional. The Kaplan-Meier estimator is a nonparametric maximum-likelihood estimator of the survival function. It incorporates information from all of the observations available, both uncensored and censored, by considering the survival function at any point in time as a series of steps defined by the observed and censored times (Hosmer and Lemeshow, 1998). Figure 18 compares the Kaplan-Meier estimate for the four different rehabilitation methods on reflective cracking. The largest time length shown is 14 years, which represents the maximum survival time from 1998 to 2012. As expected, the survival function decreases as the pavement age increases. The survival function for the rubblization treatment lies completely above the other three treatments and it has a long right-tail with

relatively constant survival probability. The survival functions for the HMA overlay is quite close to the mill & fill treatment in early service life and it gradually drops down and touches the curve for the SCR treatment, suggesting that the HMA overlay has an unfavorable survival experience in later service life with respect to reflective cracking. The estimated survivorship function for the SCR treatment lies completely below that of the other three treatments, giving it the poorest reflective cracking performance. A typical pattern for most of the treatments is: relatively early rapid descending survivor function with a gradually longer tail in the later service life. This is the result of a number of early failures and a few projects with survival near the maximum follow-up time. Table 4 summarizes the median survival time, as well as other percentiles, which are determined by linear interpolation. The median value, or 50^{th} survival percentile, is considered to be the service life that a pavement can sustain before failure (Gharaibeh and Darter, 2003). The test statistics are further examined to determine whether or not the four types of treatments are significantly different in their survival functions for reflective cracking. Log-rank and Wilcoxon tests are two simple comparison methods used in JMP software. In general, the Log-rank test places more emphasis on the differences in the curves at later survival time values, while the Wilcoxon test places more weight on early survival time values. The results show that the rubblization treatment can significantly reduce the occurrence of reflective cracking compared to the other three treatment methods, which is the cause of the high probabilities of test separation in the Log-Rank and Wilcoxon test analyses for reflective cracking.

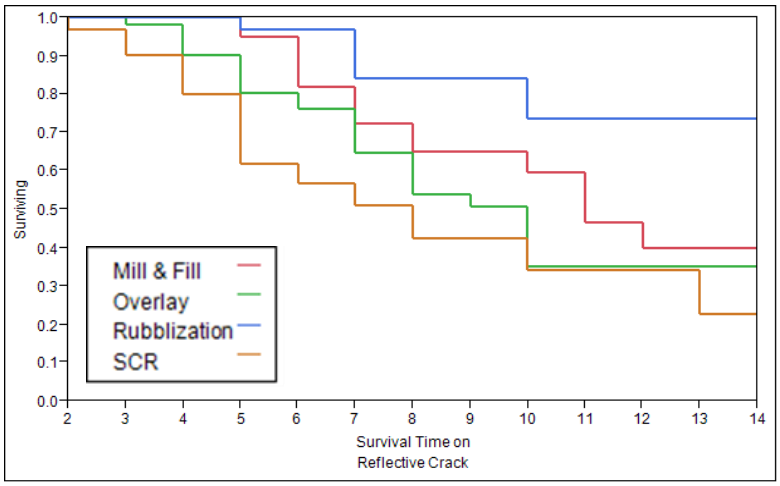

Figure 18 Kaplan-Meier estimator curves for reflective cracking treatments

Table 4 Percentile summaries and test between groups for reflective cracking

Group	Number failed	Number censored	70% Percentile (yrs)	Median (yrs)	30% Percentile (yrs)
Mill & Fill	16	26	7.6	10.7	N/A
SCR	17	14	4.5	6.8	11.5
Overlay	26	25	6.5	9.0	N/A
Rubblization	5	25	N/A	N/A	N/A
Combined	64	90	6.5	9.5	N/A
Test	**ChiSquare**	**DF**	**Prob>Chisq**		
Log-Rank	16.3	3	0.0010*		
Wilcoxon	19.5	3	0.0002*		

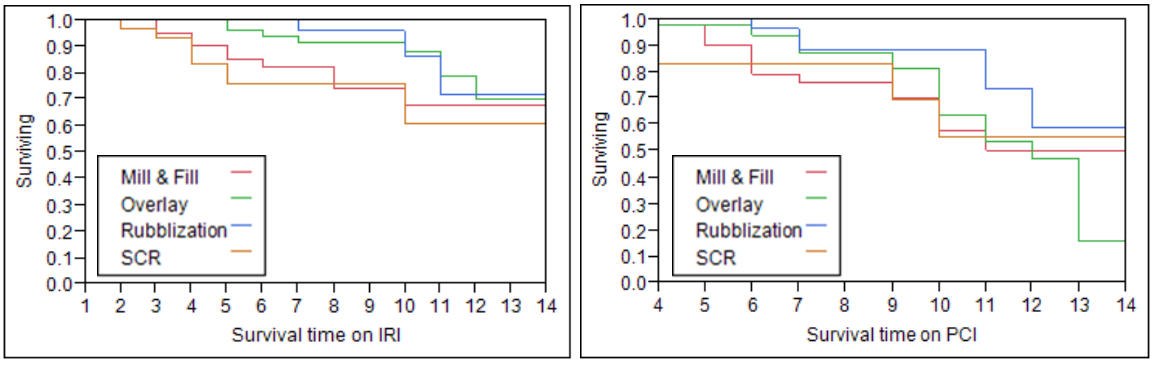

(a) (b)

Figure 19 Kaplan-Meier estimator curves for IRI (a) and PCI (b)

Table 5 Tests between groups for IRI and PCI

Test between groups for IRI			**Test between groups for PCI**	
Test	Prob>Chisq		Test	Prob>Chisq
Log-Rank	0.0252*		Log-Rank	0.391
Wilcoxon	0.0034*		Wilcoxon	0.184

Figure 19 illustrates the relationship between survival function and pavement service life based on IRI and PCI. As can be seen, all four different rehabilitation methods are effective in preserving the smoothness of composite pavements within 14 years of service life before dropping to 50% survival probability. Relatively lower survival functions for IRI are observed for the mill & fill and SCR treatments compared to the HMA overlay and rubblization treatments.

Table 5 also indicates a significant difference in IRI performance for the four treatments, especially in early survival time as indicated by the Wilcoxon test. This result is counter to previous studies which concluded that milling the existing HMA surface prior to overlay is effective in keeping the overlay smoother (Wiser, 2011). This discrepancy could be due to differences in the initial IRI conditions of pavements at the time of treatment applications. Unlike pavement distress data which typically indicates an absence of cracks soon after rehabilitation, the roughness-based initial IRI values usually vary greatly from 50 in/mile to 100 in/mile. Use of RAP in the mill & fill and SCR treatments may also be a cause for the higher initial IRI values.

Table 5 shows that there is no significant statistical difference among the survival curves for PCI. As PCI is a composite index which gives a more comprehensive indicator of pavement condition, roads treated with only HMA overlay treatment are observed to have the poorest PCI conditions in later service life (Figure 19 b).

2 Model Fitting

The Kaplan-Meier estimator is used for describing the survival experience of a population, and does not require any specific distributional assumptions about the shape of the survival function. The parametric model for survival analysis is considered next, as it may provide more information on the relationship between variables and the survival function. A best-fit model can also provide higher accuracy for predicting the survival of a given subject. Several parametric models are commonly used, including the Exponential, Weibull, Lognormal and Logistic models. The most obvious distinguishing feature between the models is in the shape of the hazard function they assume the data to follow. The Weibull distribution model is appropriate when the hazard is always increasing or decreasing. In the Exponential model, the hazard is assumed to be constant over time, while the hazard function of the Logistic model follows an "S-curve" behavior. The Log-Normal model is preferable when the hazard rises to a peak before decreasing.

A few diagnostic methods are available for the model fitness comparison, including both numerical and graphical approaches. Ideally, the selected model should reflect the physical pavement cracking and performance development patterns. In this study, Akaike's information criterion (AIC) is applied, as it performs well for both univariate and multivariable survival analyses. AIC as suggested by Akaike (1974) is an estimate of the relative distance between the unknown true-likelihood function of the data and the fitted likelihood function of the model. A lower AIC value means that a model is considered to be closer to the truth. For the general case, the method to estimate the AIC value is shown in Eq. 2, where L is the maximum likelihood function, and k is the number of free parameters in the chosen model.

$$\text{Minimize } AIC = 2k - 2\ln(L) \qquad \text{Eq.(2)}$$

Table 6 Model comparisons by the AIC values

AIC value	Lognormal	Weibull	Logistic	Exponetial
Reflective Crack	448.10	450.68	457.07	507.21
PCI	330.69	329.35	330.79	384.39
IRI	284.32	285.10	285.27	300.28

For the univariate analysis performed herein, three parameters are considered; pavement service life, intercept, and error. As shown in Table 6, the Lognormal distribution appears to be the best-suited for modeling the general trend of reflective cracking and IRI, while the Weibull model provides the best fit for the PCI. Further, the modeled hazard and survival functions are presented in Figure 20 and Figure 21 for the three pavement condition indicators. The hazard function typically provides clearer information about the underlying mechanism of failure than the survival function. Figure 20 (a) shows that there is early reflective cracking failure risk for the SCR and overlay treatments, followed by a constant hazard in the later stages of pavement life, while mill & fill has an accelerated failure rate in later service life. The hazard rate for rubblization treated pavements, on the other hand, is lowest and gradually increases during a natural failure process. In Figure 210 (b), higher hazard rates for IRI are clearly exhibited in the early life for the SCR and mill & fill treatments. As discussed previously, this could be attributed to the initial IRI condition. To test this hypothesis, the initial IRI values for all of the 155 pavement projects were sorted and displayed in the boxplot of Figure 22. As indicated by the mean lines, the average initial IRI values for mill & fill and SCR treatments are slightly higher than the other two methods. Except for a few outliers, most of the roughness-based initial IRI values vary from 45 to 90

in/mile between the lower and upper quartiles. Subgrade condition, roadway speed requirement, asphalt concrete mix type, construction quality, and surveying time can all affect the initial IRI value. Although PCI has similar survival curves to those of reflective cracking and IRI, the hazard rate for PCI follows the Weibull distribution as shown in Figure 21. The general trend is monotonically increasing, and thus the overall performance deterioration accelerates in later pavement service life for all four treatments.

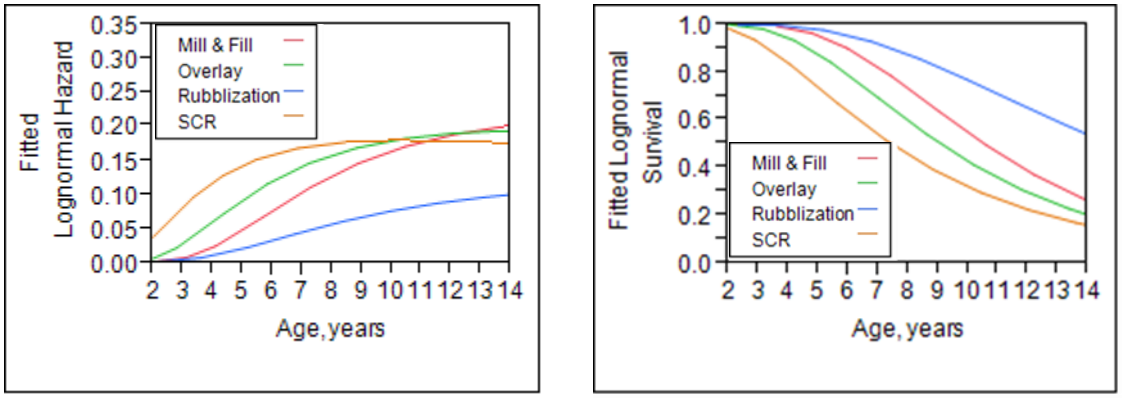

(a)

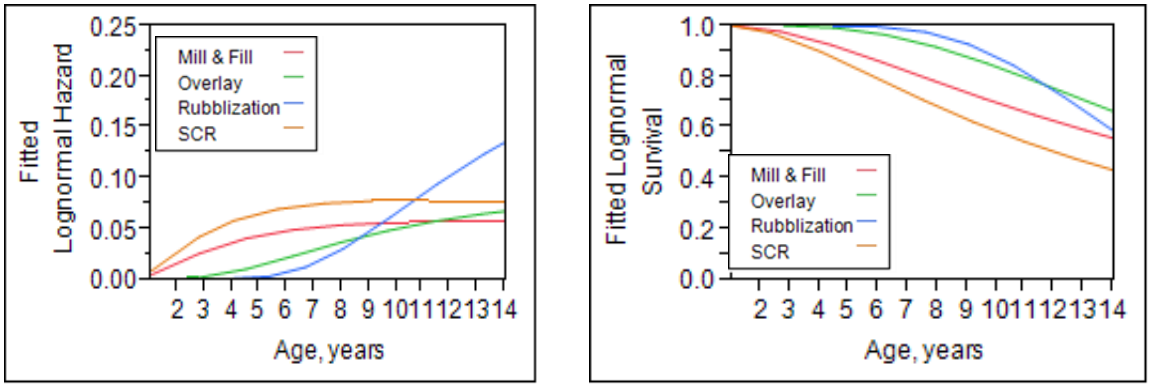

(b)

Figure 20 Summary of model fitted hazard and survival functions for reflective cracking (a), IRI (b)

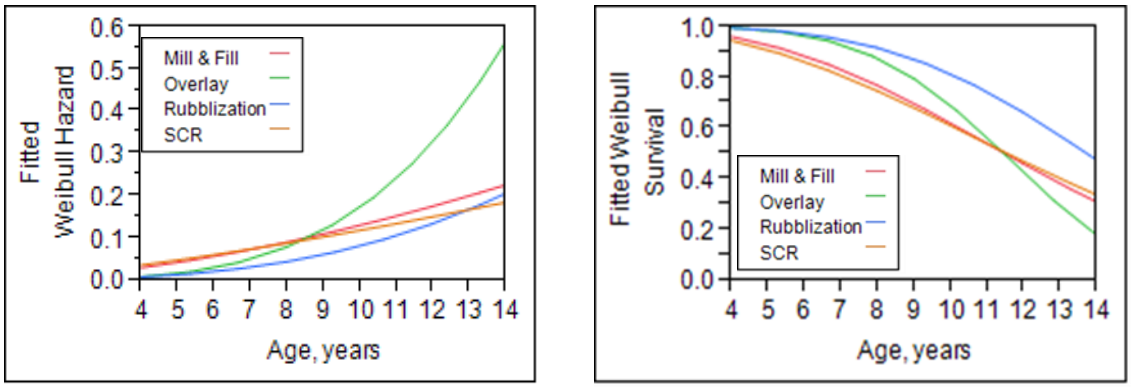

Figure 21 Summary of model fitted hazard and survival functions for PCI

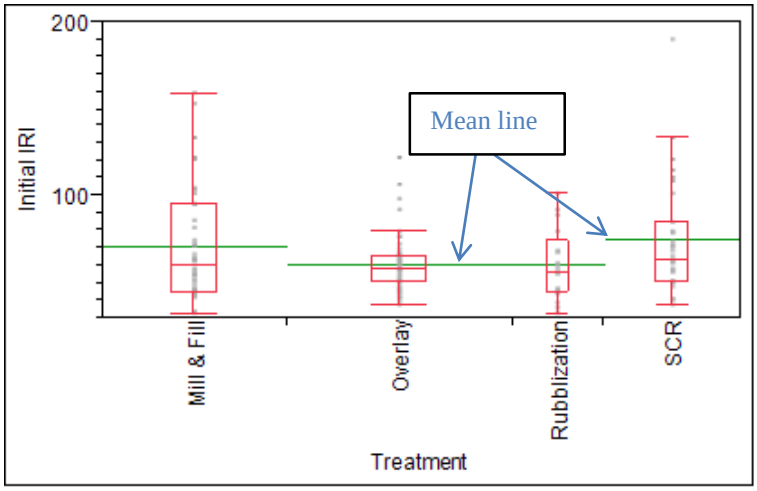

Figure 22 Initial IRI values for the four treatments

3 Multivariate Survival Analyses

In the field, various factors or covariates can influence pavement performance. The relationship between reflective cracking and a number of such factors are evaluated here. In addition to pavement performance, the traffic, pavement thickness and pre-treatment condition are also collected in the PMIS database. Average daily traffic (ADT) information is recorded in the database and used to represent the general traffic level for each project. Multivariable survival analysis using parametric survival models was performed for the four

pavement rehabilitation methods. Table 7 presents the best-fit parametric models for each treatment method via Akaike's information criterion. The selected models may differ from those used in the univariate analysis due to the influence of the additional covariates. The likelihood ratio test results shown in Table 7 determine the significance of each covariate by comparing the log-likelihood from the fitted models. The significance level is 0.05 for this test, and corresponds to a 95% level of confidence. Figure 23 displays the failure function profiler for the four rehabilitation methods. The failure function/probability is one minus the survival function. This profiler can be used to show the failure probability as one of the covariates is varied while the others are held constant by dragging the red dot line in JMP. Observations from Figure 23 are discussed below.

Table 7 Summary of AIC test and likelihood ratio test results

Method	**Fit model**	**Influence factors**	**likelihood ratio test**	
			L-R ChiSquare	Prob>Chisq
Mill &Fill	Weibull	HMA thickness	9.365	0.002*
		Removal thickness	0.316	0.574
		ADT	0.548	0.458
SCR	Lognormal	HMA thickness	9.886	0.002*
		Removal thickness	0.025	0.875
		ADT	0.137	0.711
Overlay	Lognormal	HMA thickness	3.591	0.058
		Pre-condition	0.674	0.412
		ADT	1.346	0.246
Rubblization	Lognormal	Soil type	8.24e-7	0.999
		Concrete thickness	0.408	0.523

Mill & Fill

According to the likelihood ratio tests in Table 7, the most significant factor for the failure probability of reflective cracking is the HMA thickness. The HMA thickness is the overlay thickness for the rehabilitation treatment, and the removal thickness is the milled asphalt concrete depth. In Figure 23 (a), the failure probability drops substantially as the thickness increases. The traffic level is not a significant factor; higher traffic only slightly accelerates the propagation of reflective cracking as shown in the failure probability profile.

Heater Scarification

Similar to mill & fill treatment, the most significant factor for the initiation of reflective cracking is the overlay thickness, as shown in Figure 23 (b). Removing the old HMA layer does not help retard the reflective cracking development. In the figure, pavements even exhibit a lower rate of reflective cracking failure with increasing traffic levels.

HMA Overlay

The overlay treatment does not require removal of the old HMA layer prior to placement of the new overlay during the construction process. Therefore, the pre-overlay pavement condition is involved in the analysis. The pre-condition refers to the old PCI values just before an overlay treatment. It is generally believed that cracks can more easily propagate through HMA overlays from severely cracked old pavements. However, Figure 23 (c) indicates that the pre-condition and failure function are not significantly related, which means that the pre-condition does not affect the reflective cracking in the new overlay. The most important factor for the initiation of reflective cracking is again the overlay thickness, although not significantly.

Rubblization

Three different rubblization types are usually performed. These include full rubblization, modified rubblization, and crack & seat. Concrete pavement thickness and subgrade soil types are considered in the present analysis. Soil types at the project locations were investigated using data from the National Cooperative Soil Survey System. This system provides an interactive digital map for identifying the project locations. The soil data extracted is for the surface to a depth of 60 inches' soil information and the soils around these pavement sections are divided into two groups: high silt-clay and non-high silt-clay. The high silt-clay category refers to terrains reported to have more than 70% very poorly-drained silty clay or clay loam (ASSHTO soil classification: A-6 and A-7 group). Figure 23 (d) shows that this specific categorization of soil type does not influence the survivability of pavements that have been rubblized. Modifying the rubblizing pattern to reduce impact energy and produce larger-sized broken concrete (e.g. modified rubblization and crack & seat) could provide an alternative to compensate for weak and poorly-drained subgrades. Reflective crack performance was also not significantly correlated to the underlying concrete thickness in composite pavement.

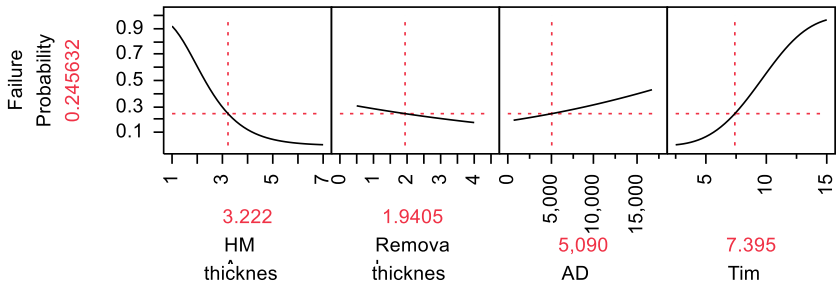

(a)

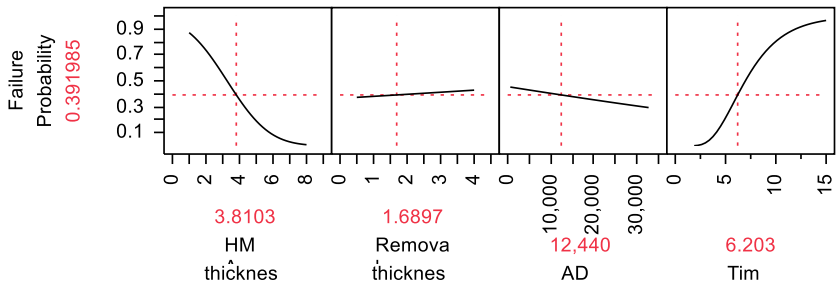

(b)

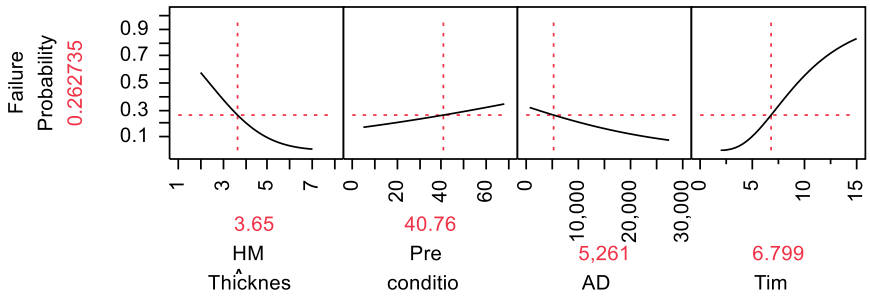

(c)

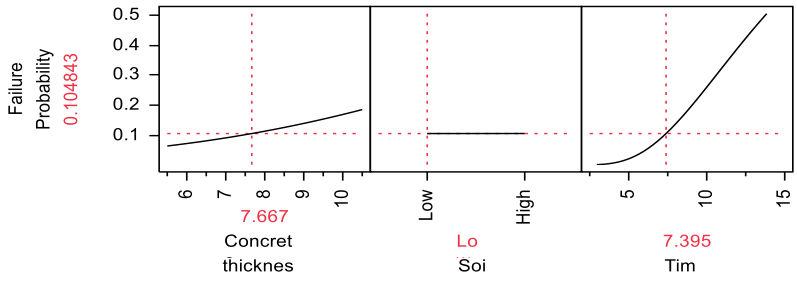

(d)

Figure 23 Influence factors on reflective cracking for Mill & Fill (a), SCR (b), Overlay (c), and Rubblization (d)

3.8 Recommendations and Conclusions

A method for understanding the performance of four pavement rehabilitation methods of traditional composite pavements, such as hot mix asphalt over PCC pavement, was outlined in this paper. A large set of data from in-service pavements was used in survival analyses to evaluate the performance of four different composite pavement rehabilitation

methods. These include mill & fill, HMA overlay, heater scarification and rubblization. Several conclusions are summarized as follows:

- The Kaplan-Meier estimator clearly illustrates that pavement rubblization can significantly retard reflective cracking development in composite pavements compared with the other three methods. The mill and fill treatment also exhibited better performance than HMA overlay in terms of reflective crack mitigation.
- The general trend of the hazard/failure function for reflective cracking follows a Lognormal distribution with an early-time increase followed by a constant or decreasing probability of failure. The corresponding survival function shows a sharp initial drop with a long tail in the later service life.
- No significant differences of PCI are seen in the survival analysis for the four rehabilitation methods. The hazard function for PCI, on the other hand, is best described by the Weibull distribution, which has an accelerated failure-time pattern.
- The SCR method shows the lowest survival probability in terms of reflective cracking and IRI. Higher initial IRI values were found for the SCR and mill & fill treatments in the database. This finally leads to lower IRI survival probabilities for the two treatments.
- Traffic level was not a significant factor for reflective cracking according to the multivariate analysis performed in this study. Higher trafficked roads even demonstrated a lower probability of reflective cracking failure.

- Increasing the new pavement thickness is effective in retarding the propagation of reflective cracking for all four treatments. The removed pavement thickness does not significantly affect the survival probability.
- The literature shows that subgrade soil properties can influence the use of rubblization in the field (Battaglia and Paye, 2011). However, this was not observed for the simple criteria considered in this paper. Modifying the rubblization pattern to compensate for weaker subgrades is commonly performed by practitioners.

Acknowledgements

The authors would like to thank the Iowa Highway Research Board and the Iowa Department of Transportation for the financial and technical support associated with this research project. The authors also recognize and appreciate Mr. Jason Omundson who provided the Iowa PMIS database. Thanks also to Antigo Construction Company for providing logistical support and information for the rubblization projects.

3.9 References

Von Quintus, L.H., Mallela, J., Lytton, L.R. 2010. Techniques for mitigation of reflective cracks. *In FAA Worldwide Airport Technology Transfer Conference*, Atlantic City, NJ.

Lytton, L.R., Tsai, L.F., Lee, S.I., Luo, R., Hu, S., and Zhou, F.J. 2010. *NCHRP report 669: models for predicting reflection cracking of hot-mix asphalt overlay.* National Cooperative Highway Research Program, Washington, D.C.

Bennert, T., and Maher, A. 2007. Evaluation of current state of flexible overlay design for rigid and composite pavements in the United States. *Transportation Research Record*, No.1991, 97-108.

Federal Highway Administration (FHWA). 2002. Pavement recycling guideline for state and local governments participant's reference book. FHWA-SA-98-042, FHWA, U.S. Department of Transportation, Washington, D.C.

Smadi, G.O., and Maze, H.T. 1998. Developing Iowa's statewide pavement management program. *4th International Conference on Managing Pavement*, Durban South Africa.

Zhou, L., Ni, F.J., and Zhao, Y.J. 2010. Evaluation method for transverse cracking in asphalt pavements on freeways. *Transportation Research Record*, No.2153, 97-105.

Vepa, T.S., George, K.P., and Shekharan, R.A. 1996. Prediction of pavement remaining life. *Transportation Research Record*, No.1524, 137-144.

Bausano, J.P., Chatti, K., and Williams, R.C. 2004. Determining life expectancy of preventive maintenance fixes for asphalt-surfaced pavements. *Transportation Research Record*, No.1866, 1-8.

Dong, Q., and Huang, B.S. 2012. Evaluation of influence factors to crack initiation of LTPP resurfaced asphalt pavements using parametric survival analysis. *Journal of Performance of Constructed Facilities* 10.1061/(ASCE)CF.1943-5509.0000409.

Yang, J.D. 2009. Development of effective remaining life prediction models for pavement management at the network level. *Transportation Research Board Conference*, CD-ROM, Washington, D.C.

Hosmer, W.D., and Lemeshow, S. 1998. Applied survival analysis: regression modeling of time to event data. John Wiley & Sons, Inc., USA.

Papagiannakis, A., Gharaibeh, N., Weissmann, J., Andrew, W. 2009. *Pavement Scores Synthesis*. FHWA/TX-09/0-6386-1, Texas Transportation Institute, Texas.

Titus-Glover, L., Fang, X.C., Alam, M., O'Toole, K., and Darter, M. 2010. Pavement health track, remaining service life forecasting models, technical information. Federal Highway Administration Office of Asset Management, Washington, D.C.

Scott, S., Ferragut, T., Syrnick, M., Anderson, S. 2011. NCHRP Report 699: Guidelines for the use of pavement warranties on highway construction projects. National Cooperative Highway Research Program, Washington, D.C.

SAS Institute. 2012. JMP user's guide version 10: Quality and Reliability Methods. SAS Institute Inc., Cary, NC.

Gharaibeh, N.G., and Darter, M.I. 2003. Probabilistic analysis of highway pavement life for Illinois. *Transportation Research Record*, No.1823, 111-120.

Wiser, L. 2011. Performance comparison of pavement rehabilitation strategies. Report No. FHWA-HRT-11-050, Federal Highway Administration, Washington, D.C.

Akaike, H. 1974. A new look at the statistical model identification. *IEEE Transctions on Automatic Control* 19 (6): 716-723.

Battaglia, I.K., and Paye, B. 2011. *Investigation of early distress in Wisconsin rubblized pavements*. Report No. WI-02-11. Wisconsin Department of Transportation.

CHAPTER 4. IN-SITU MODULUS AND PERFORMANCE EVALUATION ON FOUR REFLECTIVE CRACKING MITIGATION TREATMENTS

A paper to be submitted to the Journal of Civil Structural Health Monitoring.

Authors: Can Chen, R. Christopher Williams, Shibin Lin, Jeramy C. Ashlock

4.1 Abstract

To minimize reflective cracking in composite pavements, four treatment methods are commonly used: full rubblization, modified rubblization, crack & seat, and rock interlayer. The study objective is to evaluate the moduli and performance of the four reflective cracking treatments. A total of seventeen pavement sites were tested. In the first four sites, both falling weight deflectometer (FWD) and surface wave method (SWM) tests were conducted for preliminary analyses. The results show that SWM is a viable tool to determine the in-situ pavement modulus with relatively low statistical variation. The SWM gave concrete layer moduli that are in close agreement with FWD moduli on a conventional composite pavement. However, the SWM provided higher moduli for the rubblized concrete layer. This difference could be because SWM only records low strain moduli for subsurface layers while the FWD can measure moduli at high-strain-amplitudes for more "flexible" layers. In addition, the FWD test is found not able to measure the thin rock interlayer moduli. After the preliminary analysis was completed, an additional thirteen pavement sites were tested by the SWM. The results show that the crack & seat treatment method provides the highest moduli, followed by the modified rubblization treatment. The full rubblization and the rock interlayer methods give similar, but lower moduli.

Pavement performance surveys were also conducted during the field study. In general, none of the pavement sites had rutting problems. The conventional composite pavement site

has the largest amount of reflective cracking. A moderate amount of reflective cracking was observed for the two pavement sites with full rubblization. Pavements with the rock interlayer and modified rubblization treatments had much less reflective cracking. It is recommended that the modified rubblization and rock interlayer strategies be used for reflective cracking mitigation.

Keywords

Reflective cracking; Surface wave method; falling weight deflectometer; Rubblization

4.2 Background

Composite pavements comprise a large portion of the paved highway surfaces in the state of Iowa and throughout the U.S. Midwest. They are mostly the result of concrete pavement rehabilitation. The traditional pavement design approach has been used to construct thick full-depth Portland cement concrete (PCC) pavements. When they begin to fail years later, they are overlaid with 2-6 inches of hot-mix of asphalt (HMA). Composite pavements, compared to traditional flexible or rigid pavements, can be a more cost-effective alternative because they may provide better levels of performance, both structurally and functionally. However, this type of pavement usually leads to reflective cracking at relatively rapid rates due to the horizontal and vertical movements in the underlying concrete slabs. The commonly attributed factors that cause movements at joints and cracks in the base PCC layer include low temperatures, wheel loads, freeze-thaw cycles, and shrinkage of the PCC and cement-treated base (Von Quintus, et al., 2010). To minimize reflective cracking, four treatment methods have been widely used including full rubblization, modified rubblization, crack & seat, and rock inner layers.

Both the rubblization and crack-and-seat methods covert an existing rigid concrete layer into a “flexible” base by breaking concrete slabs into smaller pieces. These treatments thereby reduce the effective slab length and minimize its horizontal movement from thermal expansion and contraction. The sizes of pieces broken by full rubblization are usually much smaller than the crack & seat technique. However, experience has shown that a smaller broken slab size does not always mean a better performance due to the poor subgrade condition, lack of aggregate base, and the use of thin concrete pavements (Jansen, 2006). One way to compensate for a weak subgrade is to modify the full rubblizing pattern to produce larger fracture pieces which could maintain more of the existing concrete pavement’s structural support. The particle size specification and visual description for each treatment type are listed as follows:

- Full rubblization: typical 2” minus particles at surface, 6” - 12” particles at bottom of slab
- Modified rubblization: 12” minus particles on surface, significant surface spalling, surface appearance ranges from smooth to pulverized
- Crack-and-seat: typically 18” to 36” spaced cracks at surface, little to no surface spalling, spider web appearance

Rock interlayer, on the other hand, adds a “flexible” rock layer above the concrete layer to absorb the slab movement energy and distribute the loads from the HMA to the PCC laters. The rock interlayer is generally 1” - 3” thick consisting of ¾” choke stone placed wet through an asphalt paver and then static rolled (APAI, 2012). The rock interlayer is surprisingly strong and durable under construction traffic. It can be directly placed over a

failing PCC pavement for reflective cracking control, or serves as a leveling course for pavement that has received rubblization and crack-and-seat treatments.

4.3 Surface Wave Method

To measure the pavement structural moduli with the four types of treatments, nondestructive FWD and SWM testing were conducted. FWD deflection data were collected using the JILS-20 FWD equipment by applying a step loading sequence of 9-kips at each testing location. Different from the large strain/high deflection measurement by the FWD testing, moduli obtained from the SWM testing are usually in the very low-strain range. The use of SWM for nondestructive testing in pavements is not new, and its field applications have become increasingly popular since the appearance of modern spectral analyzers and powerful microcomputers (e.g. Nazarian 1984, Park et al. 1998, Ryden et al. 2002, Lin and Ashlock 2011, Lin and Ashlock 2014). Surface wave testing in this study was carried out using the multichannel simulation with one receiver (MSOR) testing system developed by Lin and Ashlock (2011, 2014). The set-up of the equipment for testing is shown in Figure 24 (a). To conduct the MOSR surface wave testing, a ball-peen hammer (12 oz) with an attached accelerometer is used as the moving triggered impact source, and the other accelerometer is fixed at zero offset on the asphalt pavement surface. 12 or 24 impacts were conducted for each testing with the first impact offset and the rest impact spacings of 10 or 5 cm (see Figure 24 b). The dispersion data of the tested sites was extracted from the field data using the phase-velocity and intercept-time scanning scheme (Lin and Ashlcok 2014). The frequencies of the dispersion data range from 100 Hz to 5000 Hz, the wavelength of which could cover the rock interlayer thicknesses of interest. Finally, the hybrid genetic-simulated annealing

algorithm (Lin and Ashlock 2014) was used to back-calculate shear-wave velocity profiles for the determination of Young's modulus.

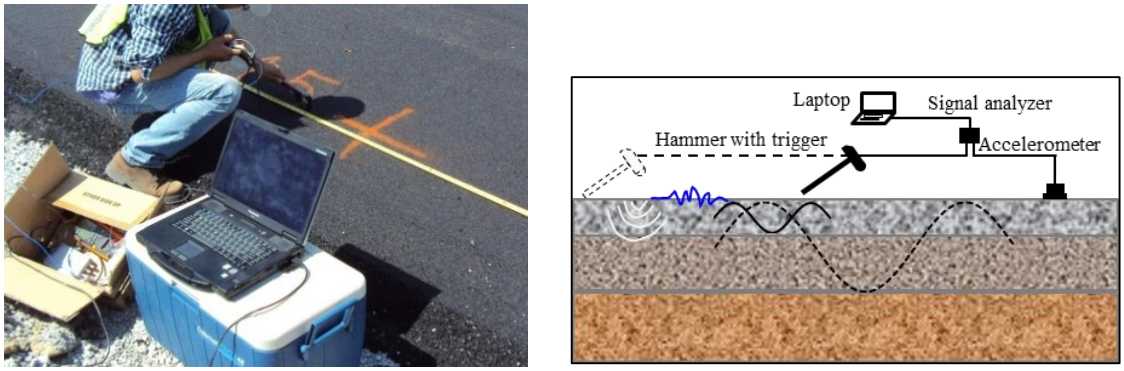

(a) (b)

Figure 24 (a) Set-up of the surface wave equipment; (b) Portable seismic acquisition system

4.4 Field Data Collection and Analysis

A total 17 pavement sites were tested in 2013 and 2014, including one conventional composite pavement (concrete without any treatment), three crack & seat pavements, two full rubblization pavements, three pavement sites with only the rock interlayer treatment, and eight modified rubblization pavements. The modified rubblization comprises a large portion of treatments in Iowa due to the wide-spread silty and clayey soil conditions. A summary of the seventeen projects route numbers, counties, treatment types, and structural information are all listed in Table 8. The route numbers for the sixteen projects are designated as the project names in this study for simplicity. At each pavement site, SWM tests were performed at 3 to 5 locations.

Table 8 A summaries of the seventeen projects

Location	Treatment	Structures	Location	Treatment	Structures
P29 (North), Webster Co.	Modified rubblization	6" HMA + 1" Rock + 6" PCC	L55, Mills Co.	Full Rubblization	7.5" HMA + 6" PCC
P29 (South), Webster Co.	Modified rubblization	6" HMA + 1" Rock + 6" PCC	D16, Black Hawk Co.	Full Rubblization	5" HMA + 7" PCC
D14, Webster Co.	Modified rubblization	4" HMA + 1" Rock + 6" PCC	P43, Webster Co.	No treatment	6" HMA + 8" PCC
P59, Webster Co.	Modified rubblization	4" HMA + 1" Rock + 6" PCC	Y4E, Scott Co.	Rock Interlayer	5" HMA + 1.5" Rock + 6" PCC
G61 (east), Adair Co.	Modified rubblization	4" HMA + 6" PCC	H14,Montgomery Co.	Rock Interlayer	4" HMA + 1.5" Rock + 6" PCC
G61 (west), Adair Co.	Modified rubblization	4" HMA + 6" PCC	J 40 (east), Davis Co.	Rock Interlayer	5" HMA + 2" Rock + 6" PCC
N72, Adair Co.	Modified rubblization	4" HMA + 6" PCC	J 40 (west), Davis Co.	Crack & Seat	5" HMA + 6" PCC
H24, Union Co.	Modified rubblization	6" HMA + 7" PCC	Y48, Scott Co.	Crack & Seat	6" HMA+ 8" PCC
			F63, Guthrie Co.	Crack & Seat	3" HMA + 6" PCC
Note: "Rock" refers to the rock interlayer in this study.					

In the first four pavement sites, moduli values for each pavement layer and underlying subgrade were measured by both the FWD and SWM in a preliminary analysis. It is intended to examine the comparability and accuracy of the measured moduli using the two methods. Temperature adjustment was not considered since the SWM tests were conducted at the same locations soon after the FWD tested and all tests were finished in one day. The moduli values for all four test sections are shown in Figure 25. As can be seen, the SWM moduli range from 4000 to 6000 ksi for the project without treatment (D43 project). A good agreement was obtained between the concrete layer moduli measured by the SWM and FWD

for the conventional composite pavement, with the FWD test results showing slightly higher values in three of the testing locations. Results of FWD subgrade moduli are almost invisible in the figure since the average subgrade modulus is just around 16 ksi. The moduli values for another three modified rubblization sections are around 1500 ksi to 3000 ksi tested by the SWM. The effect of low strain amplitude is evident during the test for the modified rubblization concrete layers. SWM moduli of modified rubblization concrete layers are typically higher than the FWD moduli by a factor of three as shown in Figure 25 (b - d). The difference could be due, in large part, to the larger strains involved in the FWD test. As the strain increases, the moduli generally decrease (Bardet et al. 2000, Ryden and Mooney 2009). The gap on the subgrade modulus is more obvious. The SWM values range from 65 to 200 ksi, while the FWD subgrade moduli are restrained between 6.5 to 20 ksi. The average FWD subgrade modulus for the modified rubblization sections is around 8 ksi, which is lower than that of the control project (P43) without any treatment. According to the minimum strength requirement (10 ksi) for the foundation layers of rubblization pavement specified by the Wisconsin Department of Transportation (DOT), the results seem to indicate that the foundation of Iowa's rubblized sections cannot provide sufficient strength (Wisconsin DOT, 2007). Moreover, it is noticed that the FWD back-calculation is quite insensitive to yield realistic predictions of pavement response for the rock interlayer, and a wide range of moduli can be obtained from 10 to 400 ksi. In this case, the researcher should consider choosing the right initial back-calculation value to decide which output is the most representative one. Finally, the initial back-calculation value is chosen to be 90 ksi as reported by Chen et al (2013) in his study and the final back-calculated moduli are restrained to 40 - 150 ksi for the rock-interlayer. Finally, Figure 26 presents FWD surface deflections in each test section. The

deflection curves match well with the back-calculated moduli that significantly lower and higher deflections were observed for the D43 and P59 projects respectively. Since the P59 project has only 4 inches overlay, a thinner HMA overlay could decrease the moduli values for both asphalt and base layers.

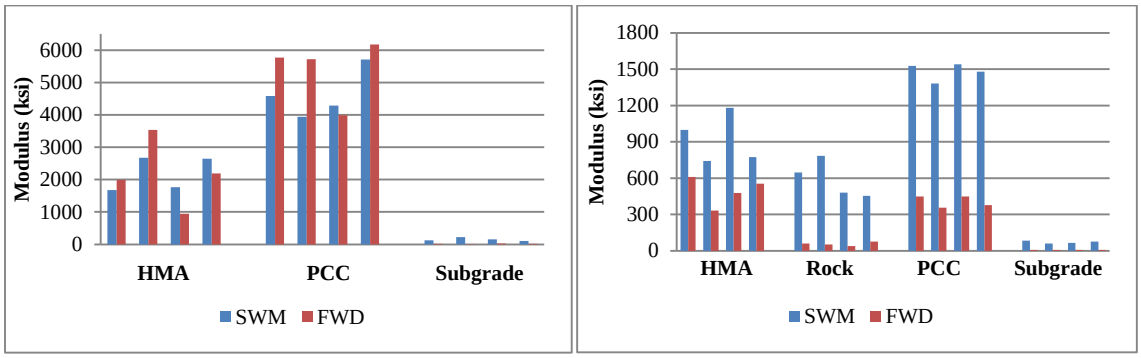

(a) (b)

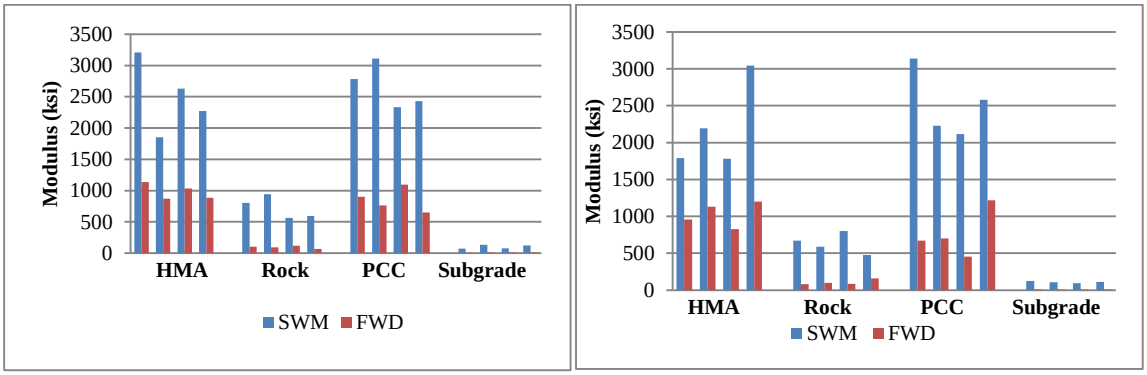

(c) (d)

Figure 25 Comparison of FWD and SWM results for the D43 project (a), P59 project (b), P29-north project (c), and P29-south project (d)

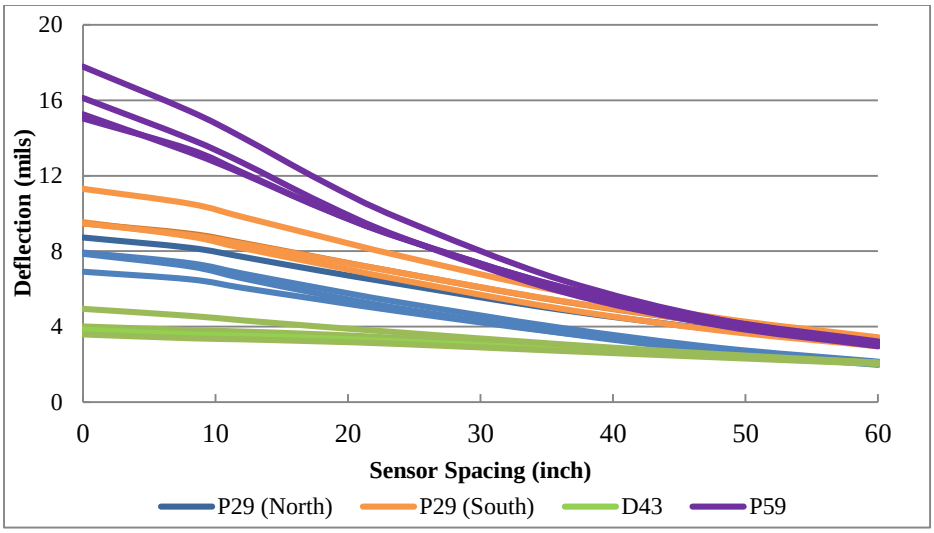

Figure 26 Comparison of FWD deflection difference

The moduli of base concrete layer are expected to decrease as the size of broken concrete pieces become smaller. Figure 27 shows the broken PCC layer and the rock interlayer moduli measured by the SWM in all of the seventeen projects. It is apparent that the moduli for rock interlayer and full rubblized layer are much lower than the modified rubblization and crack & seat treatments. During the full rubblization, the PCC slab is broken into small interconnected pieces that serve as an aggregate base course. It behaves more like a high-strength granular base, with stiffness close to the rock-interlayer formed by dense-graded choke-stone. The results also demonstrate that the Y48 project with the crack & seat treatment has higher moduli. This is because this project has 8 inches thick concrete layer and contains high density steel slags in the HMA layer. The error bar for each project is added indicating standard error. As expected, the error increases as the material get stiffer. In order to evaluate for the methods used above whether the moduli have a statistical difference or not, the all pairs were compared using the Tukey-Kramer HSD method for multiple comparisons. The fact that sample sizes were unequal was taken into account when making

these pairwise comparisons. The HSD test gives more conservative results compared with other multi-comparison tests (Hayter, 1984). The statistical test results in Table 9 prove that the intact PCC layer and crack & seat give both highest modulus values, while the rock interlayer and full rubblization both belong to the lowest group. The modified rubblization sits in the middle level. The results also indicate that the crack & seat treatment generally does not break the concrete slab and it Figure 28 shows a summary of the dispersion curves measured by the SWM. Graphical trend of the dispersion curves also seem to follow well with the statistical ranking results. The frequency range of the dispersion curves from 3000 Hz to 5500 Hz, which mainly depends on the field pavement surface condition.

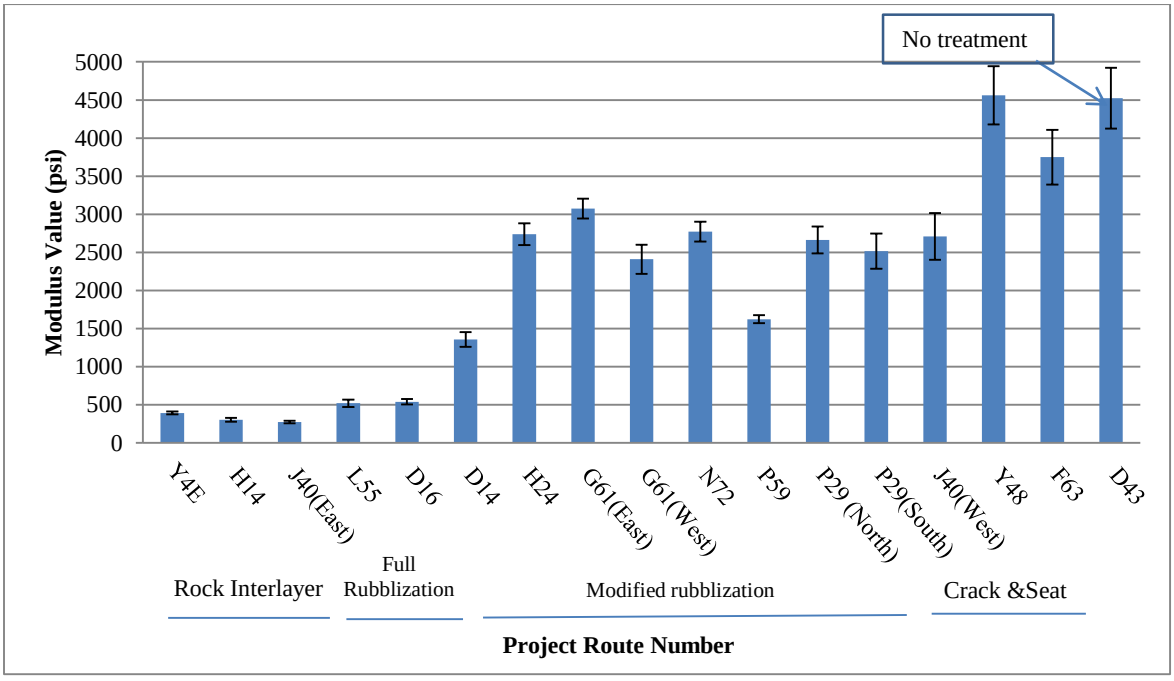

Figure 27 Mean moduli for each project

Table 9 layer moduli by multi-comparison test

Method	Ranking			Mean (ksi)
No treatment	A			4630.4
Crack-and-seat	A			3673.3
Modified rubblization		B		2381.4
Full rubblization			C	529.8
Rock interlayer			C	322.6

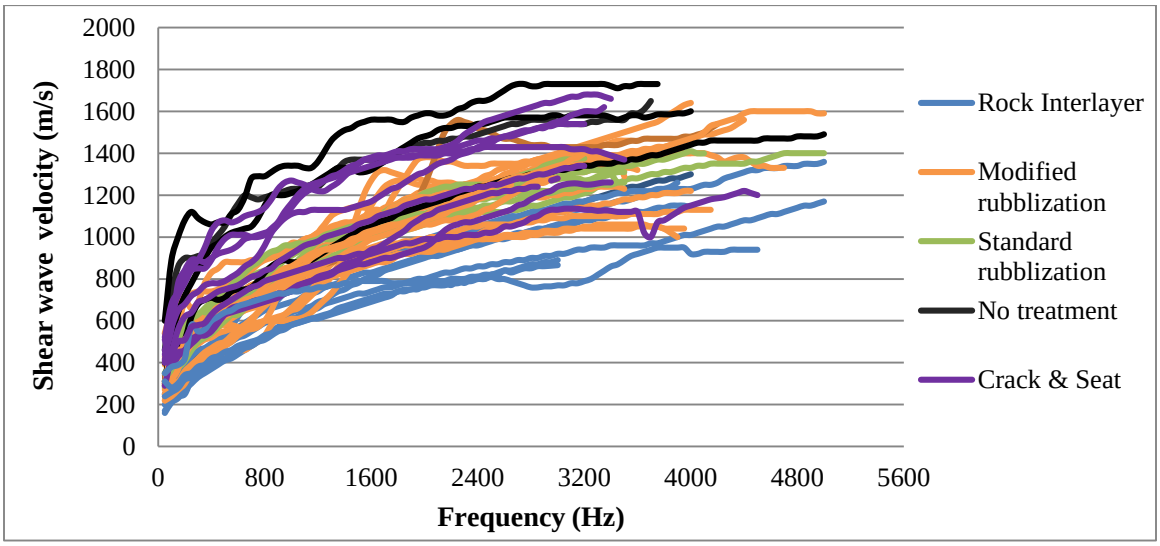

Figure 28 Comparison of dispersion curve for all tested data

Pavement performance surveys were conducted during the field study on a randomly selected 0.4 mi section along each pavement project. It is intended to investigate which treatment could be more effective in minimizing reflective cracking. Considering the common plain concrete pavement joint spacing, transverse cracks in regular and appropriate space interval (around 5-6 m apart) were considered as reflective cracks. The distress survey for reflective cracking follows the method defined in the "Distress Identification Manual for the Long-Term Pavement Performance (LTPP) Project". Reflective cracking survey results are summarized in Table 10 and only sixteen pavement projects were surveyed, and the F63

project were still in construction during the field testing. In general, none of the pavement sites have rutting problems implying that both the rubblized concrete fragments and the choke stone materials could possess enough shear strength for rutting resistance on low traffic-volume county roads. A lack of comparable control pavement sections prevents a firm conclusion about the ability for these treatments in reflective cracking mitigation. However, it is still obvious that pavements received the treatments exhibited good performance (no reflective cracks) within the first 3 years of service time. To quantify the amount of reflective cracking, a simple reflective crack index (RCI) formula is developed (Eq. 1) as proposed by Chen et al (2014).

$$RCI = Low \times 1 + Medium \times 3 + High \times 6 \qquad \text{Eq.3}$$

The index is calculated based upon the extent of reflective cracking and a weighting function of the crack severity to account for the condition of reflective cracking. A larger size reflective cracking has a higher weighting factor. Results show that the P43 project with no treatment exhibits the worst condition/highest RCI value. Both two projects by full rubblization developed moderate amount of reflective cracking, which are not well-performed as expected. The only one comparable section is the two J40 projects. The first part used crack & seat, and due to fears of pavement fails and potential cost, rock interlayer was placed later in the east part. It appears to show that the crack-and seat is less effective than the rock interlayer for reflective cracking control, but not obviously. The rock interlayer and modified rubblization projects seem to have closer pavement performance with slight amount of cracking. However, more projects should be evaluated to support the idea.

Table 10 Summary of pavement project reflective cracking condition

Project	Service Year	Reflective /Transverse cracking Condition	RCI	Project	Service Year	Reflective / Transverse cracking Condition	RCI
P29 (North)	1	No cracks	0	L55	9	4 small, 15 medium, and 3 large size	67
P29 (South)	2	No cracks	0	D16	8	3 small, 16 medium size	51
D14	3	No cracks	0	P42	8	6 small, 4 medium and 19 large size	132
P59	3	No cracks	0	Y4E	2	No cracks	0
G61 (east)	9	15 small, 15 medium, and 5 large size	90	H14	6	1 medium and 4 large size	13
G61 (west)	9	3 small, 5 medium size	18	J 40 (east)	8	6 small, 7 medium and 2 large size	39
N72	9	2 medium and 4 large size	14	J 40 (west)	8	7 small, 8 medium and 4 large size	55
H 24	8	2 small, 4 medium and 2 large size	26	Y48	3	No cracks	0
Severity levels: Low, Medium, High; representing numbers of low, medium and high severity reflective cracks							

Finally, the measured SWM moduli in this study were compared to others' research findings as presented in Table 11. As a new developed method, no literatures were found for the modified rubblization information and it is not involved in the comparison. Alexander (1992) conducted both the SWM and FWD tests on conventional composite pavement where the PCC layer moduli obtained by the SWM were slightly lower the FWD test. The same trend is seen in this study and our measured moduli are very close to his results. Using the FWD for crack & seat concrete modulus testing, Korsgaard et al. (2009) noticed that the moduli change significantly before and after the asphalt overlay, and "between" or "on" the cracks. Their reported values vary greatly from 1200 ksi to 7900 ksi. Gucunski et al (2009)

performed the SWM test directly on highly crushed full rubblized concrete layer. It shows that our SWM moduli values tested on top of a HMA overlay for the full rubblized layer are slightly higher and much less variable compared to Gucunski's results.

Table 11 Comparison of layer moduli values

	Composite pavement (PCC layer)	**Crack-and-Seat PCC**	**Full rubblized PCC**	**Rock interlayer / Granular base**
SWM in this study	3940 -5708 ksi	1118-5323 ksi	441-587 ksi	230 - 430 ksi
SWM	3512-6492 ksi (Alexander, 1992)	N/A	80-400 ksi (Gucunski et al., 2009)	N/A
FWD	6929 – 9426 ksi (Alexander, 1992)	1232-7977 ksi (Korsgaard et al., 2005)	38-122ksi (Ceylan et al., 2008)	43-100 ksi (Chen et al., 2013)

4.5 Recommendations and Conclusions

The moduli and performance of four pavement reflective cracking mitigation treatments- full rubblization, modified rubblization, crack & seat and rock interlayer-were evaluated using nondestructive testing techniques. The conclusions are summarized as follows:

- SWM is a viable method for in situ material characterization of pavement systems. PCC moduli values from the SWM agree well with the FWD result tested on traditional composite pavement.
- The effect of SWM low strain amplitude was evident in the measurement of modified rubblization layer. The SWM moduli are typically two to three times higher than the values predicted by the FWD.
- Larger gap was noticed in the modulus measurement on the thin rock interlayer and subgrade. The extremely lower FWD moduli for the rock interlayer could be due to

(a) thin layer is generally not, (b) large strain measurement on the "flexible" choke stone layer makes the results ten times lower than the SWM results.

- For the four treatment methods, the crack & seat treatment has the highest SWM moduli, followed by the modified rubblization layer. The full rubblization layer and the rock interlayer give similar, but lower moduli.
- Field performance shows that the traditional composite pavement site has the highest amount of reflective cracking followed by the full rubblization projects. Poor subgrade soil properties could be the reason to influence the use of rubblization. Breaking the concrete slabs into a tightly, interlocked material base layer have the potential to damage the subgrade support from the full rubblization. This is believed to be the cause for the unsuccess of full rubblization.
- It is recommended to use the rock interlayer and modified rubblization in the field. However, more projects should be monitored to support the recommendation.

4.6 References

APAI. 2012. *The Iowa asphalt report—the rise of the interlayer*. Published by Asphalt Paving Association of Iowa, summer report.

Alexander, D.R. 1992. *In-situ material characterization for pavement evaluation by the spectral analysis of surface waves method*. technical report-GL-92-10. US army corps of engineers.

Bardet, J. P., Ichii, K., and Lin, C. H. 2000. User's Manual for EERA. Department of Civil Engineering, University of Southern California.

Chen, X.W., Zhang, Z.J., and Lambert, J.R. 2013. Field performance evaluation of stone interlayer pavement in Louisiana. *In Transportation Research Board*, CD-COM, TRB, Washington, D.C.

Chen, C., Williams, R.C., Marasinghe, M.G., Omunderson, J., and Schram, S. 2014. Survival analysis for composite pavement performance in Iowa. *In Transportation Research Board*, CD-COM, TRB, Washington, D.C.

Ceylan, H., Gopalakrishnan, K., and Kim, S. 2008. *Performance evaluation of rubblized pavements in Iowa*. Final Report, IHRB Project TR-550, Institute for Transportation, Iowa State University, Ames, Iowa.

Gucunski, N., Sauber, R., Maher, A. and Rascoe, C. 2009. Modulus of rubblized Portland cement concrete from surface wave testing. *Transportation Research Record*, No.2104, 34-41.

Hayter, A.J. 1984. A proof of the conjecture that the Tukey-Kramer multiple comparisons procedure is conservative. *The annals of Statistics*, Vol.12, No.1, 1-104.

Jansen, J. 2006. Rubblization vs. crack and seat. *presented at 2006 Great Iowa Asphalt Conference*, Iowa.

Korsgaard H.C., Pedersen J.P., Rasmussen M. and Königsfeldt S. 2005. Rehabilitation by cracking and seating of concrete pavement optimized by FWD analysis, *BCRA* 2005.

Lin, S. & Ashlock, J.C. 2011. A study on issues relating to testing of soils and pavements by surface wave methods. *In Proceedings, 38th Annual Review of Progress in Quantitative Nondestructive Evaluation*, Burlington, VT.

Lin, S., and Ashlock, J. C. 2014. Comparison of MASW and MSOR for surface wave testing of pavements. accepted as *Near Surface Geophysics Letter for the SAGEEP 2014 conference*.

Nazarian S. 1984. In situ determination of elastic moduli of soil deposits and pavement systems by spectral-analysis-of-surface-waves method. PhD Thesis. The University of Texas at Austin.

Park, C.B., Miller, R.D., and Xia, J. 1998. Imaging dispersion curves of surface waves on multichannel record: Technical Program with biographies, *SEG, 68th Annual Meeting*, New Orleans, Louisiana, 1377-1380.

Ryden, N., P. Ulriksen, C. B. Park, and Miller, R. D. 2002. Portable seismic acquisition system (PSAS) for pavement MASW. *Proceedings of the Symposium on the Application of Geophysics to Engineering and Environmental Problems*.

Ryden, N., and Mooney, M.A., (2009). Analysis of surface waves from the light weight deflectometer, *Soil Dynamics and Earthquake Engineering*. Vol. 29, Issue 7, pp 1134-1142.

Von Quintus LH, Mallela J, Lytton LR (2010) Techniques for mitigation of reflective cracks. *In FAA Worldwide Airport Technology Transfer Conference*, Atlantic City, NJ.

Wisconsin DOT. (2007). *Facilities Development Manual.*
https://trust.dot.state.wi.us/static/standards/fdm/14/TC14.pdf.Accessed September 3

CHAPTER 5. QUALITY CONTROL/QUALITY ASSURANCE TESTING FOR LONGITUDINAL JOINT DENSITY AND SEGREGATION OF ASPHALT MIXTURES

A paper published in the journal of construction and building materials.

Authors: Can Chen, R. Christopher Williams, Taha Ahmed, Hosin "David" Lee, Scott Schram

5.1 Abstract

Longitudinal joint quality control/assurance is essential to the successful performance of asphalt pavement and it has received considerable amount of attention in recent years. Five paving projects were selected for sampling and evaluation in Iowa. For each project, joint quality is compared with regard to the "center" of the pavement mat (6' right of joint). Field densities and permeability test were made. Cores were obtained for subsequent lab permeability, density and indirect tensile (IDT) strength testing. Asphalt content and gradations were also obtained to determine the joint segregation.

In general, this study found that methods providing the most reliable measurements of joint quality are the AASHTO T166, AASHTO T331 (CoreLok) density tests and the permeability test by Karol-Warner Permeameter. The minimum required joint density for quality control should be around 90.0% and 88.5% of theoretical maximum density based on the AASHTO T166 and AASHTO T331 method respectively. Based on various mix design and longitudinal joint construction methods, the joints show differences in asphalt content and level of segregation. Results of this study indicate that poor quality of longitudinal joint should be a combination of segregation, asphalt content variation and insufficient density.

Keywords

Longitudinal joint; density; quality control; segregation

Highlights

- Evaluate available test methods for longitudinal joint quality control.
- Develop specifications to ensure the longitudinal joint with proper performance.
- Evaluate the effect of segregation on longitudinal joint density performance.

5.2 Introduction

Several methods were generally used to measure and quantify the quality of longitudinal joint construction. These include the field and in-lab permeability test, nuclear/non-nuclear density test and core density test. In recent years, a number of apparatuses have been developed to measure the permeability value of an HMA mixture and among which the NCAT field Permeameter and the Karol-Warner (K-W) in-lab Permeameter are the most popular ones. Previous studies in Arkansas, New England and Tennessee have had similar conclusions for the use of permeability test on the longitudinal joint (Williams et al., 2009; Mallick and Daniel, 2006; Huang and Shu, 2010). They all found that the joints have significantly higher permeability compared to adjacent mats and the use of infrared joint heater can greatly reduce the longitudinal joint permeability. Utilizing the two permeability testing devices, permeability criteria are determined based upon the percent within limit (PWL) of pavement air voids by Missouri Department of Transportation (DOT). The upper specification criteria for using the NCAT Permeameter and K-W Permeameter are 1560 x 10^{-5} cm/s and 530 x10^{-5} cm/s, respectively (Williams, et al., 2008). In another study conducted in the National Center for Asphalt Technology (NCAT), the critical permeability infers to the point at which a pavement becomes excessively permeable (Cooley, et al., 1999). However, none of a research currently has proposed quality control criteria using Permeameters for longitudinal joint construction. In addition to permeability tests, density

measurement is also a key indicator used to judge the quality of a HMA pavement. The most widely used core density testing method is the AASHTO T-166 method. An extensive review was conducted on longitudinal joint construction and specification documents proposed by various transportation agencies and the density at the joint are all generally recommended to be no more than 2 to 3 percent lower than the density specified in the lanes away from the joint (Sebaaly and Barrantes, 2004). Recently, another method using the CoreLok device via AASHTO T-331 method has been employed by many researchers and transportation agencies. They found that the CoreLok system tends to result in lower densities than the AASHTO T-166 method especially for lower density samples as is typical of joint cores (Williams, et al., 2009). The development of nuclear and non-nuclear density gauges offers an alternative way to measure the pavement density non-destructively. Williams and Hall (Williams and Hall, 2008) evaluated the effects of gauge model, temperature, gauge orientation and the present of sand using the PaveTracker and PQI non-nuclear gauges. They found that gauge orientation, moisture, sand and debris can significantly affect the reading of the two types of gauges.

To construct a sound longitudinal joint, mitigation of segregation is important. As stated by AASHTO (1997), the longitudinal joint area has a higher probability of being segregated. This commonly occurs from the augers not being run at sufficient speeds on the paver, allowing the coarse aggregates to roll to the outside of the mat. In addition, in order to avoid joint segregation during the paving process the auger and tunnel should be extended within 12 to 18 inches of the end gate so the material can be carried, and not pushed out to the joint. Several testing methods have been generally used to detect and measure the segregation of HMA. These include permeability test and nuclear/non-nuclear density test.

Williams et al. (Williams et al., 1996) found that the nuclear moisture/density gauge is capable of accurately measuring both asphalt content and density in a dry pavement condition. They also pointed out that the permeability test is only successful in detecting coarse segregation but not fine segregation. This is mainly because the permeability test depends more on the interconnected nature of void volume rather than simply the percent of voids. Fine dense-graded mixtures would have sufficiently low permeability that, even when moderately segregated, there is little to no statistical difference in permeability measurements. Larsen and Henault (2006) used density profiles obtained from a PaveTracker non-nuclear density gauge to quantify the level of segregation in Connecticut. However, they found that the spatial variation in density alone from the density gauge cannot distinguish the differences in segregated and low density area. Extracted asphalt content and gradations are also commonly used as a destructive way to determine segregation. As reported by Cross and Brown (1993), the pavement segregation has strong correlation with the percent passing #4 sieve, while Williams et al. (1996) used the sieve size that can separate the mix gradation into approximately equal portions to define the fine and coarse segregation. However, both of the study pointed out that segregation results in significant asphalt content variation which increases from very coarse to very fine (Williams et al., 1996; Cross and Brown, 1993).

5.3 Test Plan and Procedure

Five projects are selected for sampling and evaluation in this project study with each one represents a typical longitudinal joint construction technique as shown in Table 12. All five construction techniques are commonly used in Iowa. A summary of the five projects location, longitudinal joint construction type, lift thickness, surface mix type, and mix design are all listed out in Table 12. The route numbers for the five projects are designated as the

project names in this study for simplicity. Brief discussions for each construction method are as follows:

The butt joint applies the first roller pass with the wheel on the hot lane and overlapped onto the cold lane by about a 150 mm (6 inches), while the modified butt joint (hot pinch) applies the first roller pass with the wheel on the hot lane and about 150 mm (6 inches) away from the joint. The hot pinch has the potential to push HMA in the hot lane towards the joint during the initial roller pass. Milling and filling joint construction method include first milling a single lane, overlay that lane, and then mill the adjacent lane. Confinement can be formed during both the paving process of the cold and hot lanes by the milling and filling method. Temperature is always considered as the key in pavement construction. It is generally believed that higher compaction temperature can help increase compaction of the mix at the joint and improve the bond between the cold lane and hot lane. Higher temperature can also increase the flow ability of the mix and reduce segregation. The infrared joint heater by reheating the joint to around 230 ^{o}F before compaction is reported to be very effective (Huang and Shu, 2010; Daniel, 2006) and more detailed temperature and thermal conductivity analysis for infrared joint heater can be found in the literature (Daniel, 2006).With the same idea, longitudinal joint paved in WMA is believed to have a tight and better compaction than HMA (Tighe, et al., 2008).

The test plan contains two parts: field testing and laboratory testing. Field testing and sampling consisted of obtaining pavement density by the PaveTracker non-nuclear gauge, field permeability measurements using the NCAT Permeameter and extracting pavement cores from 6 random locations for each project. In each random selected test location, field tests were done on both the pavement longitudinal joint and the mid-section of the hot lane

(about 6’ right of longitudinal joint). Therefore, this results in testing a total number of 12 field locations and corresponding 12 core extractions from each project. Field density measurements using PaveTracker non-nuclear gauge can be greatly affected by water; therefore, they were performed firstly at each location. Once the PaveTracker density measurements were completed, NCAT permeability tests were made at the same location. After the pavement surface course is totally cooling down, core samples were taken at the same places where the field tests were performed. The core samples are from 4 to 6 inches in diameter and the thickness equals to the lift thickness of the surface course. Finally, these cores were transported to the Bituminous Materials Laboratory at the Iowa State University for further testing.

The following tests were performed on each field core samples in the laboratory: 1) voids analysis, 2) in-lab permeability, 3) indirect tensile strength, 4) determination of asphalt content and gradation. The void analysis includes the bulk specific gravity tests in accordance with AASHTO-T166 and the AASHTO T-331 method by the CoreLok® system. Karol-Warner (K-W) Permeameter was used for the in-lab permeability test based on the ASTM PS129 method. Upon completion of the laboratory density tests, core samples were tested for IDT strength following the AASHTO T-322 procedure. The joint core samples are loaded along the direction of the longitudinal joint so that failure could occur along the joint and the IDT strength at the joint can be obtained. Finally, the broken core samples were used to determine the asphalt content and gradation by the ignition method according to the AASHTO T-308 and AASHTO T-30 procedures respectively. Calibration factors were used in the ignition method from the cold-feed gradations to provide acceptable results.

Table 12 Project summaries

Projects	US-6	IA-148	IA-13	I-35	US-61
County	Iowa	Cass	Linn	Clark	Lee
Construction method	Butt joint (HMA)	Butt joint (WMA)	Butt joint + joint heater	Milling and filling	Butt joint + hot pinch
Mix Type	3M Surface 1/2 L-4	1M Surface 1/2 L-4	3M Surface 1/2 L-4	30M Surface 1/2 L-2	3M Surface 1/2 L-4
Binder Content	4.7	5.3	5.7	5.4	6.1
Lift thickness	1.5 in	1.5 in	1.5 in	2 in	2 in
Gradation					
3/4 in	100	100	100	100	100
1/2 in	93	91	97	93	97
3/8 in	87	87	86	84	88
#4	64	64	64	69	65
#8	42	44	50	50	46
#16	30	32	41	33	32
#30	21.5	18	30	20	20
#50	8.4	7.3	18	10	8.2
#100	5.5	4.1	8.8	5.3	4.5
#200	3.7	3.5	3.7	3.5	3.7

5.4 Test Results and Analysis

For each test method, the test results were firstly compared to see whether they are capable of detecting the density, permeability and tensile strength differences on longitudinal joint and 6’ right of the pavement joint (on pavement mat). Graphical comparisons for all projects are shown in Figure 29 to Figure 31.

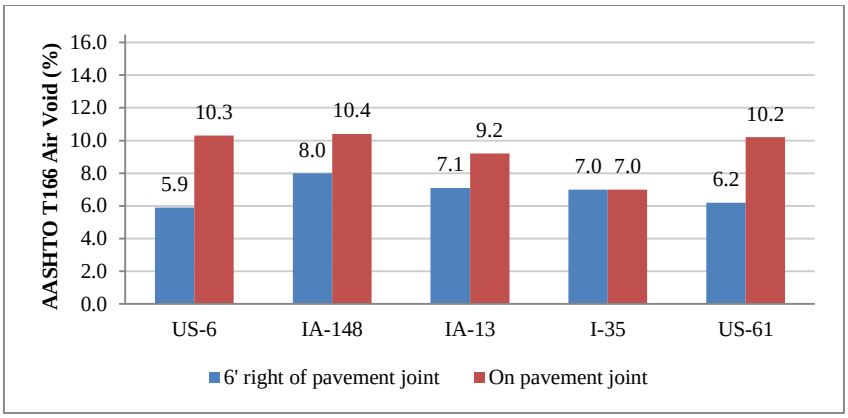

(a)

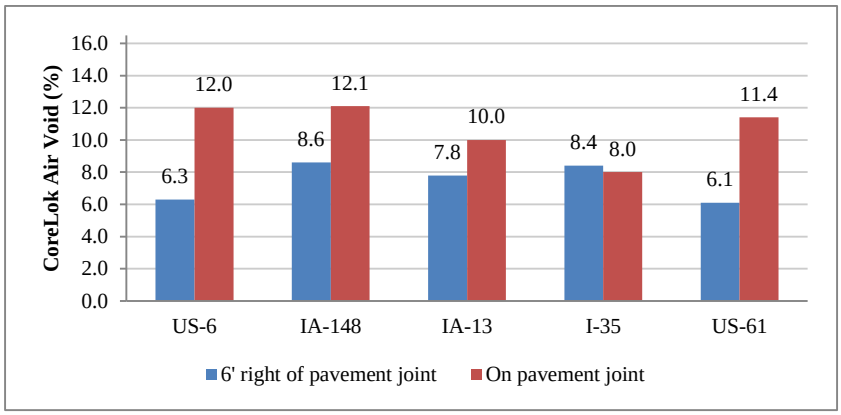

(b)

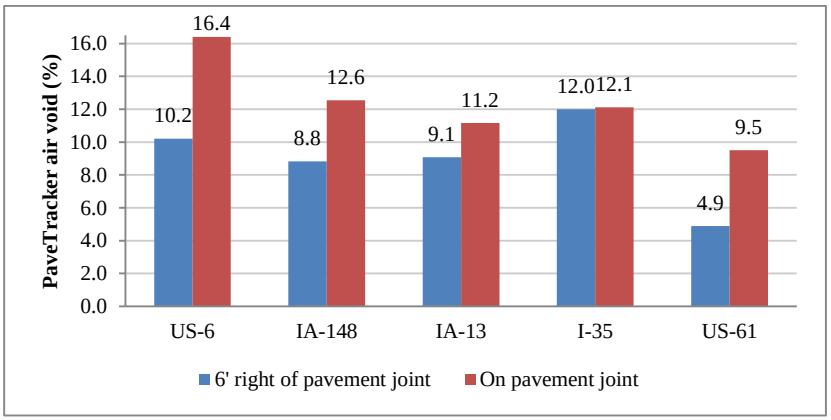

(c)

Figure 29 Comparison of mean air void values using different density testing methods: (a) AASHTO T166 method, (b) CoreLok method and (c) PaveTracker method

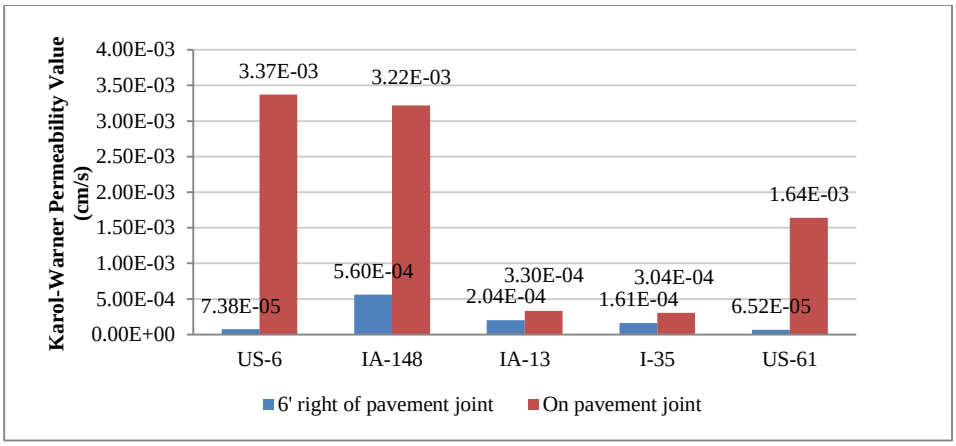

(a)

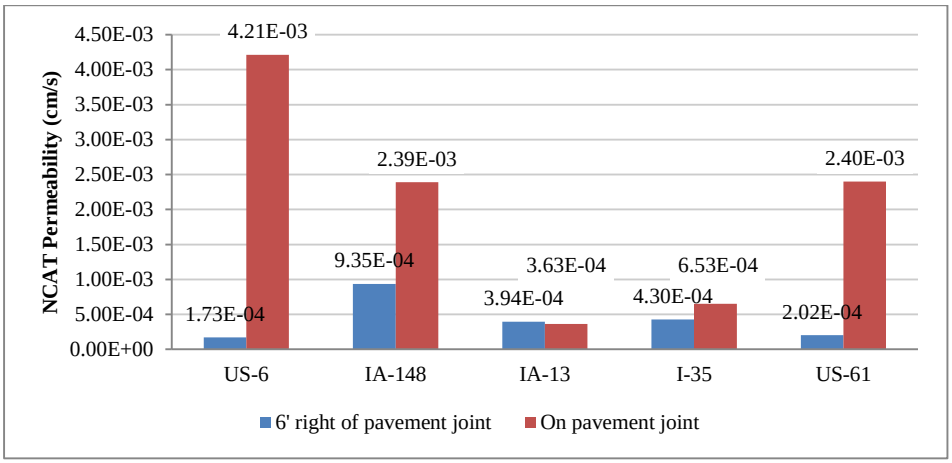

(b)

Figure 30 Comparison of mean permeability values using different permeability test methods: (a) K-W Permeameter and (b) NCAT Permeameter

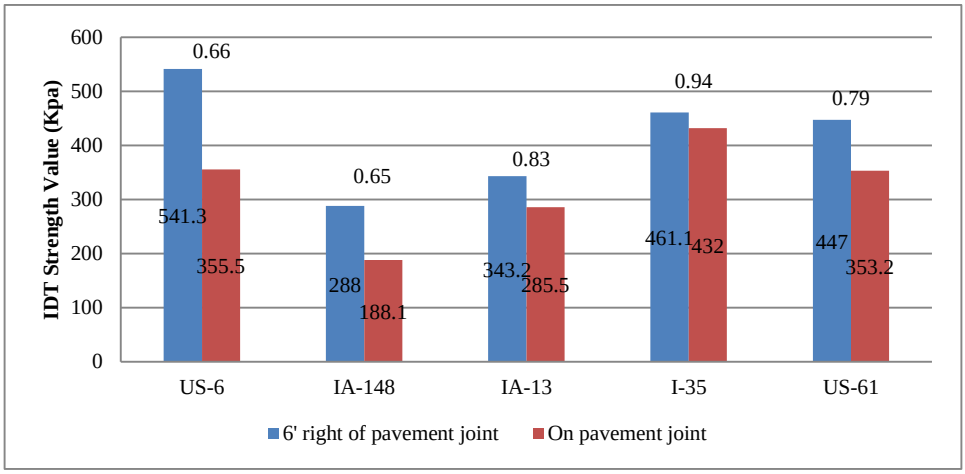

Figure 31 Comparison of mean IDT strength values

On the basis of the results comparison, the following conclusions are drawn:

From Figure 29 (a) and (b), both laboratory measures of density demonstrate the ability to detect significant differences in density with proximity to the joint. The CoreLok method did in general yield lower density values and thus higher air void values than AASHTO T166. On the longitudinal joint, the air void gap between CoreLok and AASHTO T166 methods becomes even larger.

While the PaveTracker non-nuclear gauge demonstrates the ability to detect the differences in density between the longitudinal joint and 6'right of the joint as shown in Figure 29 (c), it gives far less accurate air void values comparing with the laboratory density tests. Difference pavement temperature, moisture and surface texture could be the reasons. In addition, during the field testing it was observed that improper compaction can result in uneven longitudinal joint and this would make the density gauge placed on it not fully touching the joint surface.

Although it is not intended to compare which longitudinal joint construction method performs the best in this study, it is quite evident that the IA-13 and I-35 projects using joint heater and milling and filling technique give significantly lower lab and field permeability and air void values than the other projects. One important observation from Figure 30 is that the NCAT Permeameter provides either higher or lower values comparing with the K-W Permeameter. A problem of the NCAT Permeameter is that it is not easy to form a totally watertight seal and if water leakage happens the device would overestimate the permeability value. On the other hand, putting too much sealant material to seal the Permeameter could lead the sealant entering into the 6" testing area and thereby blocking a portion of the test

area. This would underestimate the field permeability value. Therefore, the test method is very operational dependent.

In Figure 31, the mean IDT strength on pavement mat is higher than that on pavement joint for all of the projects. The ratio values of the longitudinal joint to pavement mat IDT strength are also listed above the columns in Figure 31. Without any special treatment, the butt joints paved in HMA and WMA (US-6 Project and IA-148 Project) exhibit the lowest ratio values. It is recommended that the ratio value should not be lower than 0.8. However, more tests should be performed to support the idea. With various mix design the IDT strength are quite different. The projects IA-148 and IA-13 give lowest mean IDT strength value. This is because the project IA-148 is paved with WMA with 1.8% of water injection while the IA-13 project contains many fine aggregates, which leads to the thinnest film thickness. Therefore, without comparison on pavement mat IDT strength on longitudinal joint alone cannot be used for quality control purpose.

Of the testing methods discussed above, AASHTO T166, AASHTO T331 (CoreLok) and ASTM PS126 K-W permeability test methods are considered to be the most reliable measurements to quantitatively determine the density and permeability of longitudinal joints. Determinations of critical in-place air void and permeability values on the longitudinal joint are presented in Figure 32 and Figure 33. The critical air void is considered to be the point at which the two lines tangent to the regression line intersect. At the intersecting point of these two lines, a bisecting line was then drawn to the egression line. The point at which the bisecting line hits the regression line was defined as the critical point for air voids and permeability. Although the method gives different critical air voids for the CoreLok (AASHTO T331) and AASHTO T166 as seen in the figures, it illustrates close critical K-W

permeability values, which is around 1.5e-03 cm/s as shown in the two figures. The minimum required longitudinal joint density is around 90% of theoretical maximum density based on the AASHTO T166 method. In the same approach, the graphical representation show that the critical air voids is around 88.5% of theoretical maximum density according to AASHTO T331 (CoreLok) method. In addition, Figure 32 and Figure 33 shows that the CoreLok method has a better correlation than the AASHTO T166 method with a higher goodness of fit (R^2). On the other hand, the AASHTO T166 method is much less sensitive in the high air void region and provides more scattered results, where both fine segregation and coarse segregation are also detected on the longitudinal joint as follows.

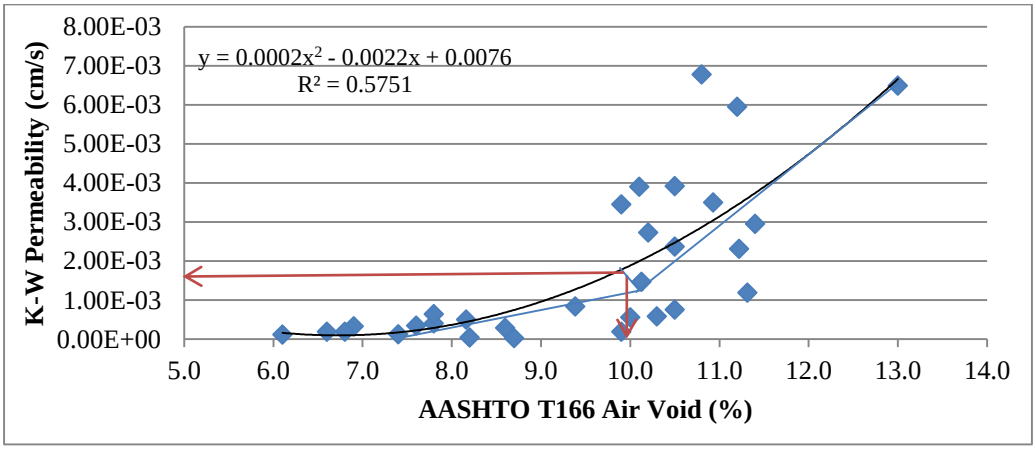

Figure 32 Selection of critical permeability and CAASHTO T166 air voids values on joint

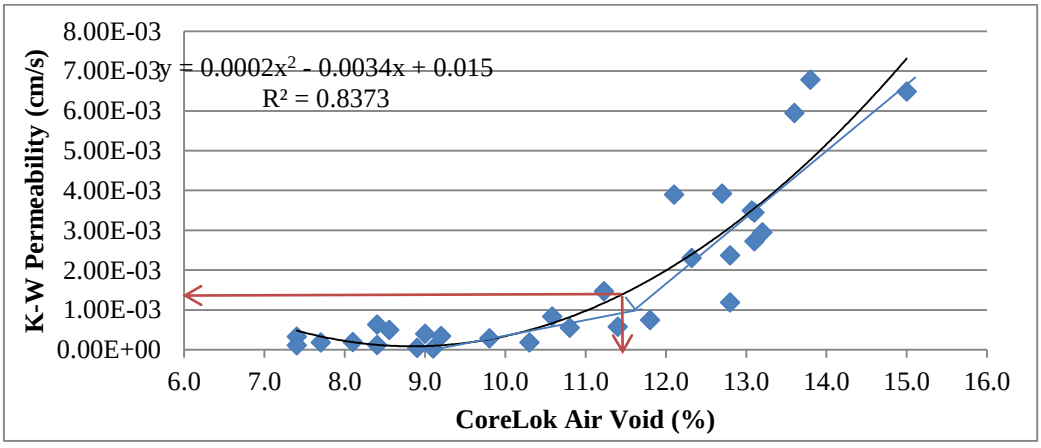

Figure 33 Selection of critical permeability and CoreLok air voids values on joint

Asphalt content and gradation of the field samples were determined according to the AASHTO T-308 and AASHTO T-30 procedures, respectively. The fineness modulus is also calculated, since the calculation of fineness modulus can serve as an overall gradation descriptor by combing the gradation data on each sieve. Finally, all of these data including the permeability, density and IDT strength data used the JMP software for the one way analysis of variance (ANOVA) to determine whether there are statistically significant differences between the paired data for on pavement joint and mat values. A 95% confidence was used in all cases. If statistically significant differences are evident, plus (+) and minus (-) signs are provided as further descriptors. A (+) sign indicates that the test values on pavement joint are significantly higher than that on pavement mat, while a (-) sign conveys that the test values on joint sample are significantly lower than those on pavement mat. Gradation results on each sieve are taken as the value retained on each sieve for comparison. Gradation results on each sieve are taken as the value retained on each sieve for comparison. Therefore, a positive sign (+) for the gradation change indicates that significantly more aggregates are retained respective sieve for the longitudinal joint samples. Based on the results of the analysis shown in Table 13, the following observations are found.

Project US-6 (HMA butt joint): The (+) positive signs on fineness modulus and percent passing the #4, #8, #30 and #50 sieves indicate that the longitudinal joint gradation is significantly coarser than the pavement mat. In addition, permeability, density and IDT strength tests are clearly able to detect the lower density and coarse segregation (coarser gradation) at the longitudinal joint.

Project IA-148 (WMA butt joint): A decrease in asphalt content and the gradation on key sieves (#8 and #16) are coarser than the pavement mat is a typical pattern for coarse

segregation. Permeability, air void and IDT strength measurements are clearly able to detect the lower density and coarse segregation at the longitudinal joint.

Project IA-13 (Infrared joint heater): significant differences in fineness modulus, percent passing the #16, #30, #50, #100 and #200 sieves are identified. The (-) negative signs reveal that the longitudinal joint gradation is significantly finer than the pavement mat. Although significantly lower density is detected at the longitudinal joint by AASHTO T166 and AASHTO T331 methods, the joint heater creates air voids lower than the recommended air void requirement. Fine segregation may also help reduce the permeability and neither the NCAT nor the K-W Permeameter shows statistical difference in the measurement.

Project I-35 (Milling and Filling): Although significant differences were detected by gradation, a consistent trend was not present for all of the sieves, which is not a typical pattern for gradation segregation. Actually, the one-way ANOVA test result shows that longitudinal joint has a more gaped gradation compared with the pavement mat. No statistical difference is found in the overall gradation comparisons and asphalt content. In addition, none of other tests (density, permeability and IDT strength tests) have shown significant differences. This tends to indicate that the longitudinal joint formed by milling and filling has slight or no segregation with close density and stiffness values to that of the pavement mat.

Project US-61 (Hot pinch): Higher asphalt content is present at the longitudinal joint by pinching and more fine aggregates are seen on the joint. In addition, significantly lower density and IDT strength are clearly shown at the longitudinal joint by the ANOVA test. Although permeability on joint and pavement mat shows significant difference, fine segregation may help reduced permeability, which can be seen in Figure 30 (a) on the comparison of permeability test.

Table 13 Summary of one-way ANOVA test results

	US-6	IA-148	IA-13	I-35	US-61
	Joint vs. Mat	Joint vs. Mat	Joint vs. Mat	Joint vs. Mat	Joint vs. Mat
NCAT Permeability	Significant (+)	Significant (+)			Significant (+)
K-W Permeability	Significant (+)	Significant (+)			Significant (+)
CoreLok Air Voids	Significant (+)	Significant (+)	Significant (+)		Significant (+)
AASHTO T166 Air Voids	Significant (+)	Significant (+)	Significant (+)		Significant (+)
PaveTracker	Significant (+)	Significant (+)			Significant (+)
IDT strength	Significant (-)	Significant (-)	Significant (-)		
Asphalt Content		Significant (-)			Significant (+)
% pass 1/2 ” change				Significant (+)	
% pass 3/8 ” change					
% pass #4 deviation	Significant (+)			Significant (+)	Significant (-)
% pass #8 change	Significant (+)	Significant (+)			Significant (-)
% pass #16 change		Significant (+)	Significant (-)	Significant (-)	Significant (-)
% pass #30 change	Significant (+)		Significant (-)	Significant (-)	
% pass #50 change	Significant (+)		Significant (-)	Significant (-)	
% pass #100 change			Significant (-)	Significant (-)	Significant (-)
% pass # 200 deviation			Significant (-)	Significant (-)	Significant (-)
Fineness Modulus	Significant (+)		Significant (-)		Significant (-)
Segregation type	Coarse	Coarse	Fine	No	Fine

In general, the last row in the table summarized the different longitudinal joint segregation type for each project that has been discussed above. Both fine and coarse segregation have been identified along the longitudinal joint and further investigation to see whether segregation affects longitudinal joint density or not. An indicator sieve is selected that can be used to represent the overall gradation segregation difference on the longitudinal

joint and pavement mat. The indicator sieve is defined as follows: 1) the selected sieve should be closest to the 50/50 passing; 2) the percent passing on the sieve should also have significant difference between pavement mat and joint. As can be seen from Table 13, No.8 sieve is considered as the indicator sieve for the project US-6 and IA-148, No.16 sieve is used for the IA-13 project, #4 sieve is used for the I-35 project, and #8 sieve is selected for the US-61 project. The relationship between the gradation segregation change on the indicator sieve and the CoreLok air voids are further shown in Figure 34 through Figure 37. The goodness of fit (R^2) for the relationship between the air void and gradation deviation on the indicator sieve may reflect out whether segregation can greatly affects the longitudinal joint density or not. The project I-35 is not involved in the analysis since the preliminary investigation has shown that it appears to have no segregation. As can be seen, the R^2 values for projects US-6, IA-13 and US-61 are around 0.4 to 0.5 showing that some correlation does exists between density variations and segregations. The correlation is relatively low, however, the trend shows that the air voids content increases on both coarse segregation and fine segregation and the coarse segregation showing a higher rate of change compared with fine segregated joints, which agrees with that in the work of others (Williams, et al., 1996). Keeping in mind only one indicator sieve is selected to correlate with the air voids, which may lead to a lower R^2 value. In addition, it also indicates that although segregation can greatly affect longitudinal joint performance, it may not be the only factor. Spatial variations in density for the longitudinal joint could be also the result of lack of roller compaction and other construction issues (mix temperature in compaction, longitudinal joint alignment, etc.), which cannot be controlled during field experimental test. The R^2 for the project IA-148 is

poor. This could be mainly because the longitudinal joint density decrease on IA-148 project is more related to the deficiency in asphalt content.

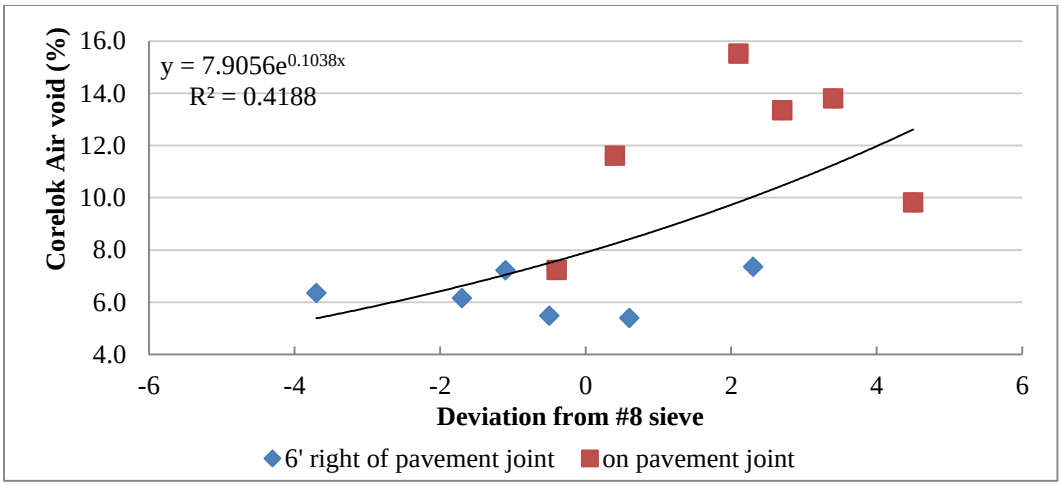

Figure 34 Air voids vs. gradation change on the indicator sieve for the US-6 project

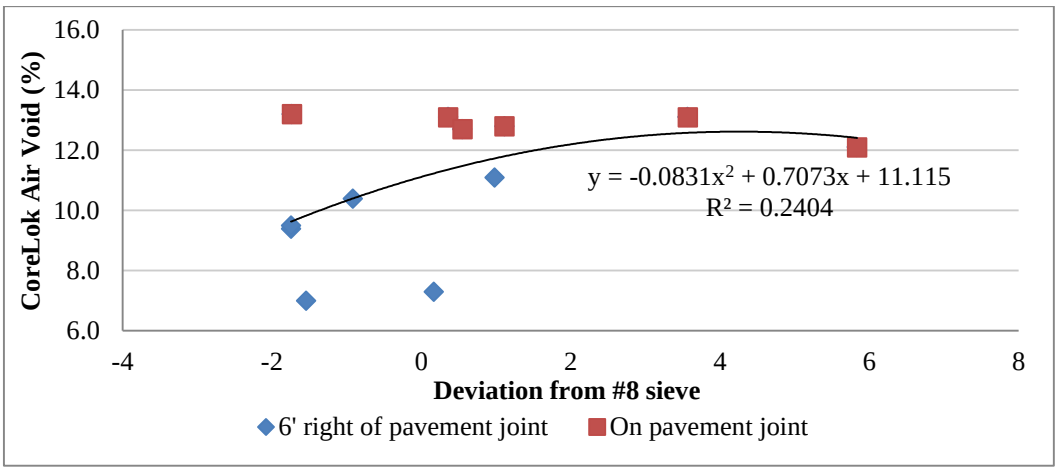

Figure 35 Air voids vs. gradation change on the indicator sieve for the IA-148 project

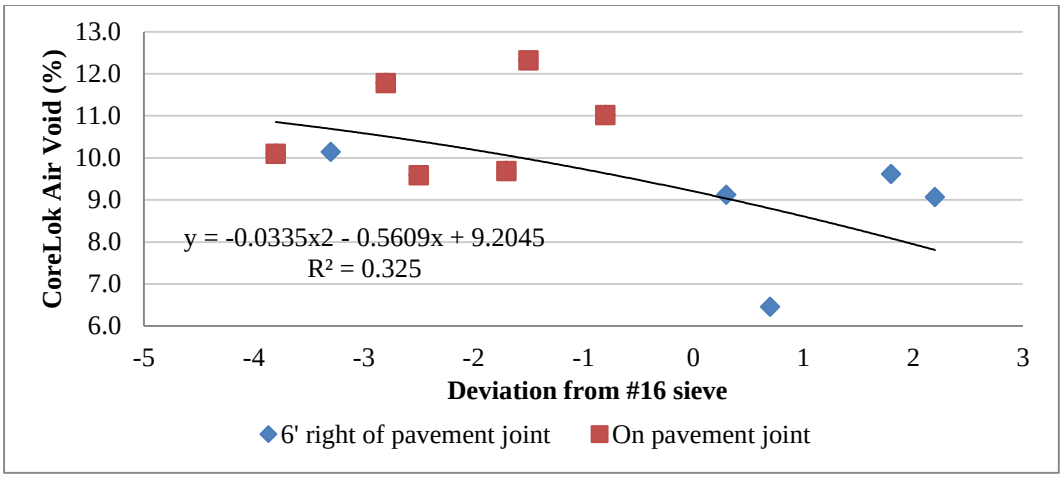

Figure 36 Air voids vs. gradation change on the indicator sieve for the IA-13 project

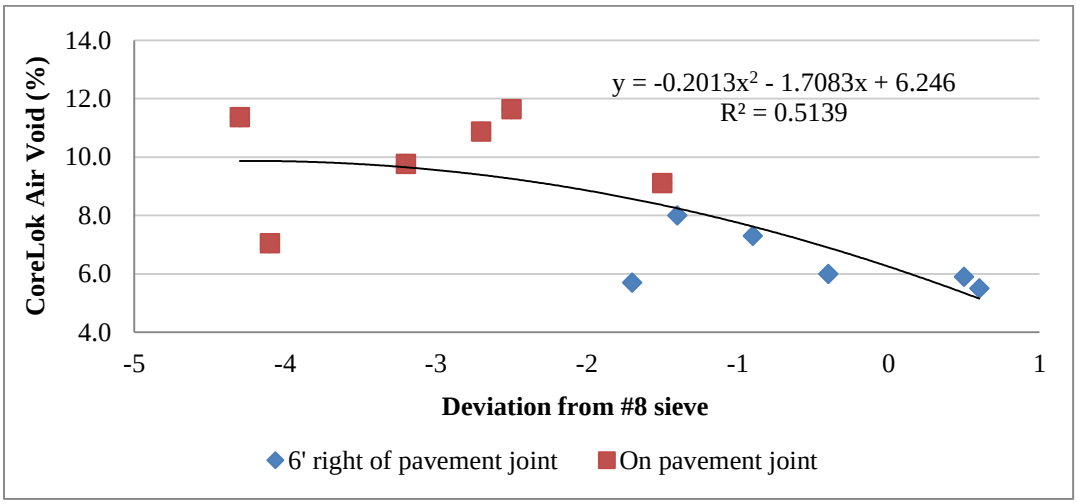

Figure 37 Air voids vs. gradation changes on the indicator sieve for the US-61 project

5.5 Recommendations and Conclusions

Premature longitudinal joint failures are a result of a combination of low density, low tensile strength, high permeability and segregation. Five paving projects were selected for sampling and evaluation in Iowa. Based on the work conducted in this study, the following conclusions and recommendations can be made.

1. The CoreLok method (AASHTO T-331) in general yields lower density values and thus higher air void values than AASHTO T-166. Greater differences in the density results are seen for the samples at the longitudinal joint.
2. The PaveTracker density gauge and NCAT Permeameter can distinguish the difference between longitudinal joint and pavement mat. However, they are not recommended as viable tools for quality control and assurance purpose.
3. It is recommended that the minimum required longitudinal joint density that the contractor to achieve should be 90.0% and 88.5% of theoretical maximum density based on the AASHTO T166 and CoreLok (AASHTO T331) methods, respectively.
4. The strong relationship between the Karol-Warner and air voids results illustrates that the Karol-Warner could be successfully used to measure the permeability of field core samples. A corresponding Karol-Warner in-lab permeability criteria identified according to the minimum required longitudinal joint density is 1.50e-03 cm/s. The Karol-Warner Permeameter is recommended for use in quality control testing,
5. IDT strength test is reliable and the ratio values for the longitudinal joint to pavement mat IDT strength is recommended no less than 0.8 for quality assurance purpose.
6. All of the projects appear to have segregation at the longitudinal joint except for the one using milling and filling method. Based on various mix design and joint construction methods, the joints show quite different changes in asphalt content and types of segregation as compared with the pavement mat. Results of this study indicate that the lower density of longitudinal joints could be a combination of gradation segregation, significant asphalt content variation and a lack of field compaction.

7. Neither the butt joint nor infrared joint heater could provide confinement during the joint compaction process. Hot pinch of the longitudinal joint by pushing extra material for compaction near to the joint could help achieve better joint density, however, fine aggregates and excess of asphalt could be stacked over the joint. The method of milling and filling one lane at a time is feasible to avoid the unsupported edge and a confinement has the potential to avoid the spread of aggregation segregation.

Acknowledgements

The authors would like to thank the Iowa Department of Transportation for financial and technical support associated with this research project. The authors also recognize and appreciate the asphalt paving contractors of Iowa that provided logistical support.

5.6 References

AASHTO. 1997. Segregation causes and cures for hot mix asphalt. American Association of State Highway and Transpiration Officials.

Cooley, L.A., Brown, E.R., and Maghsoodloo, S. 1999. Developing critical field permeability and pavement density values for coarse-graded superpave pavements. *Transportation Research Record*. (1761) 41-49.

Cross, A.S. and Brown, E.R. 1993. Effect of segregation on performance of hot-mix asphalt. *Transportation Research Record*. (1417) 117-126.

Daniel, J.S. 2006. Use of an infrared joint heater to improve longitudinal joint performance in hot mix asphalt pavements. *Journal of Performance of Constructed Facilities*. 20(2) 167-175.

Huang, B.S., and Shu, X. 2010. Evaluation of longitudinal joints of HMA pavements in Tennessee. Tennessee Department of Transportation, Project No. RES1304.

Larsen, D.A. and Henault, J.W. 2006. Field evaluation of a non-nuclear density pavement quality indicator. Connecticut Department of Transportation, Report No. 2227-F-01-3.

Sebaaly, P.E. and Barrantes, J.C. 2004. Development of a joint density specification phase I: literature review and test plan. Project No. 13DL-1.

Tighe S, Moore G, MacTaggart C and Davidson K,. 2008. Evaluating warm asphalt technology as a possible tool for resolving longitudinal joint problems. *Canadian Technical Asphalt Association Proceedings*, Saskatoon.

Williams, S.G., Pervis, A., Bhupathiraju, L.S. and Porter, A. 2009. Methods for evaluating longitudinal joint quality in asphalt pavements. *Transportation Research Record*. (2098) 113-123.

Williams, R.C., Raouf, M.A. and Schroer, J. 2010. Alternative test methods for measuring permeability of asphalt mixes. *Transportation Research Record*. 2594.

Williams, S.G., and Hall, K.D. Critical factors affecting field determination of hot-mix asphalt density using non-nuclear devices. *Transportation Research Record*. 2008; (2081) 150-157.

Williams, R.C., Duncan, G., and White, T.D. 1996. Hot mix asphalt segregation: measurement and effect. *Transportation Research Record*. (1543) 97-105.

CHAPTER 6. CONCLUSIONS AND RECOMMENDATIONS

Asphalt pavement cracking in joint area is an important consideration in pavement design and construction. In this thesis, we have used statistical method, non-destructive and destructive testing methods as well as computer simulation to evaluate the best way for pavement cracking control and understand the cause and mechanics of cracking.

In chapter three, we have identified the most appropriate reflective cracking mitigation strategy by using the PMIS and IPMP database in a netwrok-level approach. This involved collecting pavement structure, traffic, and field distress data in a number of 155 Iowa's composte pavement sections. The results of this part of research showed that rubblization treatment has the longest life span for reflective cracking control. Generally, the Lognormal distribution model performs well in fitting the reflective cracking data. The model indicates an early-time increase of failure probability followed by a constant or decreasing function. The study also analyzed the IRI and PCI other than relfetcive crakcing. Higher initial IRI values were found for the SCR and mill & fill treatments in the database. This should finally leads to lower IRI survival probabilities for the two treatments. Finally, it is found that increase pavement thickness is the only significant factor for reflective cracking control for SCR, Mill & Fill and overlay.

In chapter four, we have focued on identifying the most effective reflective cracking treatment in a project-level approach. A total seventeen pavement sites were tested. These include standard/full rubblization, modified rubblization, crack-and-seat, and rock interlayer. To provide a basis for comparison, FWD and SWM were applied at the same site in the first four projects. The results show that the SWM gives close concrete layer moduli compared with the FWD moduli on a conventional composite pavement. However, the SWM provides

higher moduli for the rubblized concrete layer. Further, other twelve projects were tested by SWM alone. The results show that the crack & seat provides the highest moduli, followed by the modified rubblization. The full rubblization and the rock interlayer give similar, but lower moduli. Pavement moduli have no close relationship with pavement performance. Based on the field distress survey result, it is recommended that use of the modified rubblization and rock interlayer treatments for reflective cracking mitigation could be best.

Longitudinal joint failure are discussed in chapter five. It is found that premature lontidunal joint cracking are a result of a combination of low density, high permeability, segregation and lack of joint adhesion. Five on-paving projects are selected for sampling and evaluation in Iowa with each one representing a typical longitudinal joint construction technique. Field and lab density, permeability and mechanical testing were performed. In general, this study finds that the minimum required joint density should be 91.5% of theoretical maximum density based on the AASHTO T166 method. The restrained-edge by milling, butt joint with infrared heat treatment and modified butt joint by hot pinch construction methods all create the joint density higher than this limit. Traditional butt joint paved in both HMA and WMA exhibits lower density and higher permeability than the criterion. In addition, all of the projects appear to have segregation at the longitudinal joint except for the one using edge-restraint by milling method. Based on various mix design and joint construction methods, the joints show quite different changes in asphalt content and types of segregation comparing with the job mix formula. Results of this study indicate that lower density of longitudinal joint is a combination of gradation segregation, significant asphalt content variation and a lack of field compaction.

APPENDIX. WATER FLOW SIMULATION AND ANALYSIS IN HMA MICROSTRUCTURE

This paper was presented in the proceeding of the International Society for Asphalt Pavements (ISAP), 2012. It is also under the publication process in the Journal of Traffic and Transportation Engineering.

Authors: Can Chen, Christopher Williams, and Baskar Ganapathysubramanian

A-1Abstract

Moisture-induced damage of asphalt mixtures is probably one of the most important factors that affect the in-service performance of asphalt pavements. Almost all of the longitudinal joint cracking is directly or indirectly related to the moisture or water damage. This paper/appendix attempts to use advanced numerical simulation techniques to investigate the internal mechanisms behind the asphalt pavement water damage. Firstly, we would introduce a method for constructing virtual two-dimensional (2-D) microstructure of Hot Mix Asphalt (HMA). Based on the method, the gradation of coarse aggregates and the film thickness of the asphalt binder can be defined by the user. The HMA microstructure then serves as the input to the Computational Fluid Dynamic (CFD) software (ANSYS-FLUENT) to investigate the water flow pattern through it. It is found that the realistic flow fields can be simulated in the 2-D microstructure and the flow patterns in some typical air void structures are identified. These flow patterns can be used to explain the mechanisms that could result in moisture damage in HMA pavement. The one-dimensional numerical permeability values are also derived from the flow fields of the 2-D HMA microstructure and are compared with the measured values obtained by the Karol-Warner permeameter. A poor agreement is seen

which is mainly because the interconnected air voids channels in actual HMA samples cannot be fully represented in a 2-D model.

A-2 Introduction

HMA is a porous medium consisting of graded coarse and fine aggregates bound with asphalt binder plus a certain amount of air voids. In HMA pavement construction, it is important that the mix be adequately compacted in-place. If the air void content exceeds about 8 percent by volume, they may be interconnected channels which allow water to easily penetrate into the HMA pavement (Cooley, et al., 2000). High permeability could result in an increased potential for moisture damage in the pavement, such as raveling and stripping. However, such a phenomenon of moisture damage and water flow pattern in HMA pavement cannot be observed on a scale visible to the human eye. Computer simulation offers attractive opportunities for depicting the simulated internal HMA structure and studying the relationship between the pore mechanism and water flow characteristics in HMA.

There are a number of attempts in the literature dealing with the water flow simulation through HMA pavement structure and subgrade soil. Water flow in an actual HMA structure captured by 2-D X-ray computer tomography images is successfully simulated by Omari and Masad (2004). Wang et al (2003) simulated the 2-D water flow in a dual-layer soil microstructure. However the parallel flow channel between clay particles used in their model is impossible to be applied here for the HMA microstructure model because of the irregularity characteristics of the HMA internal structure. Ghassemi and Pak (2011) studied the effects of permeability and tortuosity of flow through sandy soil by the Lattice Boltzmann method.

In this study, we first present a method for constructing a virtual 2-D microstructure of HMA. Next, we model pressure driven flow through the HMA microstructure by ANSYS-FLUENT. Finally, the simulated flow field pattern is used to explain the moisture damage mechanism. The numerical permeability values are also calculated and compared with in-lab measured values at similar air void contents.

A-3 HMA Microstructure Construction

There are basically two ways of numerically constructing porous structures: statistics driven reconstruction and process driven reconstruction (Ganapathysubramanian and Zabaras, 2007). The process driven technique is selected in this study, since the statistics driven method needs an X-ray CT image database containing information such as the inter-air voids distance distributions and the number of air voids in a fixed area or volume, which is not available in the current phase of research. In recent decades, one of the process driven methods developed by various researchers (Wittmann et al., 1985; Gopalakrishnan et al., 2006; Zhang, 2008) has been widely used for the visual simulation of concrete, HMA and other granular materials for its simplicity. In their model, the coarse aggregates are assumed as either spherical or polygon shapes and then these aggregates are randomly packed in a fixed area or volume by Monte-Carlo method. However, the problem with this model is obvious. Firstly, the roles of fine aggregates and asphalt binder in HMA cannot be represented. Secondly, this model can only produce material structures with medium to high porosity, which is not very suitable for the simulation of HMA microstructure. To solve these problems, a new method for constructing 2-D HMA microstructure is proposed below.

First, it is assumed that all coarse aggregates in the HMA have spherical geometries as the inner spheres shown in Figure A-1 (a). The asphalt binder modeled by the outer circle

is used to wrap the coarse aggregate particle/inner sphere and to glue with each other to form a larger and denser solid body. The thickness of the asphalt binder is assumed to be a function of the coarse aggregate dimension and can be defined as a percentage of the inner sphere diameter (e.g. 10%). Further, if we consider the area wrapped by the asphalt binder as an inscribed sphere, then a convex polygon with a random-vertices number can be generated outside as shown in Figure A-1 (b). The corner areas between the exterior polygon and interior sphere are relatively small and form different triangle-like shapes. Due to the irregular shape of the corner areas, they are considered as fine aggregates. The fine aggregate acting as a stone framework bonded outside the asphalt binder can closely reflect the HMA microstructure. Finally, the overlapped plot parts are merged together to create a whole patch as shown in Figure A-1 (c) to form the simplest unit of a HMA microstructure. In order to simulate a HMA microstructure in a larger area, many units like the type shown in Figure A-1 should be compacted or packed together. The packing algorithm follows the rule that the asphalt binder-asphalt binder, asphalt binder-fine aggregate, coarse aggregate-fine aggregate and fine aggregate-fine aggregate are all allowed to overlap with each other at their intersections but the coarse aggregate-coarse aggregate and asphalt binder-coarse aggregate are not allowed to do so (see Figure A-1). Therefore, the inter-particle distances between the coarse aggregates can serve as the controlling parameter for particle positioning in the whole domain. The packing algorithm starts with placing numbers of largest coarse aggregates first at random positions and then smaller size coarse aggregates are added one by one in the empty space among the large aggregates. If the latter placed smaller coarse aggregate overlaps with a previous large one, then the smaller one would be rejected automatically, and

another attempt would be made to place it. The HMA packing process is done when no more coarse aggregates can be placed into the domain.

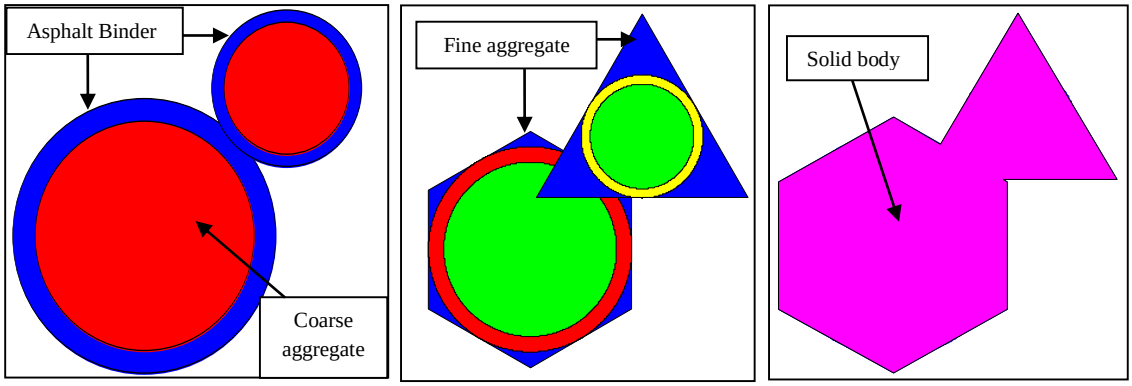

Figure A-1 Computer simulation of HMA solid body

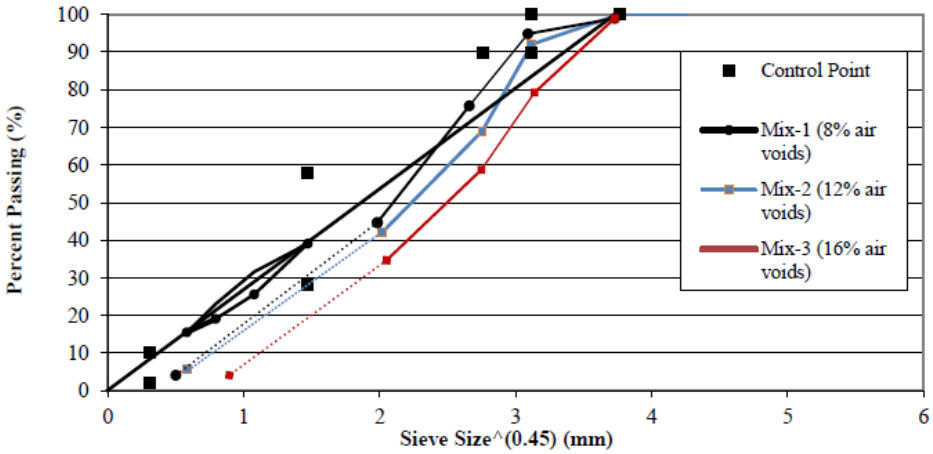

Figure A-2 Aggregate gradations for simulated HMA mixes

The maximum aggregate size used for the simulation is 12.5 mm and aggregates larger than or equal to 4.75 mm (#4 sieves) are considered as the coarse aggregates. Therefore, there are three different sizes of coarse aggregates/inner spheres in this model: 12.5 mm, 9.5 mm and 4.75 mm. The specific gravities for all aggregates are assumed to be the same in the simulation process. Then the gradation of the coarse aggregates can be

controlled based upon their diameters rather than their retained weights on each sieve. Three different mixes are simulated based upon the gradation curve shown in Figure A-2. The targets are to generate the mixes with air void contents at around 8 %, 12 % and 16 % respectively. Mix-2 with 9.5 mm Nominal Maximum Size (NMAS) is first modeled and is served as a good baseline mix for comparison with a total amount of 34 different sizes of coarse aggregates. Comparing with Mix-2, Mix-1 contains more 4.75 mm and less 12.5 mm particles, while Mix-3 with a 12.5 mm NMAS has more 12.5 mm and less 9.5 mm particles. However, the drawback of this HMA construction model is that the gradations of fine aggregates are undeterminable since the fine aggregates are allowed to be merged within other parts. Therefore, their gradation curves are expressed by dot lines extending along the coarse aggregate gradation curves.

A-4 Water Flow Simulation and Analysis

The visual HMA microstructures for Mix-1, Mix-2 and Mix-3 are shown in Figure A-3. All three mixes are made in a 3.9 x 3.9 cm simulation domain. Eq. (A-1) is used for the calculation of simulated HMA air void contents. Simulated air void contents in the HMA microstructures are very close to the target air voids. Among the three mixes, the Mix-3 has the highest air void content and most complicated interconnected air voids channels, it is chosen as a representative illustration of CFD simulation to understand the fluid flow characteristics in HMA.

$$\text{Air Voids} = \left(\frac{A_{domain} - A_{solid}}{A_{domain}} \right) \times 100 \qquad \text{(A-1)}$$

Where, A_{domain} is the simulation domain area, and A_{soild} is the solid part area in the domain.

The HMA microstructure is meshed using triangular elements. Both global and local mesh controls in ANSYS are applied since the grid sizes need to be fine enough to resolve the flow field in narrow interconnected air void channels and at the same time coarse enough to cover the whole domain without requiring an infinite computational power. This finally results in 22800 total elements for the Mix-3 microstructure. The mesh is exported to the FLUENT solver through a journal file. A steady state laminar incompressible model is adopted for the flow regime inside our virtual simulation domain. The existence of flow motion in it depends on the hydraulic pressure gradient. Water is assumed to flow into the domain through a velocity-inlet (the top boundary) and leaves it from the bottom and left boundaries. A symmetry boundary condition is used for the right side of the simulation box to double the domain area. Since permeability, as the intrinsic property of a porous material, is independent of water pressure gradient, arbitrary outlet pressure values are applied at the bottom and left boundaries. For the inlet condition, real mean inlet velocity values are used. They are obtained via the in-lab permeability test by the Karol-Warner permeameter on field HMA samples having the closest air void contents with the simulated ones. This ensuing section will further discuss how these field HMA samples are obtained. The Karol-Warner permeameter is chosen to measure the mean inlet flow velocity for its convenience to check how quick water can flow into the HMA by recording the drop in water level in a constant diameter standpipe over a given time interval. The finite volume method implemented in FLUENT solver is exploited to solve the continuity and conservation of linear momentum for an incompressible continuum medium, such as water. For the simulation, FLUENT's "standard" scheme is used for the pressure interpolation and the SIMPLE scheme is used to

represent the pressure-velocity coupling. To monitor the convergence of the simulation, the residuals are all down in the 1e-06 range in this study.

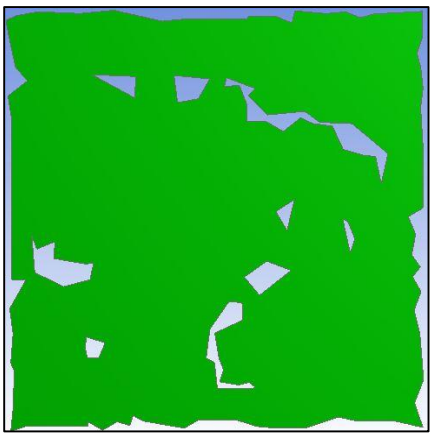

(a) Mix-1 (7.8 % air voids)

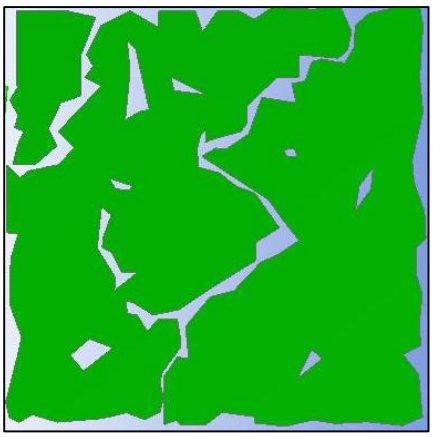

(b) Mix-2 (11.3 % air voids)

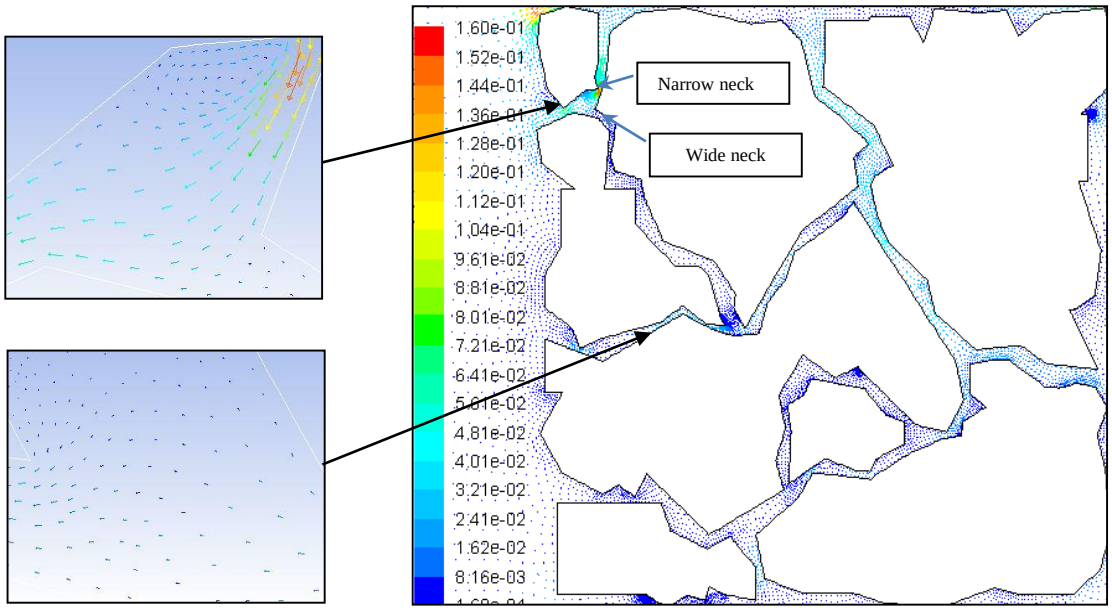

(c) Mix-3 (16.1% air voids)

Figure A-3 Water flow simulation in a 3.9 X 3.9 cm HMA microstructure

Figure A-3(c) shows the example of flow field in Mix-3 HMA microstructure. Magnitudes of flow velocity are illustrated in different colors. A brighter color shows a higher velocity. In this figure, the average breadth of the interconnected air void channel is

about 1.25 mm with the narrowest path only 0.2 mm. Some more detailed flow patterns in the HMA microstructure are observed and discussed as follows:

a. The water flow velocity depends greatly on the size of air void channel, tortuosity and the channel orientation. For example, water has two paths (A and B) in Figure A-3 (c). Higher velocity is observed along path B, which is broader and straighter. Obviously, a broader and straighter flow channel would result in higher permeability value in the local area from the view of micro-scale.

b. The existence of solid bodies reduces the area available for water flow. In order to preserve fluid continuity, water has to move through the micro-channels and hence increase the flow velocity in narrow necks.

c. Not all flow through porous media is laminar from the view of micro-scale. Many narrow and wide necks can be formed in the coarse air void channels. The top-left zoom-in view in Figure A-3 (c) illustrates the interactive effect of the wide neck and narrow neck. Local boundary layer or even turbulent flow can be formed by the increased Reynolds number, since the narrow neck can lead to high speed flow in a porous medium and the wide neck can increase the hydraulic radius. This is one of the reasons for HMA moisture damage in pavement due to the non-uniform dynamic water pressure that will be further discussed.

d. The movement of flow in the HMA microstructure is not always downward but is a function of hydraulic pressure and channel orientation. Upflow is seen in the bottom-left zoom-in view of Figure A-3 (c). Interconnected air void channels form a U-shape

tube here. If the hydraulic pressure at the right side of the tube is larger than the left side, upflow can occur at the left side.

As mentioned above, the flow velocity would increase though the narrow necks. This flow pattern is very important from an engineering point of view. Relatively high velocity (and momentum) would produce high dynamic pressure which represents the fluid flow kinetic energy and as the dynamic pressure increases the collision between water flow and solid bodies would be more forceful. In addition, in non-slip condition higher laminar flow velocity would increase the wall shear stress because the velocity gradient near the wall/solid body would become greater. Wall shear stress is also obvious in turbulent flow. As the velocity of fluid further increases, fluid is sheared across the surface of the body, instabilities would develop and eventually the flow transitions into boundary layer or turbulent motion. Figures A-4 and A-5 show the plots of dynamic pressure and wall shear stress distribution in three typical kinds of air void structures identified from the Mix-3 HMA microstructure. A brighter color shows a higher value. The same pressure difference is applied to form the flow fields in the three typical air void structures.

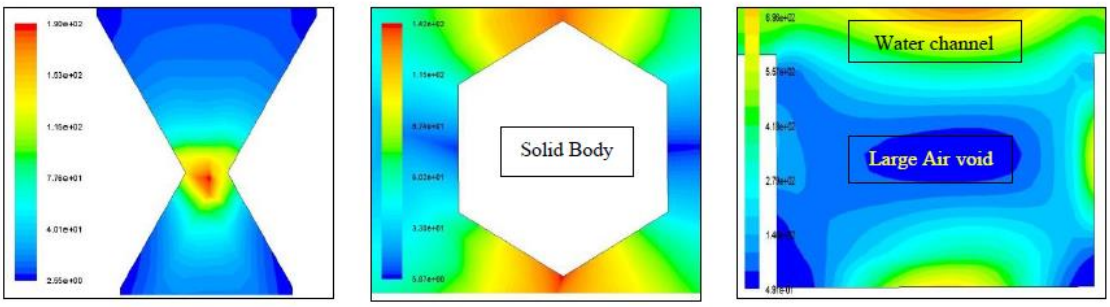

(a) (b) (c)

Figure A-4 Contours of dynamic pressure in different shapes of interconnected air voids

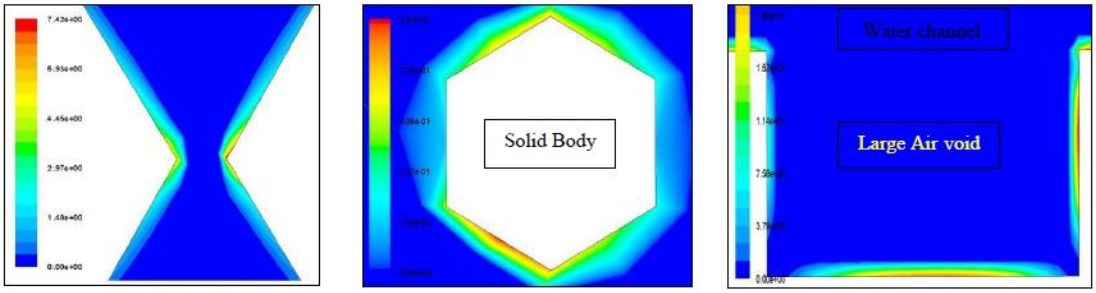

(a) (b) (c)

Figure A-5 Contours of wall shear stress in different shapes of interconnected air voids

Figure A-4 (a) and Figure A-5 (a) show the dynamic pressure and wall shear stress distribution at a typical sharp-edged narrow neck. The greatest value of dynamic pressure is seen at the edge area. As mentioned above, our model idealizes the fine aggregates as 2-D triangular structures (the sharp edges) bonded with the asphalt binder. It is believed that flow-accelerated erosion would be the most evident in areas of high wall shear stress and dynamic pressure. This shape offers a numerical modeling framework that can be used to explain one of the leading phenomenon to moisture damage in HMA pavement. In a wet condition and under heavy traffic load cycles, water in air void channels of HMA structure would repetitively crash into the surface of fine aggregates and progressively weaken the adhesive bond between the asphalt binder and aggregates. Moisture damage caused by reduction in the cohesive bond between the asphalt binder and aggregates would be the last result. Further, another two kinds of air void structures that can be generated by our visual microstructure model are also used to investigate the potential for HMA moisture damage. One is water flow around a hexagonal solid body in the vicinity of two fixed plates; another one is the turbulent flow in a square cavity. Figures A-4 (b) and A-5 (b) clearly show that along the direction of the fast moving fluid the greatest dynamic pressure and wall shear stresses are occurred at the edge parts. The distributions of pressure and stress pattern are

similar to that of the narrow-neck case in Figures A-4 (a) and A-5 (a). For the square cavity flow case, the pressure distribution would be somewhat different as shown in Figures A-4 (c) and A-5 (c). The square cavity can be considered as a large individual air void linked by other smaller interconnected voids. Flow in the interconnected air void channel would likely remain laminar, but local erosion due to turbulent flow can be formed in the cavity area. Turbulent flow can expand the space of the large individual air void by eroding the right side and bottom of the walls (see Figures A-4 (c) and A-5 (c)). It is also noticed that the erosion part is the asphalt binder in our HMA model.

Finally, the calculation of the permeability value in the HMA microstructure is discussed here. In macro-scale, water flow in HMA sample follows the Darcy's law that the hydraulic pressure loss increases linearly with the velocity of water transmitted through HMA as long as the flow of water is laminar. Darcy's permeability tensor in the vertical direction through a porous medium can be determined by Eq. A-2.

$$\frac{\partial P}{\partial y} = \frac{\gamma}{K_{yy}} U_y \qquad \text{(A-2)}$$

Where, $\partial P / \partial y$ is the pressure gradient in the vertical direction, γ is the unit weight of the fluid, U_y is the average vertical flow velocity in the porous medium, and K_{yy} is the Darcy's permeability tensor in vertical direction with unit (cm/s).

However, from a micro-scale, the Darcy's law may not be used, since the water flow is highly irregular and not evenly distributed in torturous channels of a HMA microstructure. The permeability value obtained in Eq. A-2 is the local permeability value and can only represent the viscous resistance effect on a very limited area within a porous medium. The values of local permeability obtained from micro-scale modeling need to be close to Darcy's permeability values from the macro-scale measurement in order to be used in practical

applications. Obviously, the local permeability would be approaching Darcy's permeability if one could simulate out the entire structural size of the HMA in the micro-scale modeling and this is the reason why the 3.9 cm thick simulation domain is applied in our study. The HMA core samples taken from the field for the comparison of permeability values are all around 1.5 inches (3.81 cm) in thickness and 4.0 inches (10 cm) in diameter. Since the vertical boundary of the simulation domain is set to be the line of symmetry, the simulation box increases to 3.9 cm x 7.8 cm. As can be seen, the domain size is close to the real sample size and can reduce the difference between the simulated permeability value and real measured permeability value.

The simulated permeability values in the vertical direction are calculated by Eq.A-2 with the measured top inlet flow velocity, arbitrary bottom pressure and simulated inlet pressure, bottom outlet velocity. The permeability values are shown in Figure A-6. It should be noted that the numerical permeability values in horizontal direction are unable to obtain since the Karol-Warner permeameter cannot be used to measure inlet flow velocity and permeability value horizontally. In order to compare the permeability values obtained in the simulated HMA microstructures with those in real HMA samples at similar air void content, roadway HMA core extractions were made at random locations along the longitudinal joint of US-6 highway in Iowa. It is generally believed that the longitudinal joint would be less dense than the rest of the lane away from the joint and has higher air void contents which would be closer to the level of air void contents in simulated HMA microstructures. Then the cores were transported to Iowa State University for subsequent air void and permeability tests by the Corelok$^{@}$ system and Karol-Warner permeameter, respectively. Finally, three

field core samples with the air void contents closest to the simulated HMA microstructures were chosen for permeability comparison.

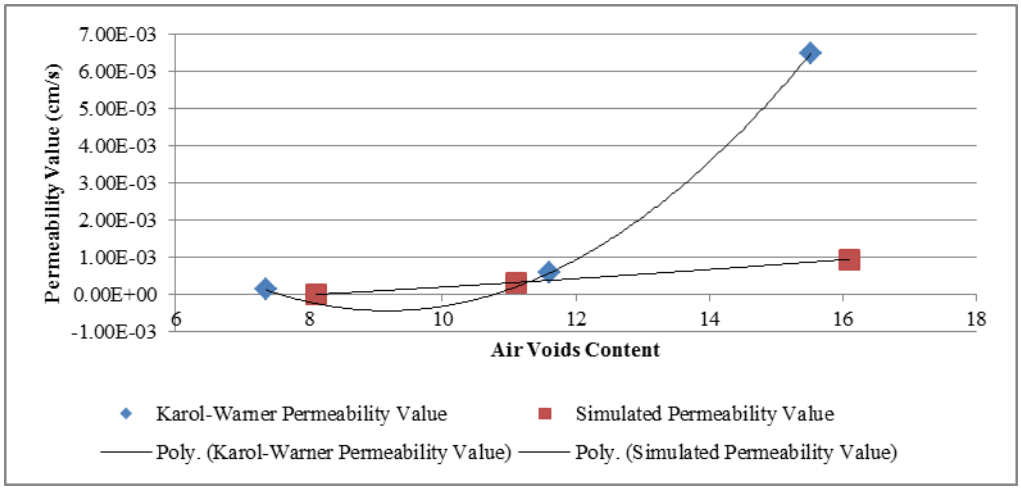

Figure A-6 Comparison of simulated and measured permeability values

Figure A-6 shows that as the air void increases, the relationship between the Karol-Warner permeability value and air void content would be no longer linear. A similar trend was observed by Williams et al (2010) and Cooley et al (2000). However, the simulated permeability values seems not follow the trend of the real permeability value and are much lower than the real ones. Reasons contributing to the result could be as follows. First, the permeability test depends on the interconnected nature of air voids in HMA rather than simply on the total percent of air voids. At 7.8 % air voids content (see Figure A-3(a)), no inter-connected air voids can be formed in the HMA microstructure based upon our HMA reconstruction method and hence no permeability value can be obtained. Another reason could be related to the position of boundary conditions. Research in CFD area indicates that too close inlet and outlet boundaries would result in inaccurate pressure and velocity predictions. The inlet and outlet boundaries considered for the permeability simulations for fibrous materials should be placed at a distance 10 times larger than the diameter of the fiber

away from the domain to obtain a relatively accurate result. However, how far away they should be placed for the simulation of granular materials is not investigated. Both the top and bottom boundaries are placed 10 cm away from the 3.9 x 3.9 cm HMA simulation domain based upon the requirement for fibrous media. This may also give inaccurate simulated pressure values. Finally, consideration should be taken into the nature limitation of the 2-D HMA microstructure. It is generally believed that interconnected air void channels can only be fully represented in a three-dimensional (3-D) system. A 2-D section of a 3-D HMA microstructure would contain more isolated air voids and underestimate the permeability value.

A-5 Recommendations and Conclusions

In this paper, a new method for constructing virtual 2-D microstructure of HMA is presented. The computer simulation technique can randomly place the particles in double layer spheres and the spheres would be further expanded into polygon shapes in an area approximately equal to the sum of coarse aggregates, fine aggregates and asphalt binder. Direct modeling of the water flow through the HMA microstructure is very complicated. This task was done in ANSYS - FLUENT commercial software which can accurately simulate the flow pattern in a given geometry. The flow pattern can be served to explain the mechanism of moisture damages in HMA pavement. The permeability values are also calculated out in post-processing work and are validated with laboratory measurements. It is found that our permeability calculation did not show a good agreement with the real laboratory results mainly due to the nature limitation of the 2-D HMA microstructure.

A-6 References

Al-Omari, A. and Masad, E. 2004. Three dimensional simulation of fluid flow in X-ray CT images of porous media, *International Journal for Numerical and Analytical Methods in Geomechanics*, 28 (13), pp. 1327-1360.

Cooley, L.A., Brown, E.R., and Maghsoodloo, S. 2000. Developing critical field permeability and pavement density values for coarse-graded Superpave pavements, *Transportation Research Record*, 1761, pp. 41-49.

Ghassemi, A. and Pak, A. 2001. Pore Scale of Permeability and tortuosity for flow through particulate media using lattice boltzmann method, *International Journal for Numerical and Analytical Methods in Geomechanics*, 35, pp. 886-901.

Ganapathysubramanian, B., and Zabaras, N. 2007. Modeling diffusion in random heterogeneous media: data-driven models, stochastic collocation and the variational multi-scale method, *Journal of Computational Physics*, 226, pp. 326-353.

Gopalakrishnan, K., Shashidhar, N., and Zhong, X.X. 2006. Study of compaction in hot-mix asphalt using computer simulations. *International Journal of Electrical and Computer Engineering*, 1:4, pp. 227-233.

Zhang, Y. 2008. Numerical simulation of dam concrete chemosmosis. Resources from http://www.paper.edu.cn/releasepaper/content/200811-769.

Williams, R.C., Raouf, M.A. and Schroer, J. 2010. Alternative test methods for measuring permeability of asphalt mixes. *In the 89th Annual Meeting of Transportation Research Board*, Washington, D.C., USA.

Wang, J.C., Leung, C.F., Chow, Y.K. 2003. Numerical solutions for flow in porous media. *International Journal for Numerical and Analytical Methods in Geomechanics*, 27, pp. 565-583.

Wittmann, F.H., Relfstra, P.E., and Sadouki, H. 1985. Simulation and analysis of composite structures, *Materials Science and Engineering*, 68, pp. 239-248.